

**Investigating low temperature carbon and nitrogen fixation of High
Arctic cyanobacterial mats**

Melissa Kozey

Department of Natural Resource Sciences

McGill University, Montreal

December 2, 2024

A thesis submitted to McGill University in partial fulfillment of the requirements of the
degree of Master of Science

©Melissa Kozey 2024

Table of Contents

Table of Contents	II
List of Tables and Figures	V
List of Abbreviations.....	VIII
Abstract.....	IX
Résumé	XI
Acknowledgements	XIII
Contribution of Authors	XIV
Chapter 1. Introduction.....	1
Chapter 2. Literature Review	3
2.1 Introduction.....	3
2.2 Climate change and biogeochemical cycles	5
2.2.1 Carbon cycle	6
2.2.2 Nitrogen cycle.....	8
2.3 Cyanobacterial carbon and nitrogen fixation.....	10
2.3.1 Photosynthesis.....	10
2.3.2 Factors affecting photosynthesis.....	12
2.3.3 Nitrogen fixation.....	13
2.3.4 Factors affecting nitrogen fixation.....	15
2.4 Stresses and adaptations in Arctic cyanobacteria.....	16
2.4.1 Cold temperatures	16
2.4.2 Desiccation.....	17
2.4.3 Osmotic stress	17
2.4.4 Solar radiation.....	18
2.4.5 Cold-tolerant cyanobacteria	19

2.5	Cyanobacterial growth and morphologies	20
2.5.1	Macroscopic microbial mats	21
2.5.2	Previous studies of cyanobacterial mat communities	22
2.6	Objectives of this thesis	24
Chapter 3. Investigating High Arctic <i>Nostoc</i> mats low-temperature carbon and nitrogen fixation through culture-independent and -dependent methods		26
3.1	Abstract	26
3.2	Introduction	27
3.3	Materials and Methods	30
3.3.1	Sample collection	30
3.3.2	Nucleic acid extraction and sequencing of an Arctic <i>Nostoc</i> mat community	31
3.3.3	Metagenomic and metatranscriptomic bioinformatic analyses of a High Arctic <i>Nostoc</i> mat community	32
3.3.4	In situ gas flux analyses of High Arctic <i>Nostoc</i> mats	34
3.3.5	Culturing and isolation of High Arctic photoautotrophs	35
3.3.6	Chlorophyll fluorescence assay of High Arctic <i>Nostoc</i> mat cultures	38
3.3.7	Acetylene reduction assay of a High Arctic mixed <i>Nostoc</i> mat culture	39
3.4	Results	40
3.4.1	Metagenomic and metatranscriptomic sequencing of a High Arctic <i>Nostoc</i> mat community	40
3.4.2	Analyses of cyanobacterial MAGs from a High Arctic <i>Nostoc</i> mat metagenome	43
3.4.3	In situ gas flux of High Arctic <i>Nostoc</i> mats	46
3.4.4	Isolation and characterization of High Arctic photoautotrophs	47
3.4.5	Chlorophyll Fluorescence Assay of High Arctic <i>Nostoc</i> mat cultures	49
3.4.6	Acetylene Reduction Assay of a High Arctic mixed <i>Nostoc</i> mat culture	50
3.5	Discussion	51

3.5.1	Metagenomic and metatranscriptomic sequencing of a High Arctic <i>Nostoc</i> mat community	52
3.5.2	Analyses of cyanobacterial MAGs from a High Arctic <i>Nostoc</i> mat metagenome	55
3.5.3	In situ gas flux of High Arctic <i>Nostoc</i> mats.....	57
3.5.4	Isolation and characterization of High Arctic photoautotrophs	59
3.5.5	Chlorophyll Fluorescence Assay of High Arctic <i>Nostoc</i> mat cultures	62
3.5.6	Acetylene Reduction Assay of a High Arctic mixed <i>Nostoc</i> mat culture	65
3.6	Conclusions.....	65
3.7	References	67
Chapter 4.	Discussion.....	74
4.1	Community composition of a High Arctic <i>Nostoc</i> mat and growth limits of its culturable photoautotrophic members.....	74
4.2	Cold adaptation mechanisms of a High Arctic <i>Nostoc</i> mat community	75
4.3	Carbon fixation and methane cycling in a High Arctic <i>Nostoc</i> mat community	77
4.3.1	Carbon fixation in a High Arctic <i>Nostoc</i> mat community	77
4.3.2	Methane cycling in a High Arctic <i>Nostoc</i> mat.....	79
4.4	Nitrogen fixation and cycling in a High Arctic <i>Nostoc</i> mat community	80
Chapter 5.	Final Conclusions and Summary.....	82
References		83
Appendix 1. Supplementary Materials for Chapter 3		91

List of Tables and Figures

Figure 2.1. Summary of the biological components of the carbon cycle. Green arrows represent photosynthesis, blue arrows represent respiration, purple arrows represent methanotrophy, and red arrows represent methanogenesis.	7
Figure 2.2. Summary of the nitrogen cycle. Blue arrows indicate denitrification, green arrows indicate annamox, red arrows indicate nitrogen fixation, purple arrows indicate nitrification, yellow arrows indicate ammonification, and black arrows indicate nitrate reduction. Gene pathways responsible for these processes are represented in italics within brackets. Abiotic sources for nitrogen fixation are represented by normal text within brackets.	10
Figure 2.3. Photosynthetic apparatus and summarized electron flow of cyanobacteria. The protein components from left to right are ATP synthase, photosystem II (PSII), plastoquinone (PQ), plastoquinol (PQH ₂), cytochrome b ₆ f (Cyt b ₆ f), cytochrome c ₆ (Cyt c ₆), photosystem I (PSI), ferredoxin (Fd), and ferredoxin-NADP reductase (FNR). The phycobillisome (PBS) is shown on PSII but can also be redistributed to PSI. In cyanobacteria, electrons can be transferred from cyt b ₆ f to PSI via Cyt c ₆ or plastocyanin (not shown). A simplified version of electron flow through the photosynthetic apparatus is demonstrated by red arrows, with cyclic electron transfer around PSI shown with a dashed arrow. For more details see Shevela <i>et al.</i> (2013).	12
Figure 2.4. <i>Nostoc</i> mat in a transient pond from the McGill Arctic Research Station on Axel Heiberg Island, Nunavut, Canada. Macroscopic <i>Nostoc</i> colonies are reddish-orange in colour. Sharpie for scale.	22
.....	31
Figure 3.1. <i>Nostoc</i> mat in a transient pond on Axel Heiberg Island, Nunavut, Canada. Red arrows point to the macroscopic <i>Nostoc</i> colonies.	31
Table 3.1 Physical measurements of 2023 <i>Nostoc</i> and control ponds from Axel Heiberg Island, Nunavut.	31
Table 3.2. Site locations and conditions at the time of <i>in situ</i> gas flux measurements of High Arctic <i>Nostoc</i> mats.	35
Table 3.3. Light levels of incubators.	37
Figure 3.2. Community structure and activity of a <i>Nostoc</i> mat from Axel Heiberg Island, Nunavut, Canada. A) By phylum. Phyla that represented less than 0.25% of the community were	

grouped into the "Other" category. B) By genus. Genera that represented less than 0.75% of the community were grouped into the "Other" category. 41

Figure 3.3. The presence and expression of cold adaptation genes in a *Nostoc* mat metagenome from Axel Heiberg Island, Nunavut, Canada, and the associated cyanobacterial metagenome-assembled genomes. Gene abundances are shown as counts per million (CPM) in the rectangles in the background, and transcript abundances are shown as transcripts per million (TPM) in the circles in the foreground. 45

Figure 3.4. Metabolic potential and expression of key genes involved in carbon fixation, methane cycling, and nitrogen cycling for a *Nostoc* mat from Axel Heiberg Island, Nunavut, Canada, and its associated cyanobacterial metagenome-assembled genomes. Gene abundances are shown as counts per million (CPM) in the rectangles in the background, and transcript abundances are shown as transcripts per million (TPM) in the circles in the foreground. 46

Figure 3.5. A) CO₂ and B) CH₄ gas flux of soils with *Nostoc* mats on the surface (*Nostoc*) and without any visible *Nostoc* mats (Control) on Axel Heiberg Island, Nunavut, Canada. Gas flux was measured using the LI-COR LI-7810 and both a clear chamber (CLEAR) and the LI-COR Smart chamber 8200-01 (DARK). 47

Figure 3.6. Microscope images of non-axenic phototrophic cultures from a *Nostoc* mat on Axel Heiberg Island, Nunavut, Canada. Panel A) MNM1, *Chloromonas* sp. B) MNM2, *Aphanizomenon* sp. NIES81 C) MNM3, *Stichococcus* sp. D) MNM4, *Tychonema* sp. CCAP_1459-11B E) MNM5 *Geitlerinema* sp. LD9. 48

Table 3.4. Summary of non-axenic culture growth characteristics from a High Arctic *Nostoc* mat community. The relative abundances of each culture in the metagenome were based on the taxonomic classification of reads. 48

Figure 3.7. The effect of temperature on the maximum quantum yield of PSII of six photoautotrophic cultures derived from a *Nostoc* mat in a transient pond from Axel Heiberg Island, Nunavut, Canada. 50

Figure 3.8. Summary of acetylene reduction at low and sub-zero temperatures of a mixed culture from a *Nostoc* mat on Axel Heiberg Island. Bars indicate the average of the cube root of biological ethylene produced by the sample +/- the standard deviation. 51

Figure 3.9. Schematic of *Nostoc* mat community carbon and nitrogen cycling on Axel Heiberg Island, Nunavut, Canada. Solid lines are representative of processes in which transcripts

indicated gene expression. Dashed lines are representative of processes that are either represented in the metagenome, with no transcripts, or indicated by in-situ gas flux measurements.....	54
Table S1. List of cold tolerance genes adapted from Raymond-Bouchard <i>et al.</i> (2018; Table 3)	91
Table S2. Selected genes to evaluate carbon fixation, methane cycling and nitrogen cycling	93
Table S3. Metagenome assembly statistics	93
Figure S1. Clear gas flux chamber sealed with a soil collar.	94
Figure S2. Gas flux sites A) N1, B) N2, C) N3, D) C1, E) C2, and F) C3. N sites contain portions of Nostoc mats (indicated by red arrows), while C sites were nearby soil sites with no mats.	94
Figure S3. Photoautotroph culture sampling sites. A) Gypsum Hill endolith (GHE) containing green striations. B) Gypsum Hill Springs microbial mats. Samples were derived from the white mat on the left (GHSWM), and the green portion in the center (GHSGM). C) White Glacier Cryoconite material (WGCM). D) White Glacier Forefield (WGF) soils that were deglaciated approx. 50 years ago.	95
Table S4. Identification and characterization of photoautotrophic cultures from high Arctic environments.....	95
Figure S4. Example ethylene standard curve generated by running standards with known ethylene concentrations through the gas chromatograph, with three technical replicates. Equation was adjusted for a set y intercept of 0.....	96
Figure S5. Tube containing photobleached cell contented following 30-day incubation under nitrogen free conditions. Arrow indicates the cell pellet.	96

List of Abbreviations

AHI: Axel Heiberg Island
BG11_o: Nitrogen-free BG11
Chl: Chlorophyll
CPM: Copies per million
DO: Dissolved oxygen
EPS: Extracellular polymeric substances
F_m: Maximum fluorescence with an oxidized PQ pool
F_o: Minimum fluorescence with an oxidized PQ pool
F_v/F_m: Maximum quantum yield of PSII
F_v: F_m – F_o
GHE: Gypsum Hill endolith
GHG: Greenhouse gas
GHSGM: Gypsum Hill Springs green mat
GHSWM: Gypsum Hill Springs white mat
HSP: Heat shock protein
MAG: Metagenome assembled genome
MARS: McGill Arctic Research Station
MNM: MARS *Nostoc* mat
PQ: Plastoquinone
PSI: Photosystem I
PSII: Photosystem II
TPM: Transcripts per million
UV: Ultraviolet
WGCM: White Glacier cryoconite material
WGF: White Glacier forefield
WHI: Ward Hunt Island

Abstract

Arctic ecosystems face unique pressures, as they are warming faster than the rest of the planet. Even with aggressive changes to greenhouse gas emissions, the Arctic is expected to see a 4°C annual temperature increase by 2050, which can cause significant disruptions to the environment, including permafrost thaw and glacial and sea ice melt. Because of the close relationship between ambient temperature and microbial activity, the threat of warming Arctic environments has raised additional concerns regarding microbial contributions to greenhouse gas emissions. Many cold-adapted organisms remain active at sub-zero temperatures, contributing to both carbon and nitrogen flux in Arctic ecosystems. Cyanobacteria are uniquely qualified for the study of biogeochemical cycles in the Arctic, as they are one of the few taxa capable of both carbon and nitrogen fixation and they are dominant primary producers in Arctic environments. For this reason, a detailed knowledge of the biogeochemical activity of Arctic cyanobacteria can contribute to a more general understanding of Arctic carbon and nitrogen cycling. We conducted metagenomic and metatranscriptomic analyses on a High Arctic *Nostoc* mat, which belongs to the Cyanobacteriota phylum, to identify the members, including transcriptionally active ones, and to evaluate the use of genes involved in cold tolerance, carbon fixation, methane cycling, and nitrogen cycling. We found that the mats had an abundance of Pseudomonadota and Cyanobacteriota members, but *Nostoc* was responsible for most of the transcripts. The Arctic *Nostoc* mat used a variety of mechanisms for cold adaptation, including those involved in membrane and peptidoglycan repair, and cold shock, stress and heat shock protein production. Within the mat community, *Nostoc* was responsible for the majority of photosynthesis and nitrogen fixation, as indicated by their transcriptional activity. To examine Arctic cyanobacterial growth, we cultured five photoautotrophs from an Arctic *Nostoc* mat and determined their

growth at a range of temperatures (-10 to 25°C), and salinities (0 to 10% NaCl). We found that four of the five isolates grew best at 15°C, and did not grow at warmer temperatures, indicating a psychrotrophic lifestyle. Additionally, one isolate grew at -5°C. None of the isolates were tolerant to high salt concentrations. To further evaluate *Nostoc* mat's role in carbon and nitrogen fixation, chlorophyll fluorescence and acetylene reduction experiments were conducted, respectively, at a variety of temperatures (-10 to 15°C). Chlorophyll fluorescence, which was conducted on the five cyanobacterial isolates, as well as a mixed culture from the *Nostoc* mat, showed that Arctic cyanobacteria are photosynthetically active at low temperatures. Acetylene reduction assay of a mixed culture of an Arctic *Nostoc* mat showed no evidence of nitrogen fixation, likely due to photobleaching early in the experiment. Arctic *Nostoc* mats are key members of Arctic carbon and nitrogen cycles as demonstrated by their transcriptional activity. Additionally, we see evidence that mat members are fixing carbon at low and sub-zero temperatures, which can be taken into consideration when examining Arctic carbon cycling.

Résumé

Les écosystèmes arctiques sont soumis à des pressions uniques, car ils se réchauffent plus rapidement que le reste de la planète. Même en réduisant radicalement les émissions de gaz à effet de serre, la température de l'Arctique devrait augmenter de 4 °C par an d'ici 2050, entraînant ainsi des perturbations importantes de l'environnement, notamment le dégel du pergélisol, la fonte des glaciers et de la glace de mer. En raison de la relation étroite entre la température ambiante et l'activité microbienne, la menace que représente le réchauffement des environnements arctiques pour les contributions microbiennes aux émissions de gaz à effet de serre soulève des préoccupations supplémentaires. De nombreux organismes adaptés au froid restent actifs à des températures inférieures à zéro, contribuant ainsi aux flux de carbone et d'azote dans les écosystèmes arctiques. Les cyanobactéries sont particulièrement qualifiées pour l'étude des cycles biogéochimiques dans l'Arctique, car elles sont l'un des rares taxons capables de fixer à la fois le carbone et l'azote et elles sont des producteurs primaires dominants dans les environnements arctiques. C'est pourquoi une connaissance détaillée de l'activité biogéochimique de ces bactéries peut contribuer à une compréhension plus générale des cycles du carbone et de l'azote dans l'Arctique. Nous avons effectué des analyses métagénomiques et métatranscriptomiques sur un tapis de *Nostoc* de l'Extrême-Arctique afin d'identifier les espèces présentes, y compris celles qui sont transcriptionnellement actives, et d'évaluer l'utilisation des gènes impliqués dans la tolérance au froid, la fixation du carbone, le cycle du méthane et le cycle de l'azote. Nous avons constaté que les tapis contenaient une abondance de Pseudomonadota et de Cyanobacteriota, mais que *Nostoc* était responsable de la plupart des transcrits. Le tapis de *Nostoc* arctique utilise une variété de mécanismes d'adaptation au froid, y compris ceux impliqués dans la réparation de la membrane et du peptidoglycane, ainsi que dans la production

de protéines de choc froid, de stress et de choc thermique. Au sein de la communauté du tapis, *Nostoc* était responsable de la majorité de la photosynthèse et de la fixation de l'azote, comme l'indique son activité transcriptionnelle. Pour examiner la croissance des cyanobactéries arctiques, nous avons cultivé cinq photoautotrophes issus d'un tapis de *Nostoc* arctique et déterminé leur croissance à une gamme de températures (-10 à 25 °C) et de salinités (0 à 10 % de NaCl). Nous avons constaté que quatre des cinq isolats poussaient mieux à 15 °C et ne poussaient pas à des températures plus élevées, ce qui indique un mode de vie psychrotrophe. Un isolat s'est même développé à -5 °C. Aucun des isolats n'était tolérant aux fortes concentrations de sel. Pour mieux évaluer le rôle des tapis de *Nostoc* dans la fixation du carbone et de l'azote, des expériences de fluorescence chlorophyllienne et de réduction de l'acétylène ont été menées à différentes températures (-10 à 15 °C). La fluorescence chlorophyllienne, réalisée sur les cinq isolats de cyanobactéries ainsi que sur une culture mixte du tapis de *Nostoc*, a montré que les cyanobactéries arctiques sont photosynthétiquement actives à basse température. Le test de réduction de l'acétylène d'une culture mixte d'un tapis de *Nostoc* arctique n'a montré aucun signe de fixation de l'azote, probablement en raison du photoblanchiment au début de l'expérience. Les tapis de *Nostoc* arctiques jouent un rôle clé dans les cycles du carbone et de l'azote dans l'Arctique, comme le montre leur activité transcriptionnelle. En outre, nous constatons que les membres du tapis fixent le carbone à des températures basses et inférieures à zéro, ce qui peut être pris en considération lors de l'examen du cycle du carbone dans l'Arctique.

Acknowledgements

I would like to thank Prof. Whyte for giving me the opportunity to join his research team and for the skills he has taught me over the course of my Master's program. I would also like to thank Prof. Brian Driscoll and Prof. Jean-Benoit Charron for their oversight and guidance of my project as committee members. My time at McGill has been full of learning experiences and has made me a better scientist. The opportunities I was given to visit the Arctic was so impactful and I will remember them fondly.

I would like to acknowledge Scott Sugden and Dr. Christina Davis for their contributions to my success and for pushing me to be a better scientist. They have provided significant advice and support that was essential to my thesis work. I would also like to thank all of the Whyte lab members that I have had the opportunity to work alongside over the course of my Masters. Dr. Nastasia Freyria, Dr. Ya-Jou Chen, Dr. Ellise Magnuson, Dr. Brady O'Connor, Esteban Góngora, Olivia Blenner-Hasset, Matthew Quinn, Lochlan Breckenridge, Emma Righi, Kyle Story, and Ke Ke Li; you have all provided guidance and support throughout this experience, for which I am forever grateful.

Finally, I would like to thank all the friends and family who have supported me throughout my thesis. You kept me sane and encouraged me the entire way. Thank you.

Contribution of Authors

Chapter 2: Literature Review

Melissa Kozey, the MSc candidate, wrote the literature review with guidance and editing provided by Scott Sugden and Prof. Lyle G. Whyte.

Chapter 3: Investigating High Arctic Nostoc mats low-temperature carbon and nitrogen fixation through culture-independent and -dependent methods

The manuscript was made in collaboration with Scott Sugden, Dr. Christina Davis, and Prof. Lyle G. Whyte from McGill University. Melissa Kozey, the MSc candidate, conducted all laboratory work, data analysis and wrote the manuscript. Scott Sugden provided assistance with data analysis and editing the manuscript. Dr. Christina Davis assisted in sample collection, experimental design, and data analysis. Prof. Lyle G. Whyte provided assistance with experimental design and editing the manuscript.

Chapter 4. Discussion and Conclusion

Melissa Kozey, the MSc candidate, wrote the discussion and conclusion with editing and counselling by Prof. Lyle G. Whyte

Chapter 1. Introduction

Climate change is a growing global crisis, with rising temperatures globally, however, the Arctic is disproportionately affected by climate change, as it is warming faster than the rest of the planet (Moon *et al.*, 2018, Overland *et al.*, 2019). It is estimated that even with aggressive reductions in greenhouse gas (GHG) emissions, the Arctic will see a 4°C annual temperature increase by 2025, causing significant disruptions to Arctic ecosystems (Overland *et al.*, 2019). The relationship between temperature and microbial activity has also raised concerns of increasing GHG emissions from Arctic microbes in a warming climate (Novis *et al.*, 2007, Nikrad *et al.*, 2016). Additionally, there are many cold-adapted microorganisms that are able to grow and metabolize at cold and sub-zero temperatures, whose annual activity will increase with rising temperatures (Mykytczuk *et al.*, 2013, Goordial *et al.*, 2016). For this reason, it is important to study how these organisms can survive the harsh conditions of the Arctic as well as the biogeochemical activity of microorganisms at cold and sub-zero temperatures.

While cold adapted heterotrophs are well studied, photoautotrophic activity in continuously cold environments is poorly understood (Mykytczuk *et al.*, 2013, Goordial *et al.*, 2016, Jungblut & Vincent, 2017). Cyanobacteria are uniquely relevant to the study of changing biogeochemical cycles as they are one of few taxa capable of both carbon and nitrogen fixation. While there have been some studies of polar cyanobacterial activity, they focus on Antarctic samples (Becker, 1982, Davey & Marchant, 1983). Additionally, there have been metagenomic and genomic studies aimed at evaluating Arctic cyanobacterial metabolisms and col-adaptations, but do not consider the activity of the cyanobacteria (Varin *et al.*, 2012, Jungblut *et al.*, 2021).

In this study, we aimed to determine what cold-adaptation genes are present and transcribed by a High Arctic *Nostoc* mat community using metagenomics and

metatranscriptomics. Additionally, we used these methods to look at marker genes involved in carbon fixation, methane cycling and nitrogen cycling. To further evaluate photoautotrophic members, five non-axenic cyanobacterial cultures from the High Arctic *Nostoc* mat, each containing one primary photoautotroph, were evaluated from growth at cold and sub-zero temperatures, high salt concentrations, and on nitrogen-limited media. An additional 14 cultures from adjacent environments were also evaluated for these characteristics. Next, chlorophyll fluorescence of the five *Nostoc* mat cultures, in addition to a mixed culture were evaluated to determine if these organisms were capable of photosynthesis at cold and sub-zero temperatures. Finally, the acetylene reduction of a mixed culture from the High Arctic *Nostoc* mat was evaluated to determine if the mat was capable of nitrogen fixation at cold and sub-zero temperatures.

Chapter 2. Literature Review

2.1 Introduction

Cryoenvironments are continuously below 0°C and include the ocean, polar and alpine regions (Morgan-Kiss *et al.*, 2006, Holmberg & Jørgensen, 2023). In general, these environments are characterized by extremely harsh conditions including low nutrient inputs, extreme fluctuation in ultraviolet (UV) radiation, freeze-thaw cycles and low water availability (Goordial *et al.*, 2013, Jungblut & Vincent, 2017, Holmberg & Jørgensen, 2023). These environments include permafrost, glacial and sea ice, and ice sheets, but can also include more unique environments such as cold lakes and ponds, and sub-zero saline springs (Goordial *et al.*, 2013, Shen *et al.*, 2021). Cryoenvironments put unique strains on life, requiring the organisms inhabiting them to adapt to survive. Despite these stresses, persistence of microbial life in the cryosphere is widely documented (Morgan-Kiss *et al.*, 2006, Goordial *et al.*, 2013, Shen *et al.*, 2021).

Although the integrity of many of these already-sensitive environments is already being challenged by climate change, Arctic regions face unique pressures because they are warming faster than the rest of the planet (Moon *et al.*, 2018, Overland *et al.*, 2019). Even with aggressive reductions in greenhouse gas (GHG) emissions, the Arctic is expected to see a 4°C annual temperature increase by 2050, which will cause permafrost to thaw and glaciers and sea ice to melt (Overland *et al.*, 2019). Because of the close relationship between ambient temperature and microbial activity (Lennihan *et al.*, 1994, Zielke *et al.*, 2005, Novis *et al.*, 2007), the threat of warming Arctic environments has raised additional concerns regarding microbial contributions to GHG emissions, as increased microbial activity generates a positive feedback loop, generating higher GHG emissions (Nikrad *et al.*, 2016). Many cold-adapted microorganisms, such as

Planococcus halocryophilis and *Rhodococcus* sp. JG3 (Mykyteczuk *et al.*, 2013, Goordial *et al.*, 2016), remain active at sub-zero temperatures, contributing to carbon and nitrogen flux in Arctic ecosystems (Nikrad *et al.*, 2016); however, both the extent of this sub-zero activity and its response to future warming remain poorly understood. To better model future geochemical cycling dynamics in a warming Arctic, it is essential to better understand how Arctic microorganisms contribute to GHG emissions at sub-zero to warmer temperatures.

Carbon fixation is a key feature of the carbon cycle; however, higher plants are sparse in polar deserts, making cyanobacteria foundational primary producers supporting other life. In addition to their role in supplying fixed carbon to Arctic ecosystems, many cyanobacterial species are capable of nitrogen fixation, generating ammonia that can also be used by other organisms to build amino acids and proteins, in turn improving growth and activity over nitrogen-limited conditions (Esteves-Ferreira *et al.*, 2017, Kohler *et al.*, 2023). Understanding the role of cyanobacteria in the carbon and nitrogen cycles at various temperatures is therefore essential to understanding how Arctic GHG flux will change with the warming climate.

Cyanobacteria (phylum Cyanobacteriota) are one of the most widely distributed and biogeochemically versatile microbial groups in Arctic ecosystems. These Gram-negative oxygenic photoautotrophs inhabit liquid brine veins within sea glacial ice (Vincent, 2002, Price, 2007). Glacial surfaces also host microbial hotspots called cryoconites, which are a complex microbial community sustained by cyanobacteria and other photosynthetic microorganisms (Morgan-Kiss *et al.*, 2006, Christmas *et al.*, 2016, Rozwalak *et al.*, 2022). Arctic and Antarctic soils and permafrost are colonized by cyanobacteria, including recently deglaciated regions (Vincent, 2002, Christmas *et al.*, 2016, Nash *et al.*, 2018, Pessi *et al.*, 2019). Cyanobacteria are also found in rocks as epiliths on the surface, hypoliths under translucent layers of rock, or

cryptoendoliths growing within the pore space of rocks (Vincent, 2002, Ziolkowski *et al.*, 2013, Goordial *et al.*, 2017). Cyanobacteria are also common in Arctic lakes, rivers, streams, and transitory ponds, often forming macroscopic mats in the same location annually (Vincent, 2002, Morgan-Kiss *et al.*, 2006).

In this review, I discuss the role of cyanobacteria in Arctic carbon and nitrogen cycles, with specific attention to the physiological and molecular mechanisms underlying their ability to provide fixed carbon and nitrogen to these otherwise nutrient-poor ecosystems. I then discuss the different stressors that Arctic cyanobacteria face and the physiological adaptations they have evolved to support life in the cryosphere. Finally, I review mat-forming cyanobacteria species and discuss previous studies of these mat communities, identifying knowledge gaps that are addressed in this thesis.

2.2 Climate change and biogeochemical cycles

Understanding geochemical cycles can help with future modelling and understanding of climate change. Geochemical cycles are the flow of energy and nutrients between the atmosphere, land, ocean, and living things, mediated by chemical, biological, and geological transformations. Human impacts on these cycles have been well documented (Falkowski *et al.*, 2000, Bernhard, 2010, Nakazawa, 2020), but knowledge of naturally occurring biogeochemical cycles is also imperative to geochemical modelling. Understanding existing geochemical cycles is most pressing in Arctic environments, which have been disproportionately affected by climate change and human activity but remain the least well studied. Annual mean temperature increases between 1880 and 2012 in the Arctic were four times higher than the global average (Moon *et al.*, 2018). Winter surface air temperatures in the Arctic are the most affected by warming, with winter temperatures in 2016 and 2018 being 6°C higher than the 1981-2010 average (Bruhwiler

et al., 2021). The consequences of this warming are numerous and include the loss of land and sea ice, associated sea level rise, permafrost thaw, changes in cloud structure, increased atmospheric water vapour, changes to atmospheric and oceanic transport of carbon, and changes in vegetation coverage (Moon *et al.*, 2018, Overland *et al.*, 2019, Bruhwiler *et al.*, 2021). One of the more subtle but pervasive effects of Arctic warming has been increased microbial activity resulting in increased GHG emissions (Martineau *et al.*, 2010, Nikrad *et al.*, 2016, Moon *et al.*, 2018, Overland *et al.*, 2019, Bruhwiler *et al.*, 2021). However, the magnitude of these changes in Arctic ecosystems, the extent to which microbial communities are affected, and their potential feedback to the global climate systems all remain poorly quantified.

2.2.1 Carbon cycle

As the Arctic continues to warm, its impact extends beyond regional ecosystems. Changes to the carbon cycle in the Arctic caused by climate change will have positive feedback, generating more GHGs, and, thus, increasing global temperatures. The carbon cycle describes the movement of carbon between the atmosphere and fixed pools in marine and terrestrial ecosystems (**Figure 2.1**). Oceans exert the strongest control on the concentration of atmospheric CO₂ via continuous gas exchange at the surface (Falkowski *et al.*, 2000, Reichle, 2020), which occurs as a combination of both biological exchange via photosynthesis and inorganic exchange via solubilization in water. In contrast, terrestrial ecosystems exchange CO₂ with the atmosphere almost exclusively via photosynthesis (Falkowski *et al.*, 2000). However, terrestrial environments absorb less net CO₂ than the ocean because the fixed CO₂ in terrestrial environments is often returned to the atmosphere either by photoautotrophic and heterotrophic respiration or by disturbances such as fires (Falkowski *et al.*, 2000, Reichle, 2020). The most stable carbon pool is the lithosphere, where carbon can remain sequestered for millions of years

in the form of carbonic rock such as limestone or as fossil fuels from decayed organic matter (Reichle, 2020). Carbonic rock is liberated into the atmosphere through volcanic activity, while fossil fuels are liberated by combustion (Reichle, 2020).

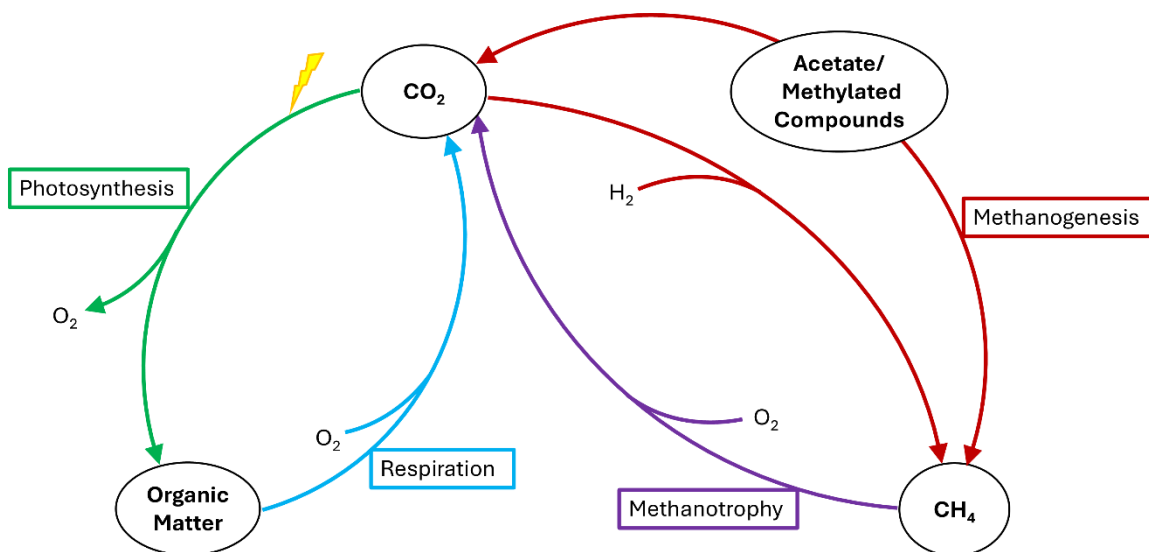


Figure 2.1. Summary of the biological components of the carbon cycle. Green arrows represent photosynthesis, blue arrows represent respiration, purple arrows represent methanotrophy, and red arrows represent methanogenesis.

Cyanobacteria play a key role in the carbon cycle as they are responsible for 20-30% of global primary production, fixing 20-30 Gt of CO₂, and releasing 50-80 Gt of O₂ into the atmosphere every year (Shevela *et al.*, 2013, Stirbet *et al.*, 2019). They are also more efficient than other primary producers: cyanobacteria convert up to 10% of the solar radiation they receive into biomass, compared to only 4-6% for C3 and C4 plants and 5% for algae (Zhu *et al.*, 2008, Esteves-Ferreira *et al.*, 2017). Because polar and high-latitude regions have lower vascular plant biomass, cyanobacterial carbon fixation is especially important as a source of primary production in these ecosystems (Chrismas *et al.*, 2018).

Another key part of the carbon biogeochemical cycle is methane, which is the second most important GHG, behind CO₂, as it is 28 times more effective at trapping heat in the atmosphere (United States Environmental Protection Agency, 2024). Methane is naturally

emitted into the atmosphere from wetlands, rivers, wild animals and geological processes, however, emissions are accelerated through anthropogenic activities, such as burning fossil fuels and ruminant farming (Nakazawa, 2020). Methane can be produced and consumed by methanogenic archaea (methanogens) and methanotrophic archaea and bacteria (methanotrophs), respectively (Nakazawa, 2020) (**Figure 2.1**). Both of these groups can be found in Arctic soils, and their activity is highly dependent on the soil moisture content, with drier conditions favouring methanotrophy, while wetter conditions favour methanogenesis (Arndt *et al.*, 2019, Voigt *et al.*, 2023). Methanogenesis requires the reduction of CO₂, H₂, acetate, or methylated compounds to CH₄ under anaerobic conditions (Evans *et al.*, 2019). On the contrary, methanotrophy oxidizes methane to carbon dioxide using methane monooxygenase enzymes (Trotsenko & Khmelenina, 2005). Methane consumption by methanotrophs typically counteracts a large fraction of emissions produced by the methanogens (Singleton *et al.*, 2018).

2.2.2 Nitrogen cycle

While the carbon cycle plays a critical role in regulating climate change and is important in the transfer of energy within ecosystems, the nitrogen cycle is also essential for the transfer of nutrients in ecosystems, with nitrogen alongside carbon being used for amino acids and nucleic acids. The nitrogen cycle (**Figure 2.2**) refers to the series of transformations that nitrogen undergoes within an ecosystem. In many ecosystems, microbial growth is limited by the availability of nitrogen more than other nutrients, making nitrogen cycling important for maintaining life (Bernhard, 2010). Nitrogen gas comprises approximately 78% of the atmosphere, but this form is inaccessible to most organisms (Bernhard, 2010, Nakazawa, 2020). However, a select few microbial taxa are capable of nitrogen fixation, which is the conversion of N₂ into biologically available ammonia (NH₃). Nitrogen can also be fixed abiotically by

lightning or using industrial processes (Bernhard, 2010). After fixation, nitrogen persists in ecosystems in both organic (amino and nucleic acids) and inorganic (ammonia and nitrate) forms (Bernhard, 2010). Organisms that use inorganic nitrogen as an electron donor contribute to nitrification, the step-wise conversion of ammonia to nitrite and then nitrate (Bernhard, 2010). Nitrate can then be returned to the atmosphere as N_2 via either anaerobic ammonia oxidation (anammox) or denitrification. In the anammox reaction, cells oxidize ammonia and use nitrate as an electron acceptor, forming N_2 (Bernhard, 2010). Denitrification is the step-wise conversion of nitrate to N_2 via the intermediates nitrite, nitric oxide, and nitrous oxide (Bernhard, 2010). Organic nitrogen molecules, such as amino and nucleic acids, can be converted to ammonia via ammonification (Bernhard, 2010). Additionally, nitrate can also be reduced to ammonium via two pathways depending on the nitrogen's fate; assimilatory nitrate reduction if the ammonium is to be incorporated into the cell's biomass and dissimilatory nitrate reduction if the ammonium is to be excreted from the cell (Sparacino-Watkins *et al.*, 2014).

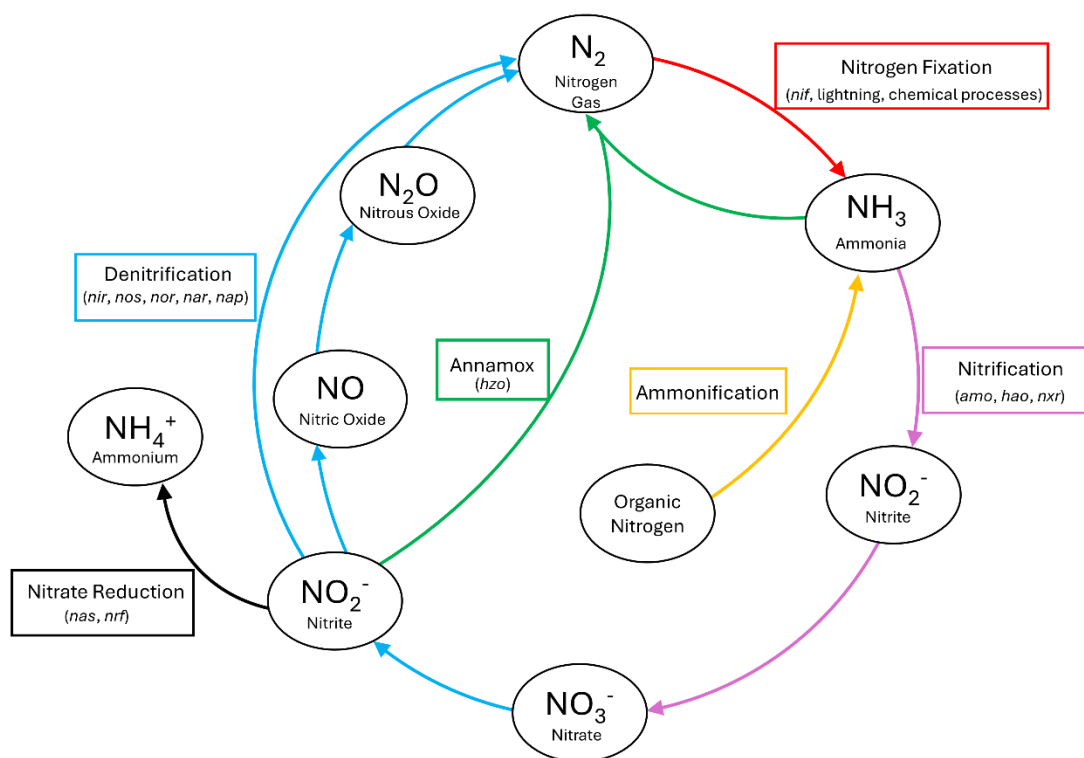


Figure 2.2. Summary of the nitrogen cycle. Blue arrows indicate denitrification, green arrows indicate annamox, red arrows indicate nitrogen fixation, purple arrows indicate nitrification, yellow arrows indicate ammonification, and black arrows indicate nitrate reduction. Gene pathways responsible for these processes are represented in italics within brackets. Abiotic sources for nitrogen fixation are represented by normal text within brackets.

2.3 Cyanobacterial carbon and nitrogen fixation

Cyanobacteria play a unique role in these biogeochemical cycles because they are one of the few taxa – from any domain of life – capable of both carbon and nitrogen fixation. For this reason, detailed knowledge of the biogeochemical activity of Arctic cyanobacteria can contribute significantly to a more general understanding of Arctic carbon and nitrogen sources and sinks.

2.3.1 Photosynthesis

Photosynthesis is the molecular process in which cells use solar radiation to generate energy-rich carbohydrates and O_2 . When water is used as the electron donor, as is the case in cyanobacteria, photosynthesis produces O_2 as a byproduct and is therefore considered oxygenic

(Shevela *et al.*, 2013). This process also requires some form of light-harvesting pigment. Cyanobacteria primarily produce chlorophyll (Chl) a for this purpose, but they can also contain Chls b and d, carotenoids, and phycobilins (phycocyanin, allophycocyanin, and phycoerythrin) (Shevela *et al.*, 2013). Phycobilins are organized into phycobilisomes, which absorb light and are attached to the reaction centre complexes, photosystem I (PSI) and photosystem II (PSII) (Shevela *et al.*, 2013). Phycobilisomes are primarily associated with PSII but can be redistributed to PSI to regulate excitation energy transfer efficiency (Shevela *et al.*, 2013).

In cyanobacteria, light conversion to ATP and NADPH occurs in the thylakoid membrane (Shevela *et al.*, 2013). For all oxygenic photosynthesis, the PSI and PSII reaction centres drive light-induced electron transfer from H₂O to NADP⁺, forming NADPH, which is used to synthesize carbohydrates (Shevela *et al.*, 2013). Light is absorbed by the large phycobilisome antenna, and the excitation energy is then transferred from the phycobilisome to the reaction centre complexes (PSII and PSI) (Shevela *et al.*, 2013). Excitation energy from the reaction centres is then transferred to the Chl a molecules P680 (in PSII) and P700 (in PSI), followed by sequential stepwise electron transfers resulting in stabilized charge separation (**Figure 2.3**) (Shevela *et al.*, 2013). Key genes involved in photosynthesis include those encoding for the phycobilisome pigments: phycocyanin (*cpc*), allophycocyanin (*apc*), and phycoerythrin (*cpe*) (Lemaux & Grossman, 1985, Reith & Douglas, 1990, Hagopian *et al.*, 2004). The apparatus protein PSI is encoded by the *psa* gene group, PSII is encoded by the *psb* gene group, and cytochrome b6f is encoded by the *pet* gene group (Mulikidjanian *et al.*, 2006). Chlorophyll is synthesized by enzymes encoded by *chl* genes (Mulikidjanian *et al.*, 2006). The resultant NADPH

and ATP are then used for carbon fixation in the Calvin-Benson-Bassham cycle, which utilizes the RubisCO enzyme (*rbc*) (Mulkidjanian *et al.*, 2006).

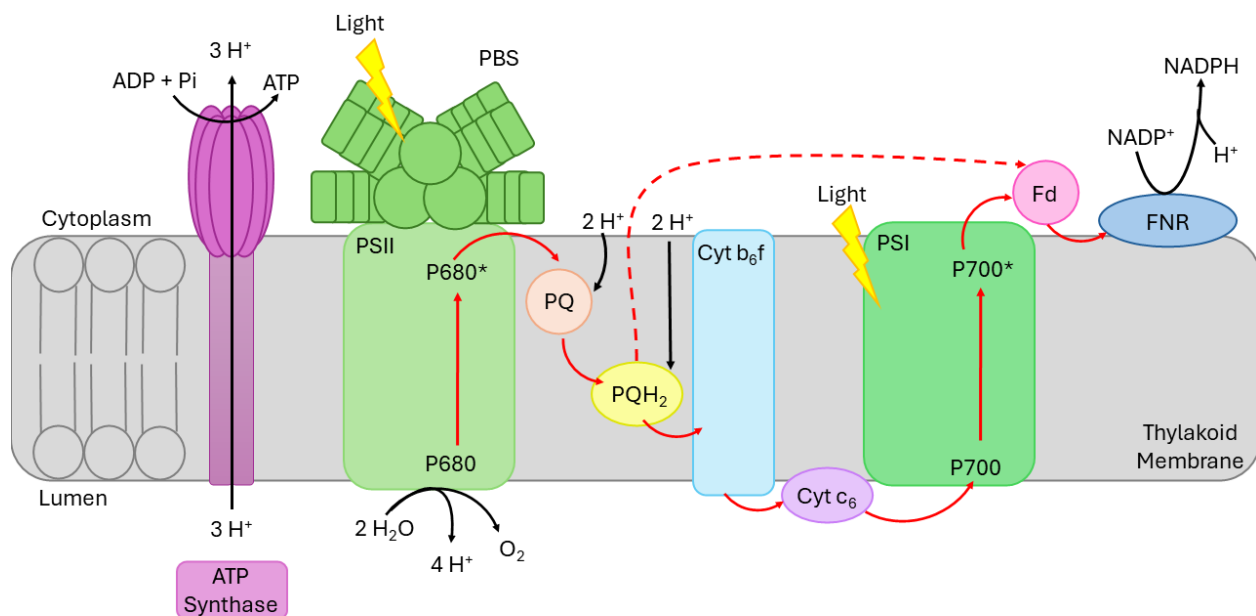


Figure 2.3. Photosynthetic apparatus and summarized electron flow of cyanobacteria. The protein components from left to right are ATP synthase, photosystem II (PSII), plastoquinone (PQ), plastoquinol (PQH₂), cytochrome b₆f (Cyt b₆f), cytochrome c₆ (Cyt c₆), photosystem I (PSI), ferredoxin (Fd), and ferredoxin-NADP reductase (FNR). The phycobillisome (PBS) is shown on PSII but can also be redistributed to PSI. In cyanobacteria, electrons can be transferred from cyt b₆f to PSI via Cyt c₆ or plastocyanin (not shown). A simplified version of electron flow through the photosynthetic apparatus is demonstrated by red arrows, with cyclic electron transfer around PSI shown with a dashed arrow. For more details see Shevela *et al.* (2013).

2.3.2 Factors affecting photosynthesis

Cyanobacterial photosynthetic rates can vary based on a variety of environmental factors. First, previous work has shown that cyanobacterial carbon fixation rates increase with both temperature (Lenniham *et al.*, 1994, Novis *et al.*, 2007) and ambient CO₂ concentrations (Qiu & Gao, 2002). Changing rates with temperature and CO₂ concentrations is a function of chemical kinetics. Higher temperatures and higher CO₂ concentrations both increase the likelihood of interactions between the enzyme and substrate, in turn increasing photosynthetic rates in both cases. Even so, a study of Antarctic *Nostoc* found measurable CO₂ fixation at −5°C, suggesting

that photosynthesis persists at sub-zero temperatures provided that sufficient light is available (Becker, 1982). Furthermore, photosynthetic rates are sensitive to light intensity: the increase in carbon fixation at higher ambient CO₂ has been shown to require higher light intensity for CO₂ saturation (Qiu & Gao, 2002), and oxygen evolution of *Nostoc commune* has been shown to plateau at light levels of 100-150 $\mu\text{mol m}^{-2} \text{s}^{-1}$ (Lennihan *et al.*, 1994). In tropical cyanobacterial mats, oxygen evolution and Chl fluorescence were reduced under both high and low light stress (Luttge *et al.*, 1995). Finally, photosynthetic rates fluctuate with water availability as water splitting is a key part of oxygenic photosynthesis, for this reason, photosynthesis ceases when the cells are desiccated or frozen, as no water is available to the cell. Novis *et al.* (2007) found that desiccation had little effect on carbon fixation in Antarctic *Nostoc* until 70% of the mat's water content was lost, with unpredictable fixation past this threshold. A different study found that photosynthetic activity was closely related to the degree of desiccation (Qiu & Gao, 2002), though mats quickly recovered activity when rehydrated (Luttge *et al.*, 1995, Qiu & Gao, 2002).

2.3.3 Nitrogen fixation

In addition to carbon fixation, some cyanobacterial taxa can also fix atmospheric nitrogen. Cyanobacteria can assimilate simple nitrogen molecules such as ammonium, nitrate and urea, but they can also fix atmospheric N₂, making them key to the nitrogen cycle (Fleming & Castenholz, 2008, Shevela *et al.*, 2013). The reaction requires N₂, 8 H⁺, 8 electrons, and 16 ATP molecules to generate two NH₃ and hydrogen gas as a by-product (Esteves-Ferreira *et al.*, 2017). Despite the high prevalence of N₂ in the atmosphere, nitrogen fixation is energetically expensive because it requires breaking the triple bond between nitrogen atoms. Because of the added stress of this reaction, cells that perform nitrogen fixation may expend less energy on other cellular processes and often exhibit reduced growth rates (Fleming & Castenholz, 2008).

Nitrogenase is oxygen-labile, with high levels of oxygen being associated with enzyme degradation and energy losses (Esteves-Ferreira *et al.*, 2017). However, cyanobacteria generate oxygen as a byproduct of photosynthesis, thus creating a challenge for maintaining enzyme integrity. To allow for both carbon and nitrogen fixation to occur without the products of the former compromising the latter, some filamentous cyanobacteria create differentiated cells called heterocysts. These unique cells have a bilayered polysaccharide and glycolipid envelope that slows the diffusion of gasses, thereby creating a microaerobic environment in which nitrogen fixation can occur. Heterocysts are spatially separated from carbon fixation in vegetative cells and cannot perform photosynthesis on their own, as most of their PSII components are degraded (Fleming & Castenholz, 2008, Esteves-Ferreira *et al.*, 2017). Instead, they are provided with fixed carbon from vegetative cells (Esteves-Ferreira *et al.*, 2017). As an alternative to spatially isolating nitrogen fixation into heterocysts, some cyanobacteria rely on temporal separation, where photosynthetic carbon fixation occurs in the light and nitrogen fixation occurs in the dark (Fleming & Castenholz, 2008, Esteves-Ferreira *et al.*, 2017). In species that use temporal separation, nitrogenase is present in all cells and nitrogen fixation rates are correlated with respiration rates (Esteves-Ferreira *et al.*, 2017).

The cellular machinery for nitrogen fixation is encoded by the *nif* gene clusters, which are organized into four operons: *nifB-fdxN-nifSU*, *nifHDK*, *nifENXW*, and *nifVZT* (Esteves-Ferreira *et al.*, 2017). Nitrogenase, the enzyme directly responsible for nitrogen fixation, consists of two subunits: dinitrogenase, which is a FeMo-protein encoded by *nifD* (alpha subunit) and *nifK* (beta subunit), and dinitrogenase reductase, which is encoded by *nifH* (Esteves-Ferreira *et al.*, 2017). Expression of the *nif* genes is controlled by the cell's carbon/nitrogen balance and cellular redox status, becoming active when carbon is abundant but nitrogen is scarce (Esteves-Ferreira *et al.*,

2017). Since ammonia is the preferred nitrogen source for cyanobacteria, ammonia indirectly represses *nif* expression by blocking the transcriptional activator NtcA (Esteves-Ferreira *et al.*, 2017). This transcriptional regulator also controls heterocyst formation, mobilization of stored nitrogen, ammonia assimilation, sensing and control of cellular nitrogen homeostasis, and NtcA itself (Esteves-Ferreira *et al.*, 2017).

2.3.4 Factors affecting nitrogen fixation

Nitrogen fixation rates, which are often measured experimentally using the acetylene reduction assay because nitrogenase can cleave small triply bonded molecules other than nitrogen gas, such as acetylene (Stewart *et al.*, 1967, David *et al.*, 1980, Capone, 1993), depend on a variety of environmental factors. First, water can affect nitrogen fixation rates because dehydration and desiccation are stressful for the cells, they shift energy expenditure from nitrogen fixation to life-sustaining activities (Davey, 1983, Davey & Marchant, 1983, Sohm *et al.*, 2020). In one study, completely desiccated cyanobacterial mats showed no nitrogenase activity, but activity immediately resumed when the mats were rehydrated (Davey, 1983). Another study found that nitrogen fixation rates in moss-associated cyanobacteria were correlated with the water content of the soil and vegetation (Zielke *et al.*, 2005). Lennihan *et al.* (1994) noted that colonies that were desiccated and then rehydrated reduced about 70% less acetylene than colonies that were never desiccated. Furthermore, when sufficient water is available, nitrogen fixation rates are correlated with temperature (Lennihan *et al.*, 1994, Zielke *et al.*, 2005). The lowest temperature at which quantifiable nitrogen fixation has been observed is -7.6°C during an *in situ* study of *Nostoc* mats in Victoria Land, Antarctica (Davey & Marchant, 1983). Third, the pH of the soil also affects the rates of nitrogen fixation, with optimal rates occurring between pH 7.0 and 8.0 (Davey & Marchant, 1983, Reynaud, 1984). Operating outside

of the optimal pH range is stressful for the cells, and as with water availability causes the cells to shift energy expenditure to more essential functions. Finally, a higher surface area-to-volume ratio has been shown to increase acetylene reduction rates, with thinner sheets having higher rates than spherical colonies due to increased surface area available for gas exchange (Lennihan *et al.*, 1994). The high energy demand of nitrogen fixation means that it is quick to cease when the cell experiences environmental stressors.

2.4 Stresses and adaptations in Arctic cyanobacteria

Cyanobacterial carbon and nitrogen fixation rates are impacted by environmental stressors. Arctic cyanobacteria experience more environmental stressors than their more temperate counterparts as they must be able to withstand cold temperatures, freeze-thaw cycles, desiccation, osmotic stress, and light stress, with high UV radiation doses in the summer, and no photosynthetically active radiation (PAR) in the winter (Morgan-Kiss *et al.*, 2006, Vincent, 2007). Cyanobacterial life in the Arctic is required to adapt and acclimate to survive these environmental stressors.

2.4.1 Cold temperatures

Arctic environments are extremely harsh and pose multiple stressors to microbial life. For example, cold temperatures persist through most of the year, which slows cellular growth and metabolism and compromises protein flexibility (Goordial, 2021). While reduced growth and metabolic rates in cold temperatures are a result of slowed molecular movement, Arctic cyanobacteria can combat this by using enzymes that are adapted to function at lower temperatures (Morgan-Kiss *et al.*, 2006, Shen *et al.*, 2021). To increase protein flexibility, cold-adapted cyanobacteria will decrease proline, which contains a carbon ring and promotes a rigid structure, or substitute arginine residues with lysine, preventing secondary structure hydrogen

bonds formed with arginine (Christmas *et al.*, 2016). Cold temperatures cause phospholipids to move closer together, compromising membrane fluidity. To combat this, cold-tolerant cyanobacteria have high concentrations of polyunsaturated fatty acids, increasing the space between the molecules, and thus maintaining membrane fluidity (Morgan-Kiss *et al.*, 2006, Shen *et al.*, 2021). Arctic environments also expose cells to freeze-thaw cycles, which can increase the risk of ice crystal formation, and these crystals can disrupt or destroy cell walls and membranes (Vincent, 2007). Polar cyanobacteria inhabiting glaciers, including *Nostoc* and *Phormidesmis*, have been shown to produce ice-binding proteins, which prevent ice recrystallization that can damage cell walls (Christmas *et al.*, 2018, Raymond *et al.*, 2021). An alternative strategy used by Arctic cyanobacteria to prevent ice crystal formation is to produce extracellular polymeric substances (EPS), which reduce the amount of water that comes in direct contact with the cell surface, preventing ice crystal-induced lysis (Vincent, 2007).

2.4.2 Desiccation

Arctic regions are cold deserts, combining low temperatures with low annual precipitation, which risks cellular desiccation (Morgan-Kiss *et al.*, 2006, Goordial, 2021). Additionally, low precipitation and snow cover make cyanobacterial communities more susceptible to temperature fluctuations and freeze-thaw cycles (Christmas *et al.*, 2016, Lim *et al.*, 2020). EPS promotes biofilm formation, which helps cyanobacteria tolerate freeze-thaw cycles and prevent desiccation in extremely cold environments (Christmas *et al.*, 2016).

2.4.3 Osmotic stress

In addition to water scarcity in Arctic environments, the available water at subzero temperatures is usually saline (Lionard *et al.*, 2012, Jungblut & Vincent, 2017), requiring cyanobacteria inhabiting the water to manage their internal water balance to prevent water loss

and plasmolysis. Because solutes are occluded from ice as it freezes, salts get concentrated into hypersaline brines, creating an osmotic stress for the microorganisms living in them (Morgan-Kiss *et al.*, 2006, Jungblut & Vincent, 2017). In sea ice, these brines are up to six times saltier than seawater and can remain liquid at temperatures as low as -12°C (Vincent, 2002). The salinity tolerance of *Nostoc* mats from the Canadian High Arctic was assessed by photosynthetic activity through Chl fluorescence (Lionard *et al.*, 2012) and found that the mats remained photosynthetically active in sodium chloride concentrations 46 times higher than their native lake environment (Lionard *et al.*, 2012). The authors postulate that the EPS surrounding the mats plays a role in buffering external salinities (Lionard *et al.*, 2012). Increased polyunsaturated fatty acids in the cell membrane and photosynthetic machinery were shown in high salt conditions (Sakamoto & Murata, 2002, Morgan-Kiss *et al.*, 2006). While the exact mechanism that explains the role of polyunsaturated fatty acids in cold tolerance is unknown, their ability to maintain membrane fluidity is believed to be a contributing factor (Sakamoto & Murata, 2002).

2.4.4 Solar radiation

While maintaining water balance is essential, Arctic cyanobacteria must also cope with a wide annual range of available daylight. In the summer, 24-hour daylight means that organisms are exposed to high levels of UV radiation, which can create reactive oxygen species that damage proteins and nucleic acids (Morgan-Kiss *et al.*, 2006, Fleming & Castenholz, 2008, Christmas *et al.*, 2016). Cyanobacteria mitigate the stress of high UV radiation during the polar summer by either filtering out or avoiding sunlight. Under high UV stress, cyanobacteria will increase their carotenoid-to-chlorophyll ratio (Morgan-Kiss *et al.*, 2006). Cyanobacterial extracellular EPS can contain protective pigments such as scytonemin or mycosporine-like amino acids, for screening UV radiation (Morgan-Kiss *et al.*, 2006, Fleming & Castenholz, 2008,

Pereira *et al.*, 2015, Christmas *et al.*, 2016, Jungblut *et al.*, 2021). To avoid high UV doses, some microbes will form colonies in which the central part is protected by the surface layers (Kvíděrová, 2018). This growth morphology is seen in microbial mats, soil crusts, and obligate symbiotes such as lichens (Kvíděrová, 2018). Alternatively, organisms can avoid UV radiation by colonizing perennially shaded areas, such as endolithic spaces (Vincent, 2002).

Conversely, cyanobacteria must also survive with zero PAR for several months during the polar winter (Morgan-Kiss *et al.*, 2006). The lack of daylight challenges not only cyanobacteria and other photoautotrophs but also the heterotrophs that rely on their primary production. To tolerate low light levels, cyanobacteria will augment the light-harvesting proteins to maximize light absorption (Morgan-Kiss *et al.*, 2006, Jungblut & Vincent, 2017). Less commonly, some cyanobacteria will acquire carbon heterotrophically under low light conditions (Morgan-Kiss *et al.*, 2006). In nutrient-limited conditions, EPS can also provide a carbon source for the microbial community (Christmas *et al.*, 2016, Kvíděrová, 2018).

2.4.5 Cold-tolerant cyanobacteria

Despite living in polar regions, most cultured cyanobacteria from polar environments grow optimally at temperatures between 15 and 35°C, well above those of their source environment (Vincent, 2002, Christmas *et al.*, 2018). Even so, many of these isolates still exhibit psychrotrophic growth, characterized by optimal growth temperatures above 15°C and maximal growth temperatures above 20°C (Shen *et al.* 2021). While not well characterized in cyanobacteria, some microorganisms also exhibit a psychrophilic lifestyle, which indicates an optimal growth temperature of around 15°C and are unable to grow above 20°C (Shen *et al.* 2021). Psychrotrophs and psychrophiles are often found in persistently cold environments may remain active at lower temperatures, and must survive long-term freezing during the winter

(Vincent, 2002). For example, *Nostoc* from cold environments show persistent viability following continual freezing at -70°C (Holm-Hansen, 1963). It has also been suggested that long periods of freezing and thawing may increase the hardiness of vegetative cells (Holm-Hansen, 1963).

2.5 Cyanobacterial growth and morphologies

Cyanobacteria can have a wide range of metabolic activities and morphologies. For example, most cyanobacteria are photosynthetic but there is a small group known as Melaniabacteria that represents four orders of non-photosynthetic bacteria: Vampiromicrobiales, Gastranaerophilales, Obscuribacterales, and Caenarcaniphiales (Monchamp *et al.*, 2019). In addition, nitrogen fixation occurs in multiple cyanobacterial orders including Synechococcales, Oscillatoriales, Chroococcales, and Nostocales, however, not all members of these orders necessarily fix nitrogen (Chen *et al.*, 2022). There are also different morphologies among cyanobacteria including unicellular, non-heterocystous and heterocystous filamentous strains, which can be associated with metabolic functions (Esteves-Ferreira *et al.*, 2017, Jungblut *et al.*, 2021, Chen *et al.*, 2022). Heterocystous filamentous strains, such as *Nostoc*, also show intercellular differentiation, with the filaments containing vegetative cells, heterocysts (for nitrogen fixation), and akinetes (spore-like cells) (Esteves-Ferreira *et al.*, 2017). Some cyanobacteria, such as the genus *Nostoc*, can exhibit a variety of relationships with other organisms. Many species are free-living, while others, especially diazotrophic species, form facultative or obligate symbiotic relationships with lichen, moss, or plants (Christmas *et al.*, 2018, Huo *et al.*, 2021). They can also grow in close association with unicellular eukaryotes or heterotrophic bacteria that feed off of and adhere to cyanobacterial sheaths (Cornet *et al.*, 2018). Due to these complex relationships between cyanobacteria and other organisms, cyanobacteria

are notably difficult to isolate in pure culture, and most cyanobacterial culture collections accordingly include non-axenic cultures.

2.5.1 Macroscopic microbial mats

In terrestrial environments, filamentous cyanobacteria, like *Nostoc*, can form mat-like macroscopic colonies (**Figure 2.4**) that appear as gelatinous masses and protect cells from desiccation, UV stress, and freeze-thaw cycles. These mats tend to form in the same place annually and form from the same seed population each year (Vincent, 2002, Morgan-Kiss *et al.*, 2006). While these mats are dominated by cyanobacteria, they also host a wide variety of heterotrophic microorganisms that rely on their primary production as a carbon source (Cornet *et al.*, 2018). Within a mat, oxygen saturation decreases from 100% at the surface to 0% at the bottom (Lionard *et al.*, 2012) and pH increases slightly (Lionard *et al.*, 2012). Pigmentation also ranges within mats; sunlight-facing surface layers contain more UV-screening pigments, such as scytonemin, whereas the bottom layers contain more carotenoids, such as zeaxanthin and myxoxanthin (Lionard *et al.*, 2012).



Figure 2.4. *Nostoc* mat in a transient pond from the McGill Arctic Research Station on Axel Heiberg Island, Nunavut, Canada. Macroscopic *Nostoc* colonies are reddish-orange in colour. Sharpie for scale.

2.5.2 Previous studies of cyanobacterial mat communities

Cyanobacterial mats pose a unique interest for research due to their contributions to biogeochemical cycles and their abundant biomass in lake and pond ecosystems. For these reasons, previous studies have characterized cyanobacterial mat communities and their geochemical activities across diverse environments in temperate ecosystems. For example, Lee *et al.* (2018) used metagenomics to analyze the taxonomic and metabolic diversity of hypersaline cyanobacterial mats from California, USA. The authors additionally binned genomes to assess the presence of functional genes for sulphur cycling, nitrogen cycling, phototrophy, autotrophy and heterotrophy. They found that the dominant cyanobacteria in the mats were *Microcoleus*. They also found that there was significant diversity of heterotrophic cycling from Bacterioides mat members (Lee *et al.*, 2018). Another study characterized the diversity of cyanobacteria in mat communities in a Bolivian lake using 16S rRNA amplicon sequencing (Fleming & Prufert-

Bebout, 2010). The authors identified over 400 unique cyanobacterial 16S rRNA sequences, with 37% of them representing a novel species (Fleming & Prufert-Bebout, 2010). More recently, researchers have examined the biogeochemical functioning of cyanobacterial mats in a low-oxygen, sulfidic sinkhole in Lake Huron using metagenomics and metatranscriptomics (Grim *et al.*, 2021). They found that under these low oxygen conditions, the dominant cyanobacteria, *Phormidium* was conducting anoxygenic photosynthesis (Grim *et al.*, 2021). Additionally, they identify that sulphide, oxygen and organic carbon are rapidly cycled among the mat community members (Grim *et al.*, 2021).

Previous studies have also explored cyanobacterial mats in polar environments, though these studies have been more limited in terms of their scope and geographic breadth. In Svalbard, Kvíderová (2018) evaluated the photosynthetic activity of sun and shade-exposed layers within high Arctic *Nostoc* mats. The author found that macroscopic *Nostoc* colonies had heterogeneous cell distribution, with more cells inhabiting the central parts of the colony than the edges. Conversely, photosynthetic activity was higher along the colony edges than the central areas, due to better access to nutrients. Finally, Kvíderová (2018) found that there was little difference in photosynthetic activity between sun and shade-exposed samples, which can be attributed to photoacclimation to a wide range of light conditions. More broadly, metagenomic analysis of cyanobacterial mats from Arctic and Antarctic ice shelves revealed a diverse but largely shared range of stress response strategies including genes involved in DNA replication, protein folding, EPS biosynthesis, and tRNA modification (Varin *et al.*, 2012). Nevertheless, few studies have included metatranscriptomics or other measures of microbial activity to identify the active members of the community and quantitatively compare the relative importance of different cellular processes, and to our knowledge, none have done so for Arctic *Nostoc* mats.

There have been strong efforts to look at photosynthesis and nitrogen fixation of polar cyanobacterial mats. *Nostoc* cultures from Antarctica fixed carbon at temperatures as low as -5°C (Becker, 1982). A more extensive study was conducted using field and laboratory measurements to determine carbon fixation rates for *Nostoc commune* from Antarctica at various temperatures, light levels, and degrees of desiccation (Novis *et al.*, 2007). The authors used this data to model annual carbon fixation rates. They estimated that hydrated terrestrial *Nostoc commune* mats fix $14.5\text{--}21.0\text{ g C m}^{-2}\text{ yr}^{-1}$ (Novis *et al.*, 2007). These estimates are within the range of estimated microbial autotrophic carbon fixation rates, which are between 4.36 and $35\text{ g C m}^{-2}\text{ yr}^{-1}$ (Li *et al.*, 2021). Davey & Marchant (1983) conducted a year-long in situ acetylene reduction experiment on *Nostoc* mats from Victoria Land, Antarctica, noting that nitrogen fixation could occur at temperatures as low as -7°C and that the mats fixed approximately $52\text{ mg N m}^{-2}\text{ yr}^{-1}$. Global nitrogen fixation averages for free-living nitrogen fixation are much higher ranging from $0.35\text{--}11.63\text{ Kg N m}^{-2}\text{ yr}^{-1}$, depending on the environment (Davies-Barnard & Friedlingstein, 2020). While these studies do focus on low temperature carbon and nitrogen fixation of polar cyanobacterial mats, they focus on the southern pole, leaving room for Arctic carbon and nitrogen fixation to be studied.

2.6 Objectives of this thesis

The objectives of this thesis are to identify and characterize the microbial community and the metabolism of macroscopic *Nostoc* microbial mats in the Canadian High Arctic and to determine which members are transcribing genes for carbon and nitrogen cycling, and cold adaptation. Finally, I want to identify the role of *Nostoc* mat communities in carbon and nitrogen cycles to increase our understanding of how climate change affects geochemical cycling in a warming Arctic. The following questions are used to address these objectives:

1. What microorganisms are present and active in Arctic macroscopic *Nostoc* mat communities?
2. What genes for carbon cycling, nitrogen cycling, and cold-tolerance are present and expressed in Arctic *Nostoc* mat communities?
3. What are the lower temperature limits of growth and activity, including photosynthesis and nitrogen fixation, of photoautotrophic members of the Arctic macroscopic *Nostoc* community?

These questions were applied to a macroscopic *Nostoc* mat near the McGill Arctic Research Station on Axel Heiberg Island, Nunavut using metagenomics, metatranscriptomics, and culture-based methods. The metabolic activity of the *Nostoc* mat community was assessed using chlorophyll fluorescence to measure photosynthesis, and acetylene reduction to measure nitrogen fixation. Photosynthetic members of the *Nostoc* mat community, cryoconite material, cryptoendoliths, and microbial mats from outflow channels of hypersaline springs were isolated and their growth characteristics at various temperatures, and salinities were determined.

Chapter 3. Investigating High Arctic *Nostoc* mats low-temperature carbon and nitrogen fixation through culture-independent and -dependent methods

Authors: Melissa H. Kozey¹, Scott Sugden¹, Christina Davis¹, and Lyle G. Whyte¹

Department of Natural Resource Sciences, McGill University, Sainte-Anne-de-Bellevue, QC, Canada

3.1 Abstract

Arctic ecosystems face unique environmental pressures, as they are warming faster than the rest of the planet. Even with aggressive changes to greenhouse gas (GHG) emissions, the Arctic is expected to see a 4°C annual temperature increase by 2050, which can cause significant disruptions to the environment, including permafrost thaw and glacial and sea ice melt. Because of the close relationship between ambient temperature and microbial activity, the threat of warming Arctic environments has raised additional concerns regarding microbial contributions to GHG emissions. Many cold-adapted organisms remain active at sub-zero temperatures, contributing to both carbon and nitrogen flux in Arctic ecosystems. Cyanobacteria are uniquely qualified for the study of biogeochemical cycles in the Arctic, as they are one of the few taxa capable of both carbon and nitrogen fixation and they are important primary producers in High Arctic environments. For this reason, a detailed knowledge of the biogeochemical activity of Arctic cyanobacteria can contribute to a more general understanding of Arctic carbon and nitrogen cycling. Here, we used metagenomic and metatranscriptomic analyses of an Arctic *Nostoc* mat to explore cold tolerance mechanisms and carbon and nitrogen cycling of the mat. The *Nostoc* mat community utilized a wide variety of cold-tolerance genes to withstand Arctic environments, favouring membrane and peptidoglycan repair and cold-shock, stress and heat shock protein production. Within the mat community, *Nostoc* was responsible for most

photosynthesis and nitrogen fixation, as indicated by the relative transcriptional activity. To gain more insights into cold-tolerance in *Nostoc* mats, five photoautotrophs were cultured from the mat and evaluated for cold growth and salt tolerance. Four of the five cultures showed a psychrotrophic lifestyle, with one capable of growth as low as -5°C . To further evaluate *Nostoc* mat's role in carbon and nitrogen fixation at low temperatures, chlorophyll fluorescence, and acetylene reduction experiments were conducted. Chlorophyll fluorescence of the five cyanobacterial isolates and a mixed culture from the *Nostoc* mat showed that Arctic photoautotrophs can be photosynthetically active at low temperatures. An acetylene reduction assay of a mixed culture of the Arctic *Nostoc* mat showed no evidence of nitrogen fixation, likely due to cell photobleaching early in the experiment. Arctic *Nostoc* mats are key members of Arctic carbon and nitrogen cycles as demonstrated by their transcriptional activity. Additionally, we see evidence that mat members are photosynthesizing at low and sub-zero temperatures, which should be included in modelling when examining Arctic carbon cycling.

3.2 Introduction

Polar environments are home to the most extreme conditions on Earth, with extremely low temperatures and low annual precipitation (Goordial *et al.*, 2013). Despite the harsh environment, microorganisms persist throughout polar environments (Morgan-Kiss *et al.*, 2006, Goordial *et al.*, 2013). To survive in Arctic conditions, microorganisms need to adapt to tolerate cold temperatures, high salt concentrations, desiccation, ultraviolet radiation, and freeze-thaw cycles (Jungblut & Vincent, 2017). However, the resilience of these microorganisms will be tested under the threat of the climate crisis. Arctic regions face unique challenges when it comes to climate change, as they are warming faster than the rest of the planet (Moon *et al.*, 2018,

Overland *et al.*, 2019), resulting in more frequent freeze-thaw cycles and changes to microbial diversity (Becker & Pushkareva, 2023). Additionally, Arctic temperature increases are expected to increase microbial greenhouse gas emissions (Nikrad *et al.*, 2016).

The extreme climate of polar ecosystems makes vegetation sparse, creating a niche that must be filled by other means of primary production. Microbial photoautotrophs, including cyanobacteria and green algae, fill this niche. A common photoautotrophic genus found in Arctic environments is *Nostoc*, a heterocystous filamentous cyanobacteria that forms macroscopic microbial mats that are often found in lakes, streams, glaciers and transient ponds on the Arctic tundra soils (Jungblut & Vincent, 2017). *Nostoc* mats typically form in the same place and from the same seed populations annually, which allows them to accrue large amounts of biomass (Vincent, 2002). While these mats are predominately made up of photoautotrophic *Nostoc*, heterotrophs are present in the community, feeding off the products of *Nostoc*'s primary production (Cornet *et al.*, 2018). To survive the harsh Arctic climate, mat members may produce cold-shock proteins, alter their membrane lipids and peptidoglycan proteins, produce extracellular polymeric substances (EPS), synthesize carotenoids, and produce DNA replication and repair enzymes (Morgan-Kiss *et al.*, 2006, Mykytczuk *et al.*, 2013, Jungblut & Vincent, 2017).

In addition to their ability to tolerate the harsh conditions of the Arctic, *Nostoc* belongs to a unique group of organisms that are capable of both carbon and nitrogen fixation. This combined with their prevalence and the low abundance of plants in Arctic environments make *Nostoc* important for studying carbon and nitrogen fixation and their relationship to Arctic carbon and nitrogen cycles. The ongoing threat of warming temperatures in the Arctic makes improving our understanding of biogeochemical cycles and microbial contributions to them imperative to

gaining insight into how these cycles will change moving forward. Previous work has shown that Antarctic *Nostoc* mats were able to fix carbon as low as -5°C and nitrogen as low as -7.6°C (Becker, 1982, Davey & Marchant, 1983). However, the extent of cyanobacterial sub-zero activity and how it will respond to future warming remains poorly understood.

Field and laboratory measurements of the annual carbon and nitrogen fixation rates of Antarctic *Nostoc* mats estimate $14.5\text{--}21.0\text{ g C m}^{-2}\text{ yr}^{-1}$ and $52\text{ mg N m}^{-2}\text{ yr}^{-1}$, respectively (Davey & Marchant, 1983, Novis *et al.*, 2007). More recently, metagenomics and metatranscriptomics have been utilized to better understand community structures and activity of difficult to culture areas, such as polar environments. This has included several metagenomic studies of non-polar cyanobacterial mats in California, Bolivia, and Lake Huron (Fleming & Prufert-Bebout, 2010, Lee *et al.*, 2018, Grim *et al.*, 2021). A metagenomic study has also explored cold stress strategies of cyanobacterial mats from Arctic and Antarctic ice shelves, finding genes involved in DNA replication, protein folding, EPS biosynthesis, and tRNA modification (Varin *et al.*, 2012). Nevertheless, Arctic *Nostoc* mats remain underrepresented and there are very few studies that have included metatranscriptomics or other measures of microbial activity to identify the active members of the community and quantitatively compare the relative importance of different cold tolerance mechanisms and selected metabolic processes.

Here, we used metagenomics and metatranscriptomics to explore the genetic basis of *Nostoc* mat survival in Arctic environments and compare the relative activities of different mat members involved in carbon and nitrogen fixation. We supported these *in situ* results by isolating five cyanobacterial and algal photoautotrophs from a *Nostoc* mat community, characterizing their growth at a range of temperatures and salinities characteristic of arctic environments, and using

chlorophyll fluorescence and acetylene reduction assays to quantify their carbon- and nitrogen-fixation activities under cold conditions.

3.3 Materials and Methods

3.3.1 Sample collection

Sampling was conducted at the McGill Arctic Research Station (MARS) (N79°22', W90°46'), Axel Heiberg Island (AHI), Nunavut, Canada, in the summer of 2023. A macroscopic *Nostoc* mat was visually identified and selected for sampling in the 2023 field season (**Figure 3.1**). In 2023, the *Nostoc* mats were hydrated in transient ponds, so a portion of the mat was collected and stored in water from its source pool for culturing, while another portion was collected in DNA/RNA shield (Zymo Research, Irvine, CA, USA) for metagenomic and metatranscriptomic sequencing. Physical measurements of the transient pond containing a visible *Nostoc* mat as well as a control pond with no visible mat were measured, including temperature, pH, and dissolved oxygen (DO) (Pico-O₂ probe with OXROB3-SUB probe; PyroScience, Aachen, Germany) (**Table 3.1**). Additionally, the nitrogen content of the ponds was measured using the CHEMetrics kits for ammonia, nitrate, and nitrite (K-1503, K-6933, and K-7003, respectively) (AquaPhoenix Scientific, Hanover, PA, USA) (**Table 3.1**).

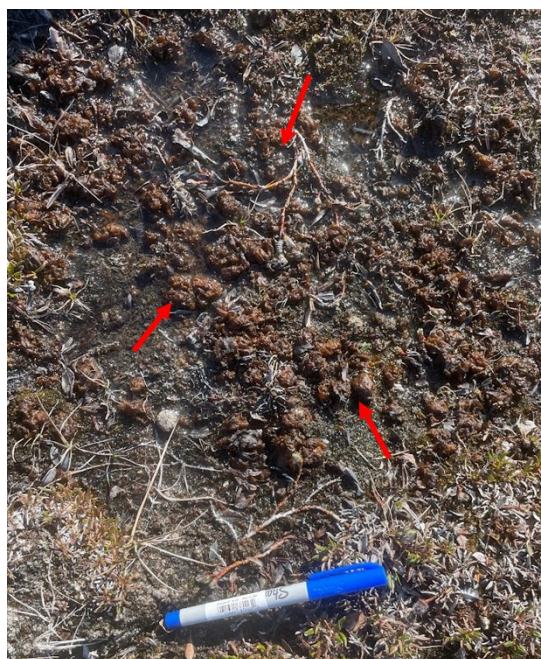


Figure 3.1. *Nostoc* mat in a transient pond on Axel Heiberg Island, Nunavut, Canada. Red arrows point to the macroscopic *Nostoc* colonies.

Table 3.1 Physical measurements of 2023 *Nostoc* and control ponds from Axel Heiberg Island, Nunavut

	Temperature (°C)	pH	DO (ppm)	Ammonia (ppm)	Nitrate (ppm)	Nitrite (ppm)
<i>Nostoc</i>	12.0	6	10.20	2.331	3.061	Below Detection
Control	13.9	6	11.77	1.379	2.701	0.028

3.3.2 Nucleic acid extraction and sequencing of an Arctic *Nostoc* mat community

We used metagenomic and metatranscriptomic sequencing to identify cold-tolerance mechanisms and the presence and expression of carbon fixation and methane and nitrogen cycling-related genes in the *Nostoc* mat community. For these analyses, DNA and RNA were extracted from the 2023 *Nostoc* mat sample using the ZymoBIOMICS DNA/RNA Miniprep Kit (Zymo Research, Irvine, CA, USA). We prepared a metagenome using 1 ng of input DNA, measured by Qubit High Sensitivity dsDNA Assay (ThermoFisher Scientific, Waltham, MA, USA), with 12 PCR cycles with the Nextera XT DNA library Prep kit (Illumina, San Diego, CA,

USA), according to the associated documentation. For the metatranscriptome, rRNA was depleted from 253 ng of input RNA, measured by Qubit High Sensitivity RNA Assay (ThermoFisher Scientific, Waltham, MA, USA), using the NEBNext rRNA Depletion kit v2 and then cDNA synthesis and library preparation were performed with 16 PCR cycles using the NEBNext Ultra RNA Library Prep Kit for Illumina (New England Biolabs, Ipswich, MA, USA) following the protocol for degraded RNA, which involves no additional RNA fragmentation. The metagenome and metatranscriptome were sequenced using the NovaSeq X platform (Illumina, San Diego, CA, USA) (2x150bp) at The Center for Applied Genomics (Toronto, ON, Canada).

3.3.3 *Metagenomic and metatranscriptomic bioinformatic analyses of a High Arctic Nostoc mat community*

To convert raw DNA and cDNA reads into interpretable data, bioinformatic analyses were needed to clean reads, assign taxonomies, assemble contigs, annotate genes, generate bins, and count annotations and transcripts. Adapters and reads were trimmed using Trimmomatic (v.0.39) (parameters: Leading: 3, Trailing: 3, Sliding Window: 4:15, Min len: 36) (Bolger *et al.*, 2014). The metagenomic reads were assigned taxonomies using Kaiju (v.1.10.1) using the nr-euk_2023-05-10 database (Menzel *et al.*, 2016). Metagenomic reads were then assembled into contigs using megahit (v.1.2.9) using default parameters (Li *et al.*, 2015). The contigs from the assembly were also assigned taxonomies using Kaiju (v.1.10.1) using the nr-euk_2023-05-10 database (Menzel *et al.*, 2016). Bowtie2 (v.2.5.1) was then used to align the reads back to the assembly. The assembly was annotated against the KEGG, COG, and TIGRFAM databases using the Joint Genome Institute IMG/M Annotation pipeline (v.5.2.1) (Chen *et al.*, 2019). The contigs were then assigned to bins generating metagenome assembled genomes (MAGs) using metabat2 (v.2.14) (Kang *et al.*, 2019) and the quality and contamination of the resulting MAGs were

determined using CheckM2 (v.1.0.1) using the uniref100.KO.1 database (Chklovski *et al.*, 2023). MAGs were classified using GTDBtk (v.2.3.2) with the GTDBtk release 214 database (Chaumeil *et al.*, 2019). Only bins assigned to Cyanobacteriota that were considered high or medium quality according to previously established thresholds for completeness and contamination (Bowers *et al.*, 2017) were used for further analyses. Gene copy and transcript copy numbers for the MAGs were pulled from the MAG-specific contigs determined based on the Bowtie2 alignments to the contigs of the metagenome assembly. Gene copy number was counted and copies per million (CPM) was calculated for normalization. Selected genes of interest, and their associated categories, for cold tolerance were adapted from Raymond-Bouchard *et al.* (2018; Table 3) (**Table S1**). Selected marker genes for carbon fixation, including components of the photosynthetic apparatus, as well as methanogenesis and methanotrophy were determined from KEGG pathways (**Table S2**). Additionally, we selected marker genes for different components of the nitrogen cycle, including nitrogen fixation, denitrification, nitrification, and nitrate reduction based on KEGG pathways (**Table S2**). These genes were used to determine the genetic potential that the *Nostoc* mats have for these processes.

For the metatranscriptome, reads identified as 16S rRNA sequences were removed using sortmeRNA (v.4.3.6). Common human contaminants were then removed from the dataset using BBMap: Remove Human (v.38.86) (Bushnell). The reads were then classified using Kaiju (v.1.10.1) using the nr-euk_2023-05-10 (Menzel *et al.*, 2016), then aligned to the metagenome assembly with Bowtie2 (v.2.5.1), and counted with htseq (v.2.0.2). To normalize raw read counts transcripts per million (TPM) was calculated, accounting for gene length, and then evaluated the transcriptional activity of the selected genes for cold tolerance (**Table S1**) and carbon and nitrogen cycling (**Table S2**) to determine the *Nostoc* mat's transcriptional activity.

3.3.4 *In situ* gas flux analyses of High Arctic *Nostoc* mats

In situ gas flux measurements were obtained to determine the *Nostoc* mat's role in CO₂ and CH₄ flux. We measured *in situ* CO₂ and CH₄ gas flux at three sites containing visible *Nostoc* mats, and three adjacent control sites with no visible mats, using a LI-COR LI-7810 (LI-COR, Lincon, NE, USA) in July 2024. The mats were desiccated when we arrived for the 2024 field season, so we rehydrated them with 13-15 L of water from Colour Lake (N79°25', W90°45') over three days before measuring gas flux, but the control sites were not. Because *Nostoc* mats contained a large amount of photoautotrophic biomass, gas flux measurements were performed using a clear chamber (**Figure S1**) and using the LI-COR Smart chamber 8200-01 (LI-COR, Lincon, NE, USA) to see if a clear chamber would improve measurements when working with photosynthetic samples, as the dark chamber blocks sunlight, and may inhibit photosynthesis. All measurements were completed in triplicate with a 30-second deadband, 5-minute measurement, and 30-second ventilation period between replicates. Physical parameters of each site can be seen in **Table 3.2** and images of each site can be found in **Figure S2**. A linear regression model for CO₂ and CH₄ for each replicate, generating a gas flux coefficient, which was then used in the following equation to obtain the gas flux in µmol per m² per second:

$$\mu\text{mol C} / \text{m}^2 / \text{s} = \frac{\text{Coefficient} * (\text{Chamber} + \text{IRGA} + \text{tubing} + \text{collar volume})}{22.4 * 10^{-3} * \left(\frac{173}{\text{Air temperature}}\right)} * \frac{1}{\text{Collar area}}$$

The resulting value was then converted to grams of carbon per m² per day. The difference between groups was determined using Welch's two-sample t-tests, with a 95% confidence interval.

Table 3.2. Site locations and conditions at the time of *in situ* gas flux measurements of High Arctic *Nostoc* mats

Site	Coordinates	Soil Temperature (°C)		Light (lux)
		Closed Chamber	Clear Chamber	
N1	N79°24'52.67" W090°45'00.57"	6	5.6	27 900
N2	N79°24'52.33" W090°44'59.16"	6.8	6.9	11 700
N3	N79°24'52.78" W090°45'02.44"	6.5	6.4	33 400
C1	N79°24'52.83" W090°45'00.27"	6.3	6.3	16 300
C2	N79°24'52.05" W090°44'59.94"	8.1	7.9	7 390
C3	N79°24'52.65" W090°45'03.11"	5.5	5.7	22 000

3.3.5 Culturing and isolation of High Arctic photoautotrophs

To gain further insights into the growth and survival of *Nostoc* mat photoautotrophs, we aimed to isolate photoautotrophic members of the mats and assessed their ability to grow in subzero and cold temperatures and various salinities, conditions commonly found in High Arctic environments (Jungblut & Vincent, 2017). All cultures were started from the 2023 MARS *Nostoc* mat sample (MNM) and grown on BG11 agar at 15°C under light. Samples were incubated in different incubators, and while the same grow lights were used in each incubator, the size of the incubator and distance from samples varied for each, in addition to cold temperatures affecting the electronics of the light, reducing light intensity. For this reason,

specific lighting conditions of the incubators can be seen in **Table 3.3**. Five morphologically unique colonies, as determined by colony morphology and light microscopy, were selected for serial subculture. This was continued until there was only one dominant, green-pigmented morphology per culture. Any further attempts to isolate for an axenic culture were unsuccessful.

To contextualize the broader photoautotroph community relative to these five cultures from the *Nostoc* mat, we followed a similar procedure to isolate a total of 14 additional photoautotrophs from four adjacent High Arctic environments. Additional culturing occurred from four Arctic environments previously demonstrated to host cyanobacteria and other photoautotrophs. Cultures were grown from a Gypsym Hill endolithic community (GHE) (Ziolkowski *et al.*, 2013), white and green pigmented microbial mats along the outflow channels from the Gypsym Hill perennial springs microbial (GHSWM, for white mats; GHSGM; for green mats) (Sapers *et al.*, 2017), cryoconite material from White glacier (WGCM) (Christmas *et al.*, 2016), and finally, from deglaciated soil collected from approximately 50 meters from the front of White Glacier (WGF) (Knelman *et al.*, 2021) (**Figure S3**). Cultures were cultured into non-axenic samples as described above.

Each of the five non-axenic *Nostoc* mat cultures, in addition to the 14 cultures from adjacent Arctic environments was examined for their ability to grow at various temperatures and salinities, as well as their ability to grow in nitrogen-free conditions. Cultures were grown on BG11 at -10, -5, 0, 5, 15 and 25°C to determine optimal temperature ranges and their subzero growth capabilities. Cultures were also grown on BG11 containing 0-10% NaCl (in 2.5% increments) to determine salinity tolerance. Finally, cultures were grown on nitrogen-free BG11 (BG11₀) to identify if they could grow in nitrogen-free conditions. The salinity and BG11₀ tests were carried out at 5°C, as it is a common summer temperature in the Canadian High Arctic

(WeatherSpark), except for cultures that could not grow at 5°C, which were grown at 15°C. All culture experiments were carried out under light, but due to differences in incubator sizes and efficiency of grow lights at cold temperatures, lighting conditions were not consistent at all temperatures (**Table 3.3**).

Table 3.3. Light levels of incubators

Temperature (°C)	Light	
	lux	μmol/s/m ²
25	2640	45.5
15	3990	68.76
5	2820	48.6
0	3590	61.87
-5	1620	27.92
-10	246	4.24

Because we could not obtain axenic cultures, we identified the dominant photoautotrophs in our five non-axenic *Nostoc* mat cultures and 14 environmental cultures using 16S and 18S rRNA gene amplicon sequencing. Amplicons were prepared using colony PCR with the 515F and 926R primers for 16S rRNA (Quince *et al.*, 2011, Parada *et al.*, 2016) and E572F and E1009R primers for 18S rRNA (Comeau *et al.*, 2011). Reactions were performed with the KAPA HiFi HotStart PCR kit (Roche, Basel, Switzerland) manufactures instructions with 25 amplification cycles. The resulting amplicons were then indexed using the Nextera XT Index primers (Illumina, San Diego, CA, USA) and the KAPA HiFi HotStart PCR kit (Roche, Basel, Switzerland) according to manufacturer instructions with 8 amplification steps. Prepared libraries were sequenced on a MiSeq platform (Illumina, San Diego, CA, USA) (2x300bp), and the resulting sequences were analyzed using the DADA2 pipeline (v.4.2.2) (Callahan *et al.*, 2016). Quality-trimmed, denoised sequences were clustered into OTUs with 97% similarity using DECIPHER (v.3.0.0) (Wright, 2016). The 16s rRNA and 18s rRNA OTUs were then

classified using the Silva nr database (v.132). The taxonomy of each non-axenic culture was assigned one taxonomic identity using the most abundant photoautotrophic OTU and confirming based on cell morphology from microscope images.

3.3.6 *Chlorophyll fluorescence assay of High Arctic Nostoc mat cultures*

Chlorophyll fluorescence imaging was used to determine if the photoautotrophic cultures were capable of photosynthesis at cold and sub-zero temperatures. Photosynthetic activity of our five non-axenic MNM isolates, as well as a mixed culture of the 2023 MARS *Nostoc* mat, using a chlorophyll fluorescence assay conducted at five different temperatures (−10, −5, 0, 5, and 15°C). The six cultures were first grown in BG11 at 15°C under light (**Table 3.3**) until visibly dense. For the fluorescence assay, we created a 3:1 culture-glycerol mixture for each culture to ensure the media remained liquid at sub-zero temperatures. The culture mixtures were then added to black-walled 96-well plates, with one plate per incubation temperature and 6 wells per plate for each culture type. Plates were sealed with an optically clear plate film and stored at their respective temperatures to acclimate under light (**Table 3.3**) for 7 days.

Chlorophyll fluorescence measurements were modified from (Ogawa & Sonoike, 2016), using the PSI Plant Screen SC System Multispectral Fluorescence Imaging Station (Photon Systems Instruments, Drásov, Czechia). Culture plates were placed in the dark at their respective incubation temperatures for one hour before measurement and then kept on ice with a black non-reflective background during measurement. The minimum fluorescence under oxidized plastoquinone (PQ) pool conditions (F_o) was measured after 5 mins of illumination ($70 \mu\text{mol m}^{-2} \text{s}^{-1}$) with blue lights peaking at 460 nm. The maximum fluorescence determined under oxidized PQ pool conditions (F_m) was measured in the presence of 20 μM DCMU under

illumination with actinic light peaking at 660 nm. The difference between F_m and F_o (F_v) is used to calculate the maximum quantum yield of PSII (F_v/F_m). A linear regression model was used to determine if the F_v/F_m was linearly correlated to temperature for each sample.

3.3.7 Acetylene reduction assay of a High Arctic mixed *Nostoc* mat culture

To assess the nitrogen fixation rates of the *Nostoc* mat at cold and subzero temperatures (-10 , -5 , 0 , 5 , and 15°C), we conducted an acetylene reduction assay. Due to resource limitations, this assay was only conducted on a mixed culture of the *Nostoc* mat, and not on the five non-axenic cultures. A mixed culture from the *Nostoc* mat collected in 2023 was grown shaking in BG11 at 15°C under light (**Table 3.3**) until visibly dense. The mixed culture was then spun down (10 minutes at $2599 \times g$), the supernatant was removed, and cells were washed with BG11_o twice. The culture was then resuspended in a 3:1 mixture of BG11_o and glycerol, to maintain a liquid state at sub-zero temperatures. 5 mL of culture-glycerol mixture was added to 30 mL serum bottles in triplicate and left to acclimate to its assay temperature for 15 days. Once acclimated, the acetylene reduction assay protocol was completed according to Stewart *et al.* (1967), David *et al.* (1980), and Capone (1993). Negative controls were prepared without biomass to determine if any non-biological acetylene reduction occurred. Samples and controls were incubated at 5 different temperatures (-10 , -5 , 0 , 5 , and 15°C) under light (**Table 3.3**). Samples were destructively sampled over 6 months at 0, 30, 60, 90, and 180 days.

A standard curve was prepared using dilutions of ethylene gas in nitrogen-free air (78% Ar, 22% O₂, and 0.004% CO₂) (**Figure S4**). Ethylene production was measured using the SRI instruments 8610C gas chromatograph (SRI Instruments, Torrance, CA, USA), with the Porapak R column (Waters, Milford, MA, USA) (Oven temperature = 60°C), Flame Ionization Detector

(low sensitivity, temperature = 300°C, H₂ flow rate = 60 ml/min), and N₂ as a carrier gas (flow rate = 25 ml/min), with an injection volume of 0.5 mL. Three technical replicates were measured for each sample.

The ethylene produced was determined by calculating the nmol of ethylene per mL using the equation derived from the standard curve, and then multiplying it by the headspace of the vial. Biological ethylene production was determined by subtracting the amount of ethylene produced in the control from the ethylene produced from the mat samples at each temperature. The biological ethylene production was then normalized by dry biomass. In order to ensure our data was normally distributed while maintaining negative values, the resulting values were transformed with a cube root and the average and standard deviation were calculated. A two-way ANOVA was used to if there was significant variance in the cube root of ethylene produced per gram of cells between temperatures and time.

3.4 Results

3.4.1 *Metagenomic and metatranscriptomic sequencing of a High Arctic Nostoc mat community*

Sequencing of the Axel Heiberg Island *Nostoc* mat produced 329,522,485 quality-filtered metagenomic paired reads, which resulted in 8,315,956 contigs with an N50 of 633, (**Table S3**), and 74,803,950 metatranscriptomic paired reads. Any reference to these samples from this point forward will include AHI, based on the location of the sample collected, Axel Heiberg Island, as a prefix for clarity. The AHI metagenome revealed that Proteobacteria made up the largest classified proportion of the DNA reads and metagenome assembly, comprising 32% and 44% respectively (**Figure 3.2**). This was followed by Cyanobacteriota, which represented 18% of

DNA reads and 4% of the AHI metagenome assembly. Notably, contigs assigned to *Nostoc* represented only 0.73% of the metagenome assembly but 12% of the quality-trimmed reads that could be classified as a genus. Other abundant genera included *Sphingomonas* (6%), and *Brevundimonas* (5%). Conversely, Cyanobacteriota accounted for the vast majority of AHI

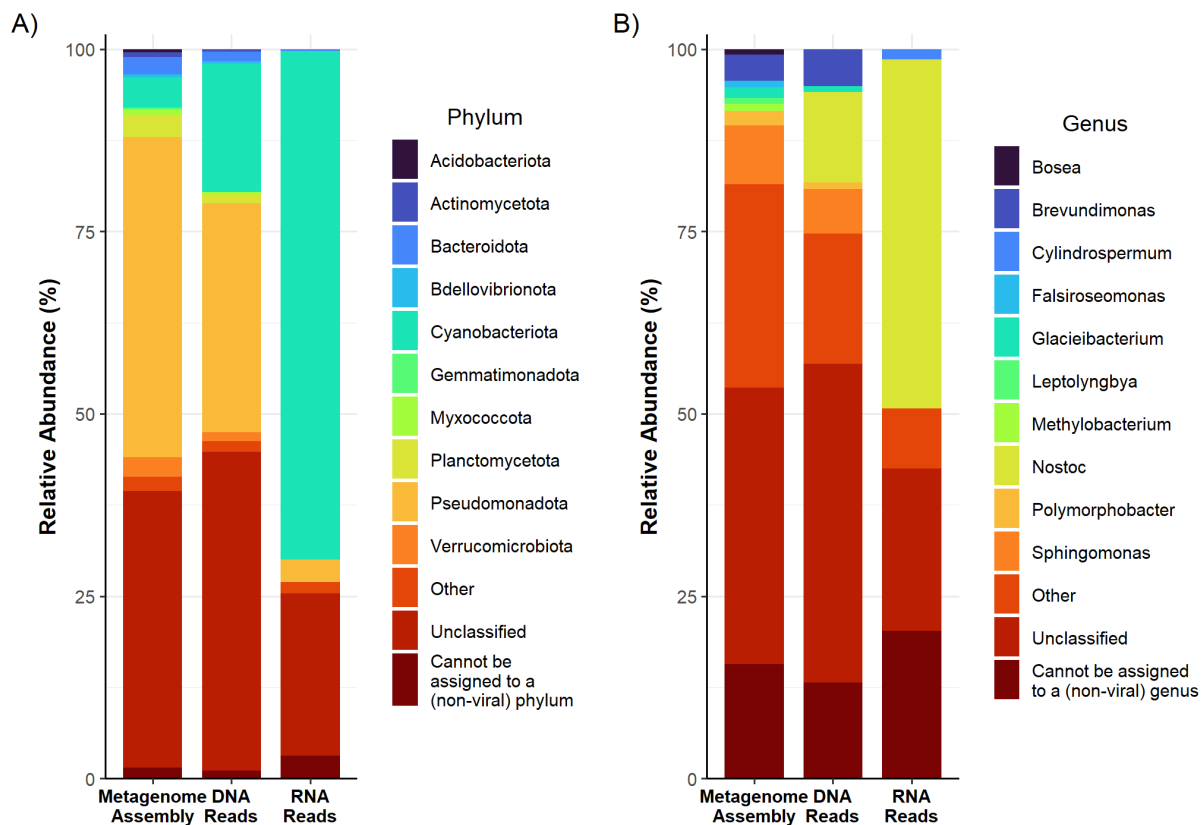


Figure 3.2. Community structure and activity of a *Nostoc* mat from Axel Heiberg Island, Nunavut, Canada. A) By phylum. Phyla that represented less than 0.25% of the community were grouped into the "Other" category. B) By genus. Genera that represented less than 0.75% of the community were grouped into the "Other" category.

mRNA reads, representing 70% of the classified reads, followed by Pseudomonadota at 3% of the reads. Interestingly, the only genera whose transcripts exceeded 0.75% relative abundance among classified AHI mRNA reads were *Nostoc* (48%) and *Cylindrospermum* (1.4%), both of which are members of Cyanobacteriota.

When we analyzed known cold adaptation genes, we found that all the tested genes were present in the AHI metagenome (**Figure 3.3**). Of the tested cold adaptation groups, genes for membrane and peptidoglycan alteration were the most abundant, with the glycosyltransferase involved in cell wall biosynthesis being the most abundant gene in the entire AHI metagenome. This was followed by transcription and translation factors, in which translation elongation factor EF-G (GTPase) was the most abundant. Genes for toxin/antitoxin modules were the least abundant of the cold adaption gene groups.

Transcripts indicated that genes for cold shock, stress, and heat shock proteins (HSP) were the most highly expressed cold adaptation genes detected in the AHI metatranscriptome. Of these genes, the molecular chaperone DnaK (HSP70) was the mostly highly expressed gene from the AHI metatranscriptome. Another highly expressed cold shock, stress, and HSP protein was chaperonin GroEL (HSP60 family). Most of the cold adaptation genes were expressed to some degree in the AHI metatranscriptome, except for the genes for Na⁺/proline symporter, trehalose-6-phosphatase, antitoxin component of RelBE or YafQ-DinJ, RecA-superfamily ATPase (KaiC/GvpD/RAD55 family), RecA/RadA recombinase, and tRNA A37 threonylcarbamoyladenine dehydratase.

The AHI metagenome and selected bins were also screened for marker genes important for carbon fixation, methane cycling, and nitrogen-cycling pathways (**Figure 3.4**). All tested genes were present in the AHI metagenome, except for the marker gene for methanogenesis, *mcrA*. The most abundant carbon fixation gene in the metagenome was for RuBisCO, which is involved in the Calvin-Benson-Bassham cycle (*rbcL*), followed by genes for photosystem II (PSII) (*psbA*) and photosystem I (PSI) (*psaA*). With the exception of methanotrophy (*mmoX*), all the genes for carbon fixation and methane cycling that were present in the metagenome were detected in the

AHI metatranscriptome. The most abundant gene for nitrogen cycling was for assimilatory nitrate reduction (*nasA*). However, nitrogen fixation (*nifH*) had the highest expression of the nitrogen cycling genes. Some denitrification (*nirK*) and nitrification (*amoA*) genes were present in the AHI metagenome, but not measurably expressed.

3.4.2 Analyses of cyanobacterial MAGs from a High Arctic *Nostoc* mat metagenome

We retrieved three medium-quality metagenome-assembled genomes (MAGs) from Cyanobacteriota species present in the mat. Bin 1 (67% completeness, 0.19% contamination) was identified as an unknown member of the Vampiromicrobiales order by GTDBtk (Chaumeil *et al.*, 2019). Bin 2 (84% completeness, 3% contamination) was identified as *Nostoc* sp. WHI, and Bin 3 (57% completeness, 0.11% contamination) was identified as a *Stenomitos* sp. These three bins were chosen for further analysis of genes involved in cold tolerance, carbon fixation, and methane- and nitrogen-cycling activities with respect to the mat community represented by the metagenome assembly.

In Bin 1 (Vampiromicrobiales), the most abundant cold adaptation gene was the glycosyltransferase involved in cell wall biosynthesis, but this bin had a total of 16 cold adaptation genes from all nine categories (**Figure 3.3**). However, the only cold adaptation gene expressed from this bin was chaperonin GroEL (HSP60 family), which accounted for 0.05% of this gene's total transcripts in the AHI metatranscriptome.

The AHI *Nostoc* sp. WHI bin (Bin 2) contained 25 cold adaptation genes across all nine categories (**Figure 3.3**). Of these genes, the most abundant and expressed gene was the glycosyltransferase involved in cell wall biosynthesis. Notably, Bin 2 was the most transcriptionally active of the three Cyanobacteriota bins we evaluated. Twenty-one cold

adaptation genes were transcribed by this MAG, with six representing over 50% of the total metatranscriptome transcripts for the corresponding gene. These genes included molecular chaperone GrpE (HSP) (84%), Rad-3-related DNA helicase (57%), 3-oxoacyl-[acyl-carrier protein] synthase (66%), glycosyltransferase involved in cell wall biosynthesis (58%), beta-carotene biosynthesis (CrtB) (90%), and thioredoxin reductase (67%).

Bin 3, *Stenomitos* sp., contained 17 cold adaptation genes from all nine categories (**Figure 3.3**). As with the other two bins, the most abundant of the cold adaptation genes was for glycosyltransferase involved in cell wall biosynthesis. The cold adaptation genes that were expressed by Bin 3 were translation elongation factor EF-G (GTPase), 3-oxoacyl-[acyl-carrier protein] synthase, glycosyltransferase involved in cell wall biosynthesis, and DNA gyrase/topoisomerase I, of which glycosyltransferase was the most highly expressed (**Figure 3.3**).

AHI Vampiiovibrionales (Bin 1) did not have any of the selected genes for carbon fixation or methane cycling, whereas Bin 2 (AHI *Nostoc* sp. WHI) contained genes for the photosynthetic apparatus including PSII (*psbA*), PSI (*psaA*), cytochrome b6/f complex (*petB*), and the phycobilisome protein phycocyanin (*cpcA*), but the gene for carbon fixation (*rbcL*) was absent (**Figure 3.4**). All these genes were also expressed in Bin 2 and accounted for over half of each gene's transcripts in the metatranscriptome. The *Stenomitos* sp. bin (Bin 3) only had genes for PSII (*psbA*) and phycocyanin (*cpcA*), and only the gene for phycocyanin was expressed. Nitrogen fixation (*nifH*) in AHI *Nostoc* sp. WHI (Bin 2) was the only nitrogen-cycling gene present in any of the bins. AHI *Nostoc* sp. WHI accounted for 98% of the *nifH* transcripts in the AHI metatranscriptome.

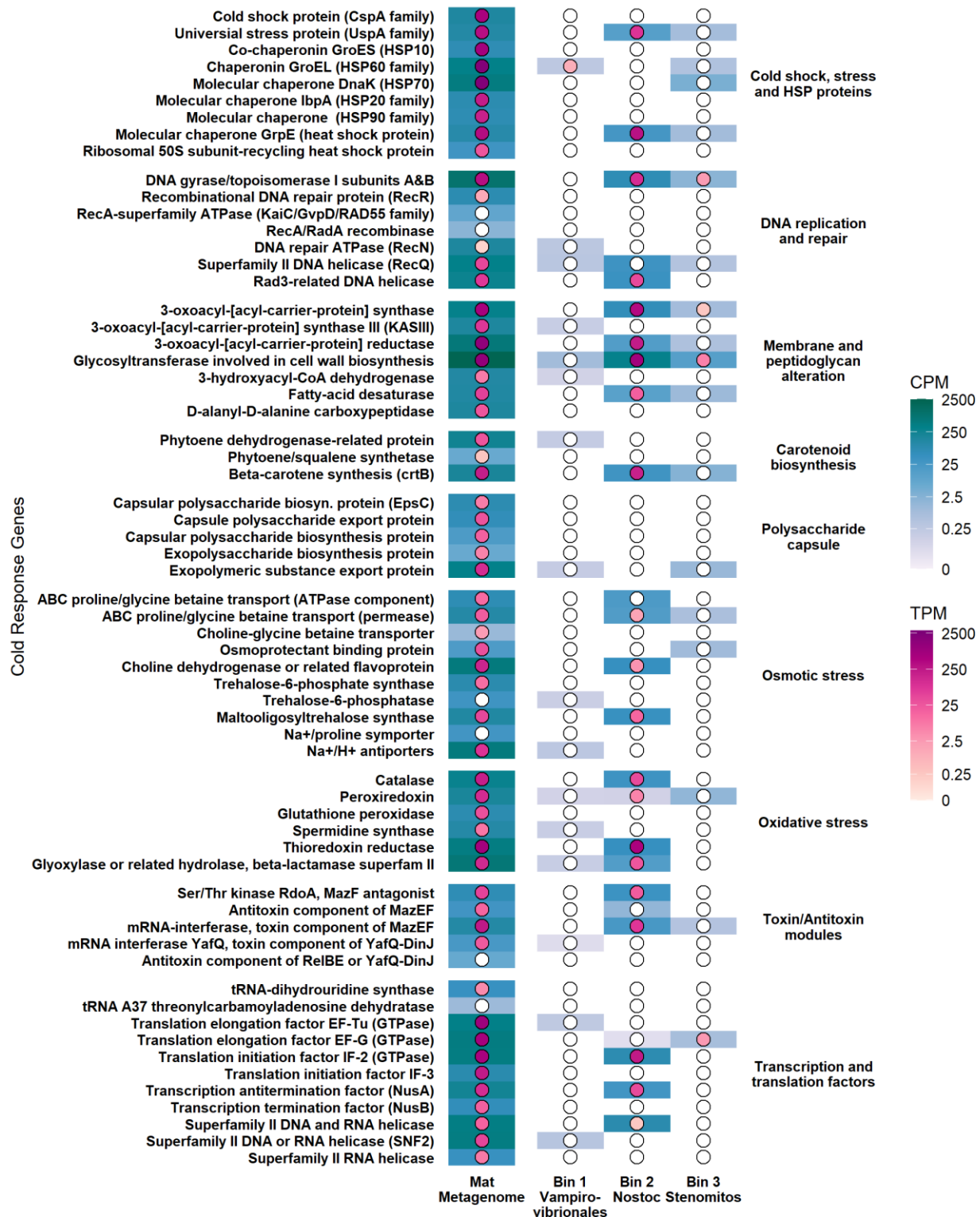


Figure 3.3. The presence and expression of cold adaptation genes in a *Nostoc* mat metagenome from Axel Heiberg Island, Nunavut, Canada, and the associated cyanobacterial metagenome-assembled genomes. Gene abundances are shown as counts per million (CPM) in the rectangles in the background, and transcript abundances are shown as transcripts per million (TPM) in the circles in the foreground.

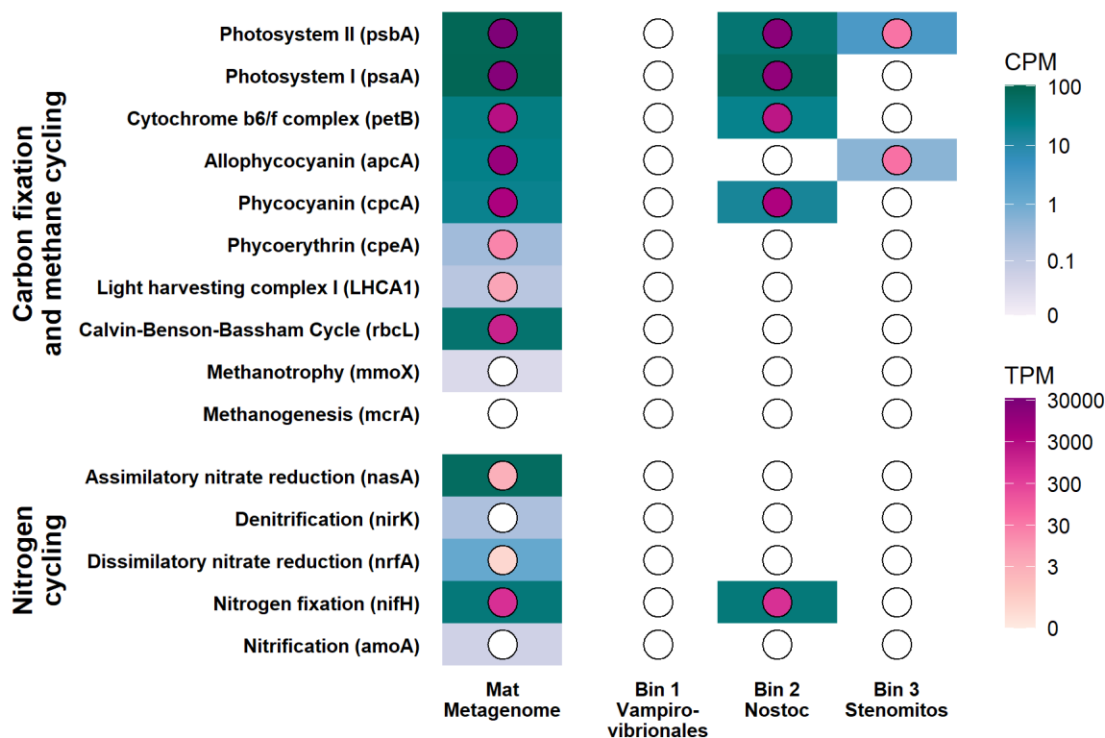


Figure 3.4. Metabolic potential and expression of key genes involved in carbon fixation, methane cycling, and nitrogen cycling for a *Nostoc* mat from Axel Heiberg Island, Nunavut, Canada, and its associated cyanobacterial metagenome-assembled genomes. Gene abundances are shown as counts per million (CPM) in the rectangles in the background, and transcript abundances are shown as transcripts per million (TPM) in the circles in the foreground.

3.4.3 *In situ* gas flux of High Arctic *Nostoc* mats

When we measured the gas flux of soils with and without visible *Nostoc* mats, we found that neither CO₂ nor CH₄ flux varied significantly between measurements taken with the clear and opaque chambers ($p = 0.0591$ and 0.6528 , respectively) (**Figure 3.5**). Similarly, there was no difference in CO₂ flux between the sites with *Nostoc* mats and those without ($p = 0.41$), but respiration is more consistent between replicates in sites containing *Nostoc* than in sites without. However, there was an 84% decrease in CH₄ uptake in samples containing visible *Nostoc* mats ($p=0.0009$). As with CO₂ flux, sites containing *Nostoc* mats have much lower variation in CH₄ flux than those without. The soils and their associated *Nostoc* mats respire approximately 0.75

grams of C per m² each day. These soils also act as a methane sink, storing 0.0008378 to 0.00055 grams of C per m² per day.

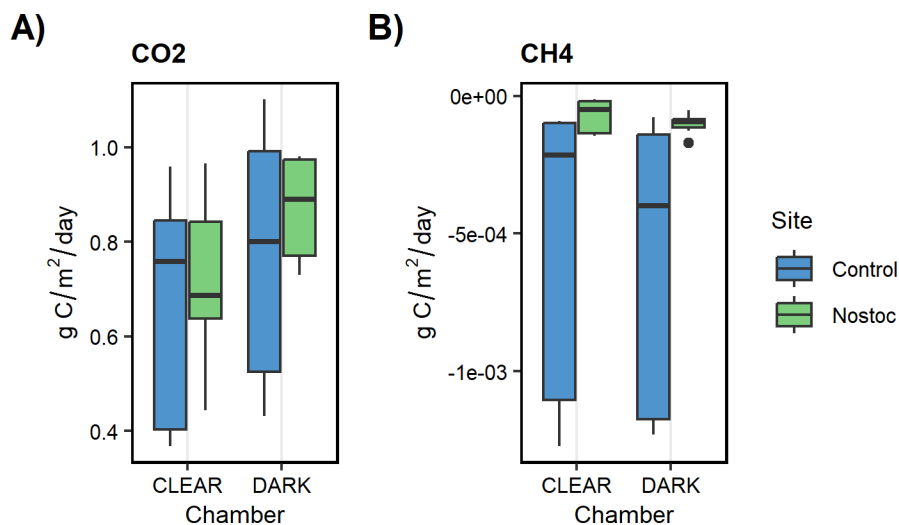


Figure 3.5. A) CO₂ and B) CH₄ gas flux of soils with *Nostoc* mats on the surface (Nostoc) and without any visible *Nostoc* mats (Control) on Axel Heiberg Island, Nunavut, Canada. Gas flux was measured using the LI-COR LI-7810 and both a clear chamber (CLEAR) and the LI-COR Smart chamber 8200-01 (DARK).

3.4.4 Isolation and characterization of High Arctic photoautotrophs

Five unique non-axenic photoautotrophic cultures were partially isolated from the *Nostoc* mat (**Figure 3.6**). Two of the cultures were identified as Eukaryotic algae, while the other three were cyanobacteria. All of these taxa were also found in the metagenome, albeit at low relative abundances (**Table 3.4**). Two of the MNM cultures, MNM2 and MNM4, exhibited psychrophilic growth, as they were unable to grow above 20°C, while MNM1 and MNM3 exhibited psychrotrophic growth, growing optimally around 15°C, but still capable of growth above 20°C. MNM5 grew optimally at 25°C and thus is likely a mesophile. All of the cultures, with the exception of MNM5, grew at 0°C, with MNM2 growing at -5°C (**Table 3.4**). Only two of the

cultures exhibited mild salt tolerance up to 2.5% NaCl (**Table 3.4**). However, all five cultures could grow under nitrogen-limited conditions on BG11_o (**Table 3.4**).

When evaluating the growth characteristics of the cultures, we see that most of the cultures are psychrotolerant, growing as low as 0°C (GHE1, GHSGMB2, WGCM1, WGCM2, WGF2, and WGF3) (**Table S4**). Most cultures showed limited salt tolerance, but GHE1 and WGF3 both demonstrated the ability to grow up to 5% NaCl. Additionally, all the cultures except for the Gypsum Hill Springs cultures were able to grow on nitrogen-limited media (**Table S4**).

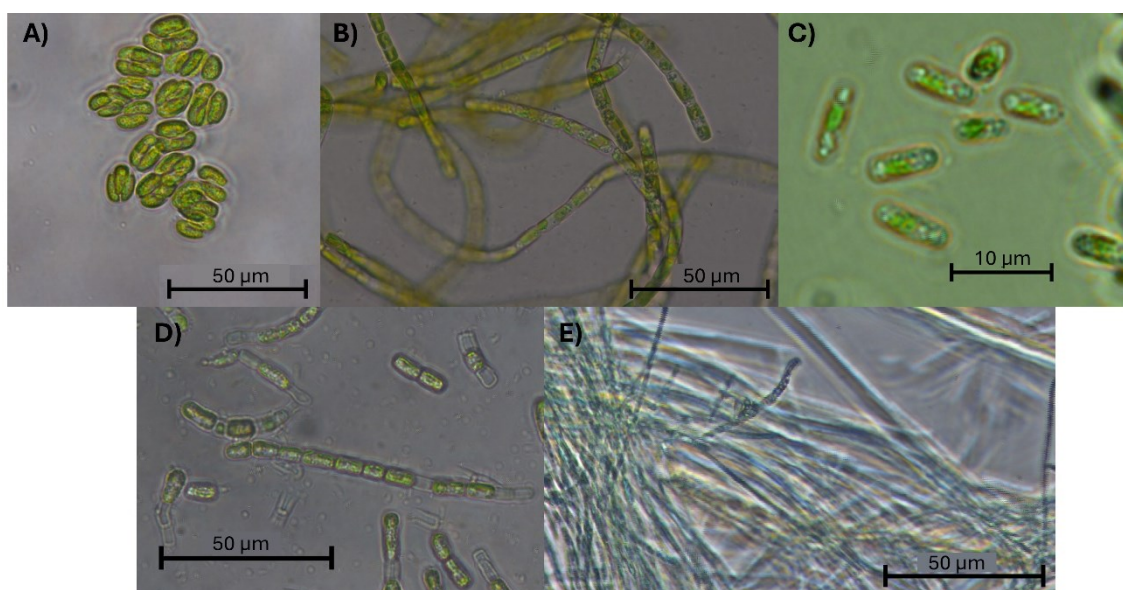


Figure 3.6. Microscope images of non-axenic phototrophic cultures from a *Nostoc* mat on Axel Heiberg Island, Nunavut, Canada. Panel A) MNM1, *Chloromonas* sp. B) MNM2, *Aphanizomenon* sp. NIES81 C) MNM3, *Stichococcus* sp. D) MNM4, *Tychonema* sp. CCAP_1459-11B E) MNM5 *Geitlerinema* sp. LD9.

Table 3.4. Summary of non-axenic culture growth characteristics from a High Arctic *Nostoc* mat community. The relative abundances of each culture in the metagenome were based on the taxonomic classification of reads

ID	Kingdom	Identity	Growth temperature (°C)	NaCl tolerance (%)	Growth on BG11 _o	Relative abundance in metagenome (%)
MARS <i>Nostoc</i> Mat (MNM)						
MNM1	Eukarya	<i>Chloromonas</i> sp.	0-25	0	Yes	1.8×10 ⁻⁵
MNM2	Bacteria	<i>Aphanizomenon</i> sp. NIES81	-5-15	0	Yes	0.005
MNM3	Eukarya	<i>Stichococcus</i> sp.	0-25	0-2.5	Yes	4.0×10 ⁻⁶

MNM4	Bacteria	<i>Tychonema</i> sp. CCAP_1459-11B	0-15	0	Yes	0.0055
MNM5	Bacteria	<i>Geitlerinema</i> sp. LD9	15-25	0-2.5	Yes	0.0061

3.4.5 Chlorophyll Fluorescence Assay of High Arctic *Nostoc* mat cultures

To determine photosynthetic activity at a variety of temperatures, chlorophyll fluorescence imaging was used to determine the F_v/F_m for six photoautotrophic cultures: the five described in section 3.4.3, and a mixed culture from a *Nostoc* mat (**Figure 3.7**). The F_v/F_m values of MNM1 and MNM5 did not have a clear relationship with temperature ($p = 0.845$ and 0.688 , respectively) (**Figure 3.7**). The F_v/F_m for MNM2 decreased weakly with increasing temperatures ($p = 0.07324$) (**Figure 3.7**), whereas the F_v/F_m for MNM3, MNM4, and the mixed mat culture all increased with increasing temperatures ($p = 0.000255$, 6.04×10^{-6} , and 3.18×10^{-5} , respectively) (**Figure 3.7**). Notably, the F_v/F_m values of MNM3 were consistent from -5 to 15°C but dropped by 30% from -5 to -10°C (**Figure 3.7**). In the mixed mat culture, F_v/F_m was consistent from -10 to 5°C but increased by 71% between 5 and 15°C (**Figure 3.7**). Photosynthetic activity was demonstrated at -5°C in MNM2, MNM3, MNM4, and the mixed culture, and at -10°C in MNM2 and MNM4 (**Figure 3.7**).

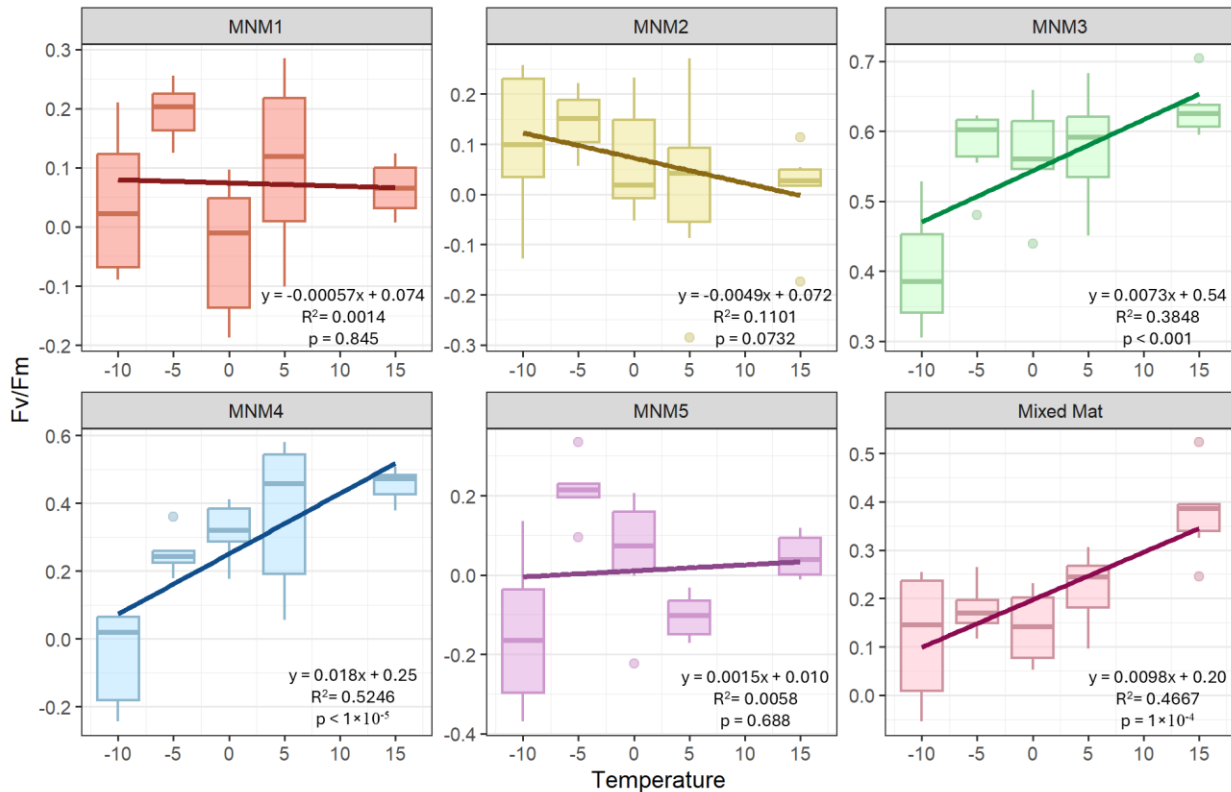


Figure 3.7. The effect of temperature on the maximum quantum yield of PSII of six photoautotrophic cultures derived from a *Nostoc* mat in a transient pond from Axel Heiberg Island, Nunavut, Canada.

3.4.6 Acetylene Reduction Assay of a High Arctic mixed *Nostoc* mat culture

A summary of acetylene reduction of *Nostoc* mat cultures at low and sub-zero temperatures over 6 months can be seen in **Figure 3.8**. At temperatures greater than 0°C, the amount of ethylene present in the controls exceeded the amount in the samples, resulting in negative measurements for biological ethylene production. A similar phenomenon occurred at 0°C on day 30. The only sample for which we obtained positive values of biological ethylene production was the culture incubated at 5°C for 60 days. No acetylene reduction was observed below 0°C at any time point (**Figure 3.8**). Despite negative biological ethylene production, the values did increase over time at 5 and 15°C (**Figure 3.8**). A two-way ANOVA indicated that both temperature and

time affected acetylene reduction ($p = <2 \times 10^{-16}$ and 2.1×10^{-5} , respectively). Notably, cells in the cultures were photobleached early in the experiment (**Figure S5**).

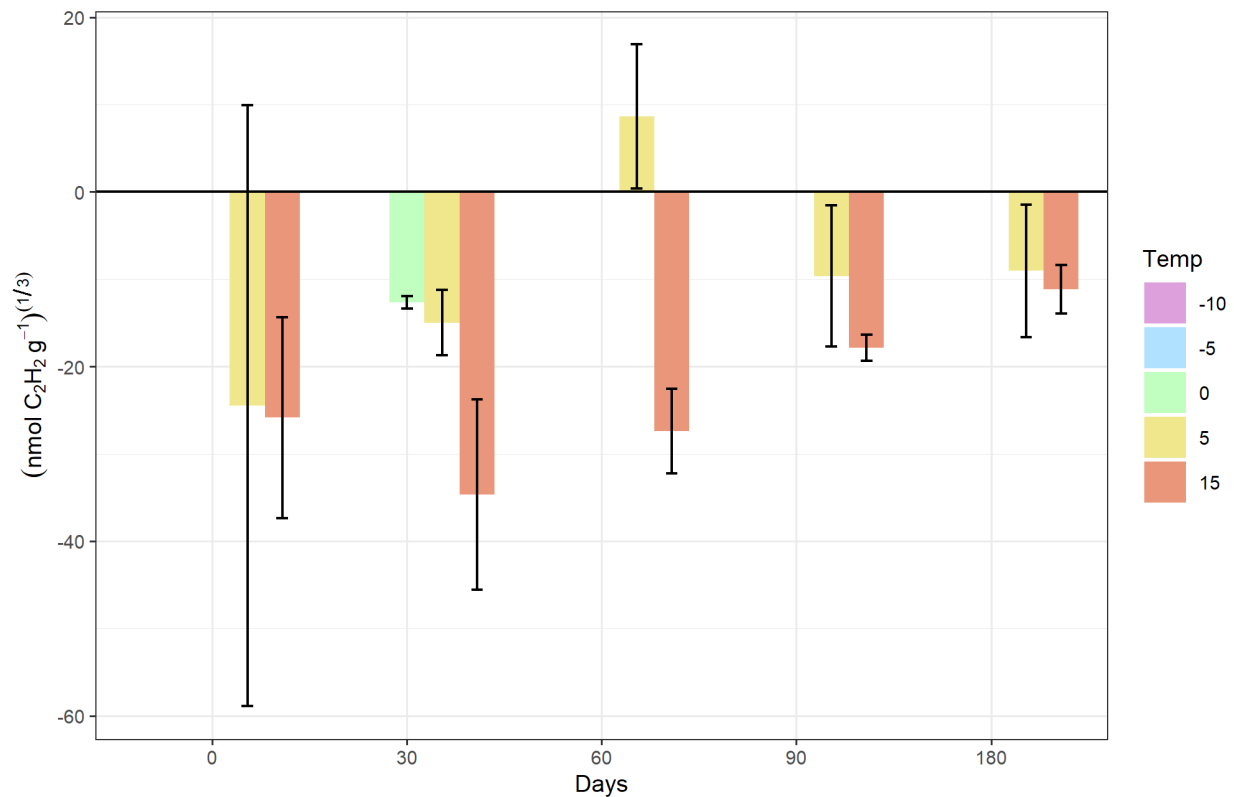


Figure 3.8. Summary of acetylene reduction at low and sub-zero temperatures of a mixed culture from a *Nostoc* mat on Axel Heiberg Island. Bars indicate the average of the cube root of biological ethylene produced by the sample +/- the standard deviation.

3.5 Discussion

In this study, we found that the *Nostoc* mat community was comprised of a wide array of genera, but most of the transcriptional activity was conducted by *Nostoc* (**Figure 3.2**). Upon further investigation, we found that the mats were transcribing a wide array of cold response genes, including, but not limited to glycosyltransferase involved in peptidoglycan alteration, molecular chaperone DnaK (HSP70), and translation elongation factor EF-G (GTPase) which may assist in their survival in extreme arctic conditions (**Figure 3.3**). Additionally, the metatranscriptome indicated that the *Nostoc* mat community was transcribing genes for

photosynthesis and carbon fixation (*psbA*, *psaA*, and *rbcL*) (**Figure 3.4**). The metagenome showed that the community possessed the marker gene for methanotrophy (*mmoX*) but was not expressing it and the marker gene for methanogenesis (*mcrA*) was absent (**Figure 3.4**).

The metagenome also showed that the community contains the marker genes for all the major nitrogen cycle components (nitrogen fixation, denitrification, nitrification, and nitrate reduction), but genes for nitrogen fixation and nitrate reduction are the only ones being expressed (**Figure 3.4**). To further investigate the cyanobacterial member's role in the mat's cold tolerance, carbon fixation and nitrogen cycling activity, three MAGs were evaluated (*Vampriovibrionales*, *Nostoc* sp. WHI, and *Stenomitos* sp.). Of the three MAGs, *Nostoc* sp. WHI was the most transcriptionally active.

To expand our understanding of cold growth and activity, five non-axenic cultures were grown from the *Nostoc* mat and their growth at low and sub-zero temperatures was tested along with their salt-tolerance (**Table 3.4**). One of these cultures (MNM2) demonstrated sub-zero growth at -5°C (**Table 3.4**). Chlorophyll fluorescence was also measured for the five non-axenic *Nostoc* mat cultures, and a mixed culture to determine if photosynthesis was occurring at low and sub-zero temperatures. We found that four of the six cultures were photosynthetically active at sub-zero temperatures (**Figure 3.7**). We also tested for cold and sub-zero nitrogen fixation via acetylene reduction, but the results were inconclusive (**Figure 3.8**).

3.5.1 Metagenomic and metatranscriptomic sequencing of a High Arctic *Nostoc* mat community

The community makeup of the AHI *Nostoc* mat was primarily Pseudomonadota, followed by Cyanobacteriota (**Figure 3.2**). This aligns with previous research suggesting that macroscopic *Nostoc* mats in low-nutrient environments, such as the Arctic, host a community of heterotrophic

organisms (Jungblut & Vincent, 2017). The high prevalence of *Nostoc* in the DNA reads but comparatively lower abundance in the metagenome assembly indicates that while there was a high abundance of *Nostoc* in the sample, there were few *Nostoc* strains within the community. The RNA reads indicated that *Nostoc* was the most active member of the community, accounting for half of all the transcripts that we detected.

When looking at the AHI metagenome as a whole community, we observed a diverse pattern of presence and transcription of cold adaptation genes (**Figure 3.3**). Notably, many of the genes tested for cold tolerance are house keeping genes, so their presence is expected within the metagenome, but gene expression is more informative with regard to cold tolerance. Expression profiles were slightly biased towards genes related to cold shock, stress and HSP proteins, membrane and peptidoglycan alteration, and transcription and translation factors. The diversity in cold adaptation strategies is common among polar communities, as cold temperatures are associated with other stressors, such as high salt concentration, low water availability, and freeze-thaw cycles (Lionard *et al.*, 2012, Christmas *et al.*, 2016, Jungblut & Vincent, 2017, Goordial, 2021).

The metagenome and metatranscriptome AHI *Nostoc* mat also show the *Nostoc* mat's role in carbon fixation, methane cycling and nitrogen cycling activity (**Figure 3.9**). In the mats, we did not see any transcription of methanotrophy or methanogenesis, suggesting that there is no synthesis or breakdown of methane in the mat community. We do see high relative expression of genes related to photosynthesis and carbon fixation (*psbA*, *psaA*, *petB*, and *rbcL*), which suggests that the mats are actively fixing carbon via photosynthesis. As for the nitrogen cycle, we observed high relative activity of *nifH*, indicating that nitrogen fixation is occurring in the mats. There was also some expression of genes for assimilatory and dissimilatory nitrate reduction,

which suggests that ammonia is being produced within the mats but not being transformed into other forms of nitrogen. In fact, the transcripts suggest that nitrate is being transformed into ammonia. The *Nostoc* mat contained 51% more ammonia than the adjacent control pond, but only 12% more nitrate, corroborating the transcript data. The persistence of ammonia within the mat community has advantages and disadvantages when considering their role in climate change. On one hand, without nitrification, and subsequent denitrification, there is no opportunity for the release of nitrous oxide into the atmosphere, which acts as a potent greenhouse gas that is considered third in importance behind carbon dioxide and methane (Bernhard, 2010, Voss *et al.*, 2024). On the other hand, while some ammonia will be taken up by members of the mat, some may be leached to surrounding areas, increasing nutrient availability to heterotrophic organisms and therefore increasing CO₂ emissions.

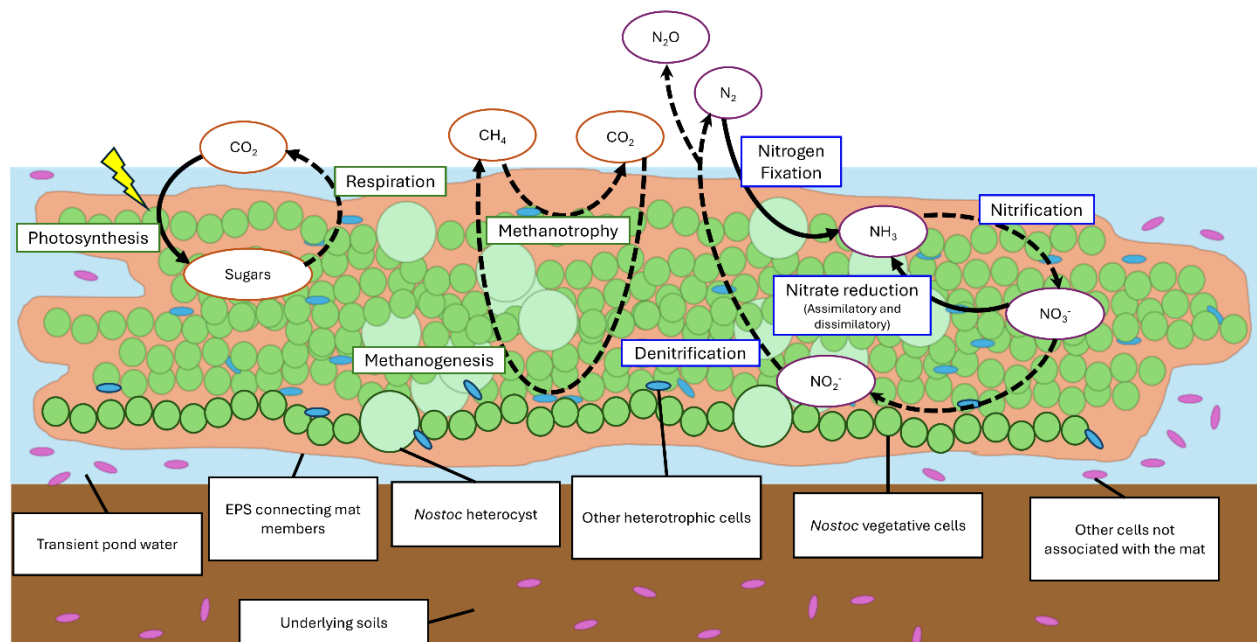


Figure 3.9. Schematic of *Nostoc* mat community carbon and nitrogen cycling on Axel Heiberg Island, Nunavut, Canada. Solid lines are representative of processes in which transcripts indicated gene expression. Dashed lines are representative of processes that are either represented in the metagenome, with no transcripts, or indicated by in-situ gas flux measurements.

3.5.2 Analyses of cyanobacterial MAGs from a High Arctic *Nostoc* mat metagenome

The three cyanobacterial MAGs were analyzed to identify and understand the genetic basis of cold adaptation, carbon fixation, methane cycling, and nitrogen cycling, in the cyanobacterial members of the mats. The first of the MAGs selected for further analyses was an unknown member of the Vampirovibrionales order, as identified by GTDBtk (Chaumeil *et al.*, 2019). This order only has one named species, *Vampirovibrio chlorellavorus*, a non-photosynthetic member of Cyanobacteriota that preys on the microalgae *Chlorella vulgaris* by attaching to its surface and producing peripheral vacuoles that gradually dissolve cell contents (Soo *et al.*, 2015).

Chlorella vulgaris was identified in the metagenome, accounting for 0.0033% of the reads, further supporting the presence of a member of Vampirovibrionales. The AHI

Vampirovibrionales MAG possessed some genes known for cold adaption, but we only detected transcripts for one of these, chaperonin GroEL (HSP60 family) (**Figure 3.3**), a protein used to modulate and accelerate protein folding (Georgescauld *et al.*, 2014). The MAG had none of the carbon fixation or methane- and nitrogen-cycling genes that we tested for (**Figure 3.4**), which is unsurprising due to members of the family being non-photosynthetic and instead opting to acquire nutrients through predation (Soo *et al.*, 2015).

The second MAG that was selected for analyses was identified as *Nostoc* sp. WHI, which was first isolated from Ward Hunt Island (WHI), Nunavut, Canada (Jungblut *et al.*, 2021) and had its genome sequenced. Previous genomic analyses of this strain (RefSeq:

GCF_015714725.1) focused on its metabolic pathways, stress genes, secondary metabolites, and CRISPR-cas systems (Jungblut *et al.*, 2021). We found that the AHI *Nostoc* transcribed a wide array of the tested cold adaptation genes, suggesting that it utilizes multiple strategies to survive Arctic conditions (**Figure 3.3**). Actively transcribed genes included cold shock, stress and HSP,

DNA replication and repair, membrane and peptidoglycan alteration, carotenoid biosynthesis, osmotic stress, oxidative stress, toxin/anti-toxin modules and transcription and translation factors. Many of the cold adaptation genes found by Jungblut *et al.* (2021) were detected in both the AHI MAG and its corresponding reads from the AHI metatranscriptome. These include DNA gyrase/topoisomerase, molecular chaperones DnaK and GrpE, maltotriose synthase, and translation initiation factor IF-2 (**Figure 3.3**). Notably, the selected genes for polysaccharide capsules were absent from the AHI MAG, which is unexpected as *Nostoc* is known to produce large amounts of EPS to create the sheath that connects individual cells in the filament (Lionard *et al.*, 2012). However, exopolysaccharide biosynthesis and export proteins are present in the *Nostoc* sp. WHI genome, some of which were included in our search, and others that were not (Jungblut *et al.*, 2021). The absence of these genes can be attributed to a combination of limited search parameters and the fact that this MAG was only 84% complete, so not all genes harboured by the organism were present in the MAG. This limitation of MAG incompleteness is common in metagenomic studies, as binning programs struggle with high-complexity samples and closely related strains (Sczyrba *et al.*, 2017).

The AHI *Nostoc* MAG also showed transcription of the photosynthetic apparatus genes PSII, PSI and Cytochrome b6/f, as well as one of the phycobilisome proteins, phycocyanin (cpcA) (**Figure 3.4**). However, RuBisCO—the marker gene for photosynthesis-associated carbon fixation—genes and transcripts were absent from the AHI MAG, suggesting that while the photosynthetic apparatus was active, carbon fixation was not occurring. To ensure that this is not a product of MAG incompleteness, sequences annotated as *rbcL* should be compared to a reference database to determine which organisms contain and express the marker gene for carbon fixation. Members of the *Nostoc* genus are known to grow under mixotrophic conditions (Yu *et*

al., 2009), which could explain the lack of *rbcL* transcripts, but copies of the gene would still be expected withing the genome.

The final cyanobacterial MAG selected for analyses was identified as a species of *Stenomitos* (Bin 3), which are simple filamentous members of the Leptolyngbyaceae (Lee *et al.*, 2023). While this MAG had 17 cold adaptation genes, we only detected transcripts for four of these genes (**Figure 3.3**). This suggests that, while capable of multiple cold tolerance strategies, this *Stenomitos* species transcribes fewer, with higher expression of glycosyltransferase, which helps to increase flexibility and reduce turgor pressure and cell permeability at low temperatures (Benforte *et al.*, 2018). With respect to carbon fixation, methane-cycling, and nitrogen-cycling genes, the AHI *Stenomitos* MAG had genes for PSII and phycocyanin but did not have any of the tested genes for nitrogen cycling (**Figure 3.4**). The only transcribed gene in our carbon- and nitrogen-related gene set was for phycocyanin, which is a phycobilisome pigment. This suggests that while some of the pigments are being expressed, it is unlikely that *Stenomitos* is photosynthetically active in this community, or the mRNAs for these genes were below the detection level. The lack of nitrogen fixation genes is unsurprising, as *Stenomitos* are not known nitrogen fixers (Hirose *et al.*, 2021).

3.5.3 *In situ* gas flux of High Arctic *Nostoc* mats

To quantify the CO₂ and CH₄ flux associated with the *Nostoc* mats, we measured the *in situ* gas flux of soils with and without visible *Nostoc* mats. *In situ* gas flux measurements taken in 2024 indicated that *Nostoc* mats did not affect the CO₂ respiration from the soils (**Figure 3.5**). This was unexpected, as the metatranscriptomic analysis on our 2023 samples showed high relative expression of photosynthesis and carbon fixation genes in these mats (**Figure 3.4**). This discrepancy could be attributed to mat dehydration, as the mats had only been hydrated for

approximately three days at the time of measurement, and photosynthetic rates may have been decreased for this reason. Alternatively, because carbon fixation is a slower process than respiration, it may not be properly captured in short measurements (Spohn *et al.*, 2020). The similar flux could also be a result of microscopic cyanobacteria and other photoautotrophs that were present in the soils, that were also fixing carbon, which would result in more similar CO₂ flux than soils free of all photoautotrophs. Another reason for the similar CO₂ respiration rates could be that respiration by heterotrophic microorganisms associated with the *Nostoc* mat may offset the CO₂ being fixed by photoautotrophic members of the community. Unfortunately, there is no one marker gene for heterotrophy, making it difficult to compare the relative expression levels of autotrophic and heterotrophic metabolisms in an -omics-based data set. Further studies, such as NanoSIMS could be conducted to measure the carbon respiration rates and compare them to carbon fixation rates. Even so, our data suggests that at the time of measurement, the *Nostoc* mats and underlying soils act as a net source of CO₂ (Li *et al.*, 2023). Historically, Arctic soils were a carbon sink, which created a significant carbon reservoir; however, as the Arctic continues to be affected by warming, it is shifting to a carbon source, as is reflected by our soil flux data (Altshuler *et al.*, 2019, Liu *et al.*, 2024).

The *Nostoc* mats and their underlying soils also acted as a methane sink, suggesting the presence of methanotrophic microorganisms; however, this sink was weaker in the *Nostoc* mats than the surrounding soils (**Figure 3.5**), and transcripts for both methanogenesis and methanotrophy were not detected in the *Nostoc* mat metatranscriptome (**Figure 3.4**), suggesting that the mats may have a lower incidence of methanotrophy than the soils alone. Methane source-sink dynamics are reliant on the soil conditions at the time of measurement, as wetter conditions favour methane release, while drier conditions favour methane uptake (Arndt *et al.*,

2019, Voigt *et al.*, 2023). However, previous studies have shown that permafrost near the *Nostoc* mat sampling site is a methane sink (Altshuler *et al.*, 2022). This soil moisture effect may explain the reduction in methane uptake in the presence of *Nostoc* mats; the mats were rehydrated before measuring gas flux, and their EPS naturally holds water, creating slightly wetter conditions that would have reduced the net methane sink. Alternatively, there is evidence of cyanobacteria in terrestrial and freshwater environments producing methane (Bižić *et al.*, 2020); however, this was not evidenced in our metagenome (**Figure 3.4**). We could better understand the role of these *Nostoc* mats in methane cycling by obtaining gas flux measurements when the transient ponds are filled, to see the change with naturally rather than artificially wetter conditions.

Notably, both CO₂ and CH₄ flux was more consistent for the sites containing the *Nostoc* mats than those without them. This may be a result of rehydrating the sites containing the *Nostoc* mats, as previous work has shown that carbon fixation is inconsistent when water is unavailable (Novis *et al.*, 2007), and the control sites were not rehydrated. A similar phenomenon could be occurring for methane cycling activity, as water is key for maintaining most enzymatic processes.

3.5.4 Isolation and characterization of High Arctic photoautotrophs

To further explore the cold adaptations and carbon- and nitrogen-cycling activities of specific photoautotrophic members of the *Nostoc* mat community, we partially isolated five unique non-axenic photoautotrophic cultures. Several of these cultures were capable of growth at near- or sub-zero temperatures, suggesting that the diverse cold tolerance mechanisms identified in the metagenome allow *Nostoc* mat activity to persist well into the arctic shoulder seasons. In two of the cultures, (MNM1 and MNM3) dominant photoautotrophs were eukaryotic microalgae, and three (MNM2, MNM4, MNM5) were filamentous cyanobacteria (**Table 3.4**). MNM5 was

not able to grow below 15°C, suggesting that it is mesophilic. In contrast, MNM1, MNM3, and MNM4 were all able to grow as low as 0°C. MNM2 was able to grow at –5°C and is likely a true psychrophile, as it grew best around 15°C, and was unable to grow at temperatures higher than that (Shen *et al.*, 2021). Interestingly, none of the cultures displayed significant salt tolerance, which is typically coupled with subzero temperature microbial growth as the exclusion of salts from freezing water often makes sub-zero environments hyper-saline (Mykytczuk *et al.*, 2013, Jungblut & Vincent, 2017). This suggests that MNM2 is utilizing other mechanisms to withstand subzero temperatures and obtain liquid water. This is especially true for MNM2, which grew at sub-zero temperatures.

The two eukaryotic genera that we cultured were identified as *Chloromas* sp. and *Stichococcus* sp., respectively (**Table 3.4**). *Chloromonas* is a genus of green algae that have been isolated from a wide variety of environments, including the High Arctic (Barcytė *et al.*, 2018). There have been multiple psychrotolerant *Chloromonas* strains isolated, including one from snow algae in Svalbard, Norway (Barcytė *et al.*, 2018). The presence of snow algae in the *Nostoc* mat community is unsurprising, as the transient ponds that they inhabit are supplied by the spring and summer snow melt. *Stichococcus* is a genus of green microalgae that is found globally, with incidences in terrestrial and freshwater environments in the Arctic and Antarctic (Hodač *et al.*, 2016). *Stichococcus* has been found in a wide variety of polar permafrost from Siberia, Canada, Svalbard, the USA, and Russia (Vishnivetskaya *et al.*, 2020).

MNM2 was identified as *Aphanizomenon* sp. NIES81. This species was first isolated from a lake in Japan and identified as a toxic, nitrogen-fixing, filamentous, algal bloom-forming species (Cao *et al.*, 2014, Cirés & Ballot, 2016). There is some evidence of *Aphanizomenon* species being salt tolerant, as isolates from the Baltic Sea can survive in waters up to 7.4 PSU

compared to local freshwater lakes with 0.1 PSU; however, to our knowledge, there are no reported cold-tolerant species (Laamanen *et al.*, 2002). Our finding of an *Aphanizomenon* isolate growing as low as -5°C , and unable to grow above 15°C , may therefore be the first report of cold tolerance in *Aphanizomenon* (**Table 3.4**). This is important because psychrophilic growth has previously not been identified in cyanobacteria, with most polar cyanobacterial isolates exhibiting psychrotrophic growth, with optimal growth temperatures above 20°C but still tolerating cold temperatures (Vincent, 2002, Christmas *et al.*, 2018, Shen *et al.*, 2021).

MNM4 and MNM5 were identified as *Tychonema* sp. CCAP_1459-11B, and *Geitlerinema* sp. LD9, respectively. *Tychonema* sp. CCAP_1459-11B was originally isolated from Loughgall, Northern Ireland, UK (Suda *et al.*, 2002). Previous work showed that this strain grows between 20 and 30°C and up to 0.43% NaCl (Suda *et al.*, 2002). While our data corroborates *Tychonema* sp. CCAP_1459-11B's low salt tolerance, we found that the species could only grow between 0 and 15°C (**Table 3.4**), indicating that MNM4 is psychrophilic. *Tychonema* sp. has previously been found in Arctic and Antarctic cyanobacterial mats (Jungblut & Vincent, 2017). Finally, *Geitlerinema* sp. LD9 was first identified in soil crusts from the Tibetan Plateau in Ladakh, India (Čapková *et al.*, 2016). This area is considered a cold desert, similar to the Canadian High Arctic (Čapková *et al.*, 2016). To our knowledge, this strain has not been previously cultured, but its inability to grow temperatures below 15°C in our study is unusual considering its prevalence in cold environments, although summer air temperatures can reach 15 - 20°C at AHL.

All five non-axenic cultures were detected in our metagenome of the *Nostoc* mat community, but at abundances too low to effectively assemble into medium- or high-quality MAGs. MNM1 made up $1.8 \times 10^{-5} \%$ of the metagenomic reads, and 0.0018% of the metatranscriptomic reads (**Table 3.4**). MNM2 comprised 0.005 and 0.008% of the DNA and

RNA reads, respectively. MNM3 was assigned to 4.0×10^{-6} and $2.3 \times 10^{-5}\%$ of the metagenomic and metatranscriptomic reads, respectively. MNM4 made up 0.0055% of the DNA reads and 0.0026% of the RNA reads. Finally, MNM5 was the most abundant of the non-axenic cultures, making up 0.0061% of the metagenomic reads. MNM5 also made up 0.0048% of the metatranscriptomic reads.

The additional 14 cultures from other arctic environments were mostly psychrophilic and psychrotolerant, however, one GHE strain was unable to grow below 15°C (**Table S4**). This is expected as these samples are derived from a cold environment, and thus have likely adapted to be able to tolerate those conditions. Additionally, most of the cultures were not or only mildly salt tolerant, as we found in the MNM cultures. All of the cultures with the exception of those from the Gypsum Hill mats were capable of growth on nitrogen-limited media, which is interesting as nitrogen fixation is not common among algae; however, could be from a nitroplast – a nitrogen-fixing organelle found in some algae that is a result of primary endosymbiosis (Coale *et al.*, 2024).

3.5.5 Chlorophyll Fluorescence Assay of High Arctic *Nostoc* mat cultures

Chlorophyll fluorescence measurements of our five non-axenic *Nostoc* mat isolates revealed the persistence of photosynthetic activity even at low or sub-zero temperatures in several cultures, though photosynthetic stress in the overall mat community became evident at 5°C (**Figure 3.7**). The chlorophyll fluorescence parameter F_v/F_m measures the maximum quantum yield of PSII and is commonly used as a measure of photosynthetic efficiency and is used to determine how photosynthesis is affected by stressors (Stirbet *et al.*, 2019). In healthy unstressed plants, this value is typically around 0.7-0.8; however, this value is typically lower in cyanobacteria as the PQ pool is shared between the photosynthetic and respiratory electron

transport chains, making total oxidation of the PQ pool before measurement difficult (Ogawa *et al.*, 2017, Stirbet *et al.*, 2019). Unstressed cyanobacteria will usually have an F_v/F_m ratio of 0.45-0.6 following the addition of DCMU to oxidize the PQ pool (Ogawa *et al.*, 2017, Stirbet *et al.*, 2019).

Interestingly, MNM2 was the only culture to show a decrease in the quantum yield of PSII with increasing temperature (**Figure 3.7**). While the highest measured F_v/F_m was still considered low for cyanobacteria, this may be a sign of cold-adapted photosynthesis. Notably, this was also the strain that demonstrated sub-zero growth (**Table 3.4**). Further work should repeat this assay at lower temperatures to see the total range of photosynthetic activity in this strain.

Conversely, MNM3, MNM4 and the mixed mat culture all showed increasing F_v/F_m with increasing temperature (**Figure 3.7**). This increase is expected based on previous studies showing that temperature is positively correlated with photosynthetic activity (Lennihan *et al.*, 1994, Novis *et al.*, 2007). MNM3 showed a sharp decrease in F_v/F_m at -10°C , whereas the F_v/F_m from -5 to 15°C was consistent (**Figure 3.7**). This suggests that -10°C is a critical point at which the *Stichococcus* sp. begins to experience photosynthetic stress. This culture also had the highest F_v/F_m values of all the tested cultures; however, this does not provide evidence of increased photosynthetic activity because MNM3 is a green alga, so its unstressed F_v/F_m values are expected to be in the same range as plants (0.7-0.8) (Stirbet *et al.*, 2019). MNM4 followed a similar pattern to MNM3, with a gradual decrease in chlorophyll fluorescence from 15 to -5°C followed by a large decrease at -10°C . At temperatures greater than 5°C , MNM4 showed unstressed photosynthetic efficiency (**Figure 3.7**). In the mixed mat, F_v/F_m was consistent from -10 to 5°C but then increased at 15°C , suggesting that the critical point where photosynthetic stress occurs in the whole mat is around 5°C even if some mat members continue photosynthesis

at lower temperatures. Both MNM1 and MNM5 could not be described by a linear model, and the F_v/F_m for both of these cultures was close to 0 at all temperatures tested (**Figure 3.7**). This suggests that these cultures were stressed, and photosynthesis had ceased at all tested temperatures. It is also important to note that the light levels in the sub-zero temperature incubators were much lower than those at and above 0°C (**Table 3.3**). This could be the reason for lower F_v/F_m at lower temperatures, however, because F_v/F_m values were above zero at sub-zero temperatures in multiple samples, it suggests that the photoautotrophs in the cultures are adaptable to a wide variety of light conditions. This is an adaptation that was previously described (Morgan-Kiss *et al.*, 2006, Jungblut & Vincent, 2017).

In summary, we see that the relationship between F_v/F_m and temperature varies among the different photoautotrophs present in the *Nostoc* mat, however there are photoautotrophic members of the community that are able to perform photosynthesis at sub-zero temperatures (**Figure 3.7**), expanding our previous understanding of cold photosynthesis, which was believed to be at -5°C (Becker, 1982), however the data presented here suggests that this should be revised to -10°C. Although F_v/F_m and chlorophyll fluorescence imaging can provide an idea of photosynthetic activity, they are not always directly proportional to carbon fixation rates, as the activity of light harvesting apparatuses does not guarantee the activity of carbon fixation machinery (Hupp *et al.*, 2021). A definitive assessment of carbon fixation rates across a range of temperatures will require additional experiments, such as measuring oxygen evolution or using $^{13}\text{CO}_2$ and NanoSIMS to directly measure carbon fixation over time (Hupp *et al.*, 2021, Li *et al.*, 2023).

3.5.6 Acetylene Reduction Assay of a High Arctic mixed *Nostoc* mat culture

Acetylene reduction and the resulting production of ethylene is used as an indirect measurement of nitrogen fixation in diazotrophic microorganisms, as the nitrogenase enzyme can cleave other low-molecular-weight, triple-bonded molecules like acetylene (Capone, 1993). Although we found that the amount of acetylene reduced biologically by the mixed *Nostoc* mat culture was significantly higher at 5 and 15°C than at lower temperatures, the high levels of ethylene produced in the 5 and 15°C negative controls confound these results. Indeed, ethylene was detected in both the 5 and 15°C negative controls as early as day 0, suggesting that some non-biological reaction quickly converted some of the added acetylene into ethylene (**Figure 3.8**). Furthermore, most of the cultures photobleached (i.e., lost their chlorophyll pigmentation; **Figure S5**) soon after the vials were sealed. Photobleaching damages the photosynthetic apparatus pigments, preventing the excitation of electrons from light (Hsieh *et al.*, 2014). For this reason, photobleached cells cannot perform carbon fixation. Because our mixed mat culture was provided with carbon-free media for the acetylene reduction assay, the cells were presumably carbon-limited and would have decreased or ceased all nitrogenase activity. Future assessments of nitrogen-fixing activity in *Nostoc* mats should repeat this experiment under less carbon-stressed conditions to confirm the relationship between temperature and nitrogen fixation.

3.6 Conclusions

This study showed that High Arctic *Nostoc* mats both encode and express the cold tolerance genes required to withstand low-temperature environments as well as the key genes for carbon and nitrogen fixation, which were detected in multiple photoautotrophic members of the mat community. Culture-based analyses identified multiple photoautotrophic mat members that

maintained chlorophyll fluorescence, and therefore presumed photosynthetic activity, even at sub-zero temperatures; one isolate, *Aphanizomenon* sp. NIES81 (MNM2), was also capable of growth sub-zero temperatures. Given these results, the continued activity of Arctic photoautotrophic communities at low and sub-zero temperatures should be accounted for in future studies of biogeochemical cycles in the context of climate change, as these communities may comprise a significant portion of terrestrial microbial biomass in rapidly warming polar regions. Further work is therefore needed to expand both *in situ* and culture-based knowledge of the role of *Nostoc* mats in Arctic biogeochemical cycles, including explicit quantitation of their carbon and nitrogen fixation rates at low and sub-zero temperatures so that these communities can be better considered in biogeochemical models.

3.7 References

- Altshuler I, Raymond-Bouchard I, Magnuson E, Tremblay J, Greer CW & Whyte LG (2022) Unique high Arctic methane metabolizing community revealed through in situ $^{13}\text{CH}_4$ -DNA-SIP enrichment in concert with genome binning. *Scientific Reports* **12**: 1160.
- Altshuler I, Hamel J, Turney S, Magnuson E, Lévesque R, Greer CW & Whyte LG (2019) Species interactions and distinct microbial communities in high Arctic permafrost affected cryosols are associated with the CH_4 and CO_2 gas fluxes. *Environmental Microbiology* **21**: 3711-3727.
- Arndt KA, Oechel WC, Goodrich JP, Bailey BA, Kalhori A, Hashemi J, Sweeney C & Zona D (2019) Sensitivity of Methane Emissions to Later Soil Freezing in Arctic Tundra Ecosystems. *Journal of Geophysical Research: Biogeosciences* **124**: 2595-2609.
- Barcytė D, Hodač L, Nedbalová L & Elster J (2018) *Chloromonas arctica* sp. nov., a psychrotolerant alga from snow in the High Arctic (Chlamydomonadales, Chlorophyta). *International Journal of Systematic and Evolutionary Microbiology* **68**: 851-859.
- Becker B & Pushkareva E (2023) Metagenomics Provides a Deeper Assessment of the Diversity of Bacterial Communities in Polar Soils Than Metabarcoding. *Genes* **14**: 812.
- Becker E (1982) Physiological Studies on Antarctic *Prasiola crispa* and *Nostoc commune* at Low Temperatures. *Polar Biology* **1**: 99-104.
- Benforte FC, Colonnella MA, Ricardi MM, Solar Venero EC, Lizarraga L, López NI & Tribelli PM (2018) Novel role of the LPS core glycosyltransferase WapH for cold adaptation in the Antarctic bacterium *Pseudomonas extremaustralis*. *PLOS ONE* **13**: e0192559.
- Bernhard A (2010) The Nitrogen Cycle: Processes, Players, and Human Impact. *Nature Education Knowledge* **3**: 25.
- Bižić M, Klintzsch T, Ionescu D, Hindiyeh MY, Günthel M, Muro-Pastor AM, Eckert W, Urlich T, Keppler F & Grossart HP (2020) Aquatic and terrestrial cyanobacteria produce methane. *Science Advances* **6**: eaax5343.
- Bolger AM, Lohse M & Usadel B (2014) Trimmomatic: a flexible trimmer for Illumina sequence data. *Bioinformatics* **30**: 2114-2120.
- Bowers RM, Kyrpides NC, Stepanauskas R, *et al.* (2017) Minimum information about a single amplified genome (MISAG) and a metagenome-assembled genome (MIMAG) of bacteria and archaea. *Nature Biotechnology* **35**: 725-731.

Bushnell B BMap.

Callahan BJ, McMurdie PJ, Rosen MJ, Han AW, Johnson AJA & Holmes SP (2016) DADA2: High-resolution sample inference from Illumina amplicon data. *Nature Methods* **13**: 581-583.

Cao H, Shimura Y, Masanobu K & Yin Y (2014) Draft Genome Sequence of the Toxic Bloom-Forming Cyanobacterium *Aphanizomenon flos-aquae* NIES-81. *Genome Announc* **2**.

Čapková K, Hauer T, Řeháková K & Doležal J (2016) Some Like it High! Phylogenetic Diversity of High-Elevation Cyanobacterial Community from Biological Soil Crusts of Western Himalaya. *Microbial Ecology* **71**: 113-123.

Capone DG (1993) Determination of Nitrogenase activity in Aquatic Samples Using the Acetylene Reduction Procedure. *Handbook of Methods in Aquatic Microbial Ecology*, (Kemp PF, Sherr BF, Sherr EB & Cole JJ, eds.), p.^pp. 621-631. Lewis Publishers, Boca Raton, Fla.

Chaumeil PA, Mussig AJ, Hugenholtz P & Parks DH (2019) GTDB-Tk: a toolkit to classify genomes with the Genome Taxonomy Database. *Bioinformatics* **36**: 1925-1927.

Chen IA, Chu K, Palaniappan K, *et al.* (2019) IMG/M v.5.0: an integrated data management and comparative analysis system for microbial genomes and microbiomes. *Nucleic Acids Res* **47**: D666-D677.

Chklovski A, Parks DH, Woodcroft BJ & Tyson GW (2023) CheckM2: a rapid, scalable and accurate tool for assessing microbial genome quality using machine learning. *Nat Methods* **20**: 1203-1212.

Christmas NAM, Anesio AM & Sánchez-Baracaldo P (2018) The future of genomics in polar and alpine cyanobacteria. *FEMS Microbiol Ecol* **94**: 10.

Christmas NAM, Barker G, Anesio AM & Sánchez-Baracaldo P (2016) Genomic mechanisms for cold tolerance and production of exopolysaccharides in the Arctic cyanobacterium *Phormidesmis priestleyi* BC1401. *BMC Genomics* **17**: 14.

Cirés S & Ballot A (2016) A review of the phylogeny, ecology and toxin production of bloom-forming *Aphanizomenon* spp. and related species within the Nostocales (cyanobacteria). *Harmful Algae* **54**: 21-43.

Coale TH, Loconte V, Turk-Kubo KA, *et al.* (2024) Nitrogen-fixing organelle in a marine alga. *Science* **384**: 217-222.

Comeau AM, Li WKW, Tremblay J-É, Carmack EC & Lovejoy C (2011) Arctic Ocean Microbial Community Structure before and after the 2007 Record Sea Ice Minimum. *PLOS ONE* **6**: e27492.

Cornet L, Bertrand AR, Hanikenne M, Javaux EJ, Wilmotte A & Baurain D (2018) Metagenomic assembly of new (sub)polar Cyanobacteria and their associated microbiome from non-axenic cultures. *Microbial Genomics* **4**.

Davey A & Marchant HJ (1983) Seasonal Variation in Nitrogen Fixation by *Nostoc Commune* Vaucher at the Vestfold Hills, Antarctica. *Phycologia* **22**: 377-385.

David KA, Apte SK, Banerji A & Thomas J (1980) Acetylene reduction assay for nitrogenase activity: gas chromatographic determination of ethylene per sample in less than one minute. *Appl Environ Microbiol* **39**: 1078-1080.

Fleming ED & Prufert-Bebout L (2010) Characterization of cyanobacterial communities from high-elevation lakes in the Bolivian Andes. *J Geophys Res-Biogeosci* **115**: 11.

Georgescauld F, Popova K, Gupta AJ, Bracher A, Engen JR, Hayer-Hartl M & Hartl FU (2014) GroEL/ES chaperonin modulates the mechanism and accelerates the rate of TIM-barrel domain folding. *Cell* **157**: 922-934.

Goordial J (2021) Cryomicrobial Ecology: Still Much To Learn about Life Left Out in the Cold. *mSystems* **6**: e0085221.

Goordial J, Lamarche-Gagnon G, Lay C-Y & Whyte L (2013) Left Out in the Cold: Life in Cryoenvironments. *Polyextremophiles: Life Under Multiple Forms of Stress*, (Seckbach J, Oren A & Stan-Lotter H, eds.), p.^pp. 335-363. Springer Netherlands, Dordrecht.

Grim SL, Voorhies AA, Biddanda BA, Jain S, Nold SC, Green R & Dick GJ (2021) Omics-Inferred Partitioning and Expression of Diverse Biogeochemical Functions in a Low-O₂ Cyanobacterial Mat Community. *Msystems* **6**: 16.

Hirose Y, Ohtsubo Y, Misawa N, *et al.* (2021) Genome sequencing of the NIES Cyanobacteria collection with a focus on the heterocyst-forming clade. *DNA Res* **28**.

Hodač L, Hallmann C, Spitzer K, Elster J, Faßhauer F, Brinkmann N, Lepka D, Diwan V & Friedl T (2016) Widespread green algae *Chlorella* and *Stichococcus* exhibit polar-temperate and tropical-temperate biogeography. *FEMS Microbiol Ecol* **92**.

Hsieh P, Pedersen JZ & Bruno L (2014) Photoinhibition of cyanobacteria and its application in cultural heritage conservation. *Photochem Photobiol* **90**: 533-543.

Hupp J, McCoy JIE, Millgan AJ & Peers G (2021) Simultaneously measuring carbon uptake capacity and chlorophyll a fluorescence dynamics in algae. *Algal Research* **58**: 102399.

Jungblut AD & Vincent WF (2017) Cyanobacteria in Polar and Alpine Ecosystems. *Psychrophiles: From Biodiversity to Biotechnology*, (Margesin R, ed.) p.^pp. 181-206. Springer International Publishing, Cham.

Jungblut AD, Raymond F, Dion MB, *et al.* (2021) Genomic diversity and CRISPR-Cas systems in the cyanobacterium Nostoc in the High Arctic. *Environ Microbiol* **23**: 2955-2968.

Kang DD, Li F, Kirton E, Thomas A, Egan R, An H & Wang Z (2019) MetaBAT 2: an adaptive binning algorithm for robust and efficient genome reconstruction from metagenome assemblies. *PeerJ* **7**: e7359.

Knelman JE, Schmidt SK & Graham EB (2021) Cyanobacteria in early soil development of deglaciated forefields: Dominance of non-heterocystous filamentous cyanobacteria and phosphorus limitation of N-fixing Nostocales. *Soil Biology and Biochemistry* **154**.

Laamanen MJ, Forsström L & Sivonen K (2002) Diversity of Aphanizomenon flos-aquae (Cyanobacterium) Populations along a Baltic Sea Salinity Gradient. *Applied and Environmental Microbiology* **68**: 5296-5303.

Lee JZ, Everroad RC, Karaoz U, Detweiler AM, Pett-Ridge J, Weber PK, Prufert-Bebout L & Bebout BM (2018) Metagenomics reveals niche partitioning within the phototrophic zone of a microbial mat. *Plos One* **13**: 19.

Lee N, Kim D & Lee O (2023) Stenomitros terricoa sp. nov. (Leptolyngbyaceae, Cyanobacteria) from the moist soil of Mt. Gwanggyo, Republic of Korea. *Phycological Research* **17**: 154-165.

Lennihan R, Chapin DM & Dickson LG (1994) Nitrogen fixation and photosynthesis in high arctic forms of Nostoc commune *Canadian Journal of Botany* **72**: 940-945.

Li D, Liu CM, Luo R, Sadakane K & Lam TW (2015) MEGAHIT: an ultra-fast single-node solution for large and complex metagenomics assembly via succinct de Bruijn graph. *Bioinformatics* **31**: 1674-1676.

Li Q, Chang J, Li L, Lin X & Li Y (2023) Research progress of nano-scale secondary ion mass spectrometry (NanoSIMS) in soil science: Evolution, applications, and challenges. *Science of The Total Environment* **905**: 167257.

Lionard M, Péquin B, Lovejoy C & Vincent WF (2012) Benthic cyanobacterial mats in the high Arctic: multi-layer structure and fluorescence responses to osmotic stress. *Front Microbiol* **3**: 10.

- Liu Y, Zhang W, Danielsen BK, Elberling B, Hansen BU & Westergaard-Nielsen A (2024) Snow redistribution decreases winter soil carbon loss in the Arctic dry heath tundra. *Agricultural and Forest Meteorology* **356**: 110158.
- Menzel P, Ng KL & Krogh A (2016) Fast and sensitive taxonomic classification for metagenomics with Kaiju. *Nat Commun* **7**: 11257.
- Moon T, Ahlstrom A, Goelzer H, Lipscomb W & Nowicki S (2018) Rising Oceans Guaranteed: Arctic Land Ice Loss and Sea Level Rise. *Curr Clim Change Rep* **4**: 211-222.
- Morgan-Kiss RM, Priscu JC, Pocock T, Gudynaite-Savitch L & Huner NP (2006) Adaptation and acclimation of photosynthetic microorganisms to permanently cold environments. *Microbiol Mol Biol Rev* **70**: 222-252.
- Mykytczuk NCS, Foote SJ, Omelon CR, Southam G, Greer CW & Whyte LG (2013) Bacterial growth at -15°C ; molecular insights from the permafrost bacterium *Planococcus halocryophilus* Or1. *The ISME Journal* **7**: 1211-1226.
- Nikrad MP, Kerkhof LJ & Haggblom MM (2016) The subzero microbiome: microbial activity in frozen and thawing soils. *FEMS Microbiol Ecol* **92**: fiw081.
- Novis PM, Whitehead D, Gregorich EG, Hunt JE, Sparrow AD, Hopkins DW, Elberling B & Greenfield LG (2007) Annual carbon fixation in terrestrial populations of *Nostoc commune* (Cyanobacteria) from an Antarctic dry valley is driven by temperature regime. *Glob Change Biol* **13**: 1224-1237.
- Ogawa T & Sonoike K (2016) Effects of Bleaching by Nitrogen Deficiency on the Quantum Yield of Photosystem II in *Synechocystis* sp. PCC 6803 Revealed by Chl Fluorescence Measurements. *Plant Cell Physiol* **57**: 558-567.
- Ogawa T, Misumi M & Sonoike K (2017) Estimation of photosynthesis in cyanobacteria by pulse-amplitude modulation chlorophyll fluorescence: problems and solutions. *Photosynth Res* **133**: 63-73.
- Overland J, Dunlea E, Box JE, Corell R, Forsius M, Kattsov V, Skovgård Olsen M, Pawlak J, Reiersen L & Wang M (2019) The urgency of Arctic change. *Polar Science* **21**: 6-13.
- Parada AE, Needham DM & Fuhrman JA (2016) Every base matters: assessing small subunit rRNA primers for marine microbiomes with mock communities, time series and global field samples. *Environmental Microbiology* **18**: 1403-1414.
- Quince C, Lanzen A, Davenport RJ & Turnbaugh PJ (2011) Removing Noise From Pyrosequenced Amplicons. *BMC Bioinformatics* **12**: 38.

Raymond-Bouchard I, Goordial J, Zolotarov Y, Ronholm J, Stromvik M, Bakermans C & Whyte LG (2018) Conserved genomic and amino acid traits of cold adaptation in subzero-growing Arctic permafrost bacteria. *FEMS Microbiol Ecol* **94**.

Sapers H, Ronholm J, Raymond-Bouchard I, Comrey R, Osinski G & Whyte L (2017) Biological Characterization of Microenvironments in a Hypersaline Cold Spring Mars Analog. *Front Microbiol* **8**: 2527.

Sczyrba A, Hofmann P, Belmann P, *et al.* (2017) Critical Assessment of Metagenome Interpretation—a benchmark of metagenomics software. *Nature Methods* **14**: 1063-1071.

Shen L, Zhang S & Chen G (2021) Regulated strategies of cold-adapted microorganisms in response to cold: a review. *Environ Sci Pollut Res Int* **28**: 68006-68024.

Soo RM, Woodcroft BJ, Parks DH, Tyson GW & Hugenholtz P (2015) Back from the dead; the curious tale of the predatory cyanobacterium *Vampirovibrio chlorellavorus*. *PeerJ* **3**: e968.

Spohn M, Müller K, Höschen C, Mueller CW & Marhan S (2020) Dark microbial CO₂ fixation in temperate forest soils increases with CO₂ concentration. *Glob Change Biol* **26**: 1926-1935.

Stewart WD, Fitzgerald GP & Burris RH (1967) In situ studies on N₂ fixation using the acetylene reduction technique. *Proc Natl Acad Sci U S A* **58**: 2071-2078.

Stirbet A, Lazár D, Papageorgiou GC & Govindjee (2019) Chlorophyll a Fluorescence in Cyanobacteria: Relation to Photosynthesis. *Cyanobacteria: From Basic Science to Applications*, (Mishra AK, Tiwari DN & Rai AN, eds.), p. 79-130. Academic Press.

Suda S, Watanabe MM, Otsuka S, Mahakahant A, Yongmanitchai W, Nopartnaraporn N, Liu Y & Day JG (2002) Taxonomic revision of water-bloom-forming species of oscillatorioid cyanobacteria. *International Journal of Systematic and Evolutionary Microbiology* **52**: 1577-1595.

Varin T, Lovejoy C, Jungblut AD, Vincent WF & Corbeil J (2012) Metagenomic Analysis of Stress Genes in Microbial Mat Communities from Antarctica and the High Arctic. *Applied and Environmental Microbiology* **78**: 549-559.

Vincent WF (2002) Cyanobacterial Dominance in the Polar Regions. *The Ecology of Cyanobacteria: Their Diversity in Time and Space*, (Whitton BA & Potts M, eds.), p. 321-340. Kluwer Academic Publishers.

Vishnivetskaya TA, Almatari AL, Spirina EV, Wu X, Williams DE, Pfiffner SM & Rivkina EM (2020) Insights into community of photosynthetic microorganisms from permafrost. *FEMS Microbiol Ecol* **96**.

Voigt C, Virkkala A-M, Hould Gosselin G, *et al.* (2023) Arctic soil methane sink increases with drier conditions and higher ecosystem respiration. *Nature Climate Change* **13**: 1095-1104.

Voss M, Choisnard N, Bartoli M, Bonaglia S, Bourbonnais A, Frey C, Holtermann P, Jennerjahn TC, Jickells T & Weston K (2024) Coastal Nitrogen Cycling – Biogeochemical Processes and the Impacts of Human Activities and Climate Change. *Treatise on Estuarine and Coastal Science (Second Edition)*, (Baird D & Elliott M, eds.), p.^pp. 225-250. Academic Press, Oxford.

WeatherSpark Climate and Average Weather Year Round at Eureka, N.W.T., Nunavut, Canada. 2024. Weather Spark.

Wright ES (2016) Using DECIPHER v2.0 to Analyze Big Biological Sequence Data in R. *The R Journal* **8**: 352-359.

Yu H, Jia S & Dai Y (2009). Growth characteristics of cyanobacterium *Nostoc flagelliforme* in photoautotrophic, mixotrophic and heterotrophic cultivation. *Journal of Applied Phycology* **21**: 127-133.

Ziolkowski LA, Mykytczuk NCS, Omelon CR, Johnson H, Whyte LG & Slater GF (2013) Arctic gypsum endoliths: a biogeochemical characterization of a viable and active microbial community. *Biogeosciences* **10**: 7661-7675.

Chapter 4. Discussion

The global objectives of this thesis were to identify the community composition and active members of a high Arctic *Nostoc* mat community and to identify the low-temperature limits of photoautotrophic growth, photosynthesis, and nitrogen fixation. This was achieved through metagenomic and metatranscriptomic analyses, microbial culturing, chlorophyll fluorescence, and acetylene reduction assays.

4.1 Community composition of a High Arctic *Nostoc* mat and growth limits of its culturable photoautotrophic members

The AHI *Nostoc* mat community was comprised of many different microbial members with a wide variety of metabolisms. Members of Pseudomonadota were the most abundant in the metagenome, comprising 32% of the reads, followed by Cyanobacteriota, which made up 18% of the reads (**Figure 3.2**). When scaled to the genus level, *Nostoc*, a Cyanobacteriota member, had the highest abundance of the classified quality-trimmed DNA reads (12%), followed by two Pseudomonadota members, *Sphingomonas* (6%) and *Brevundimonas* (5%) (**Figure 3.2**). This data aligns with previous research on *Nostoc* mats in cold low-nutrient environments, in which photoautotrophic members of the community supply carbon to heterotrophic members (Jungblut & Vincent, 2017, Cornet *et al.*, 2018). Metatranscriptomic analyses showed that Cyanobacteriota represented most of the transcriptional activity (70%), while Pseudomonadota was only assigned to 3% of the metatranscriptome (**Figure 3.2**). At the genus level, *Nostoc* was the most active member of the mat community, representing approximately half of the mRNA reads (**Figure 3.2**). This shows that while heterotrophic members of the mat community were more prevalent, photoautotrophic members exhibited higher transcriptional activity.

Five photoautotrophic members, two Chlorophyta and three Cyanobacteriota, from the *Nostoc* mat community, were partially isolated, resulting in non-axenic cultures each with one dominant photoautotroph (**Table 3.4**). Each of the cultured genera was found in both the metagenome and metatranscriptome, albeit at very low abundances (<0.01%) (**Table 3.4**). These cultures were grown at a variety of temperatures and salinities to determine their limits for low-temperature growth. All of the non-axenic cultures, except MNM5, could grow at 0°C and MNM2 was the only non-axenic culture to grow at sub-zero temperatures (−5°C) (**Table 3.4**). However, none of the cultures were more than mildly salt tolerant, indicating that while some of these organisms used adaptations for salt tolerance, they likely also utilized alternative strategies to maintain a liquid environment in cold conditions (**Table 3.4**). Additionally, 14 non-axenic photoautotrophic cultures were grown from adjacent High Arctic environments, and most of these cultures exhibited psychrotrophic or psychrophilic growth characteristics, with mild salt tolerance (**Table S4**). This research has identified several psychrophilic photoautotrophs, which have been underrepresented in studies of cold tolerance and adaptation (Vincent, 2002, Christmas *et al.*, 2018).

Further isolation of these non-axenic cultures could be beneficial to allow for genomic sequencing of the strains. Additionally, a more in-depth analysis of these organisms' cold adaptation mechanisms, carbon fixation and nitrogen cycling could be evaluated by conducting comparative transcriptomics on the isolates at different cold and sub-zero temperatures.

4.2 Cold adaptation mechanisms of a High Arctic *Nostoc* mat community

Genes associated with cold adaptation were searched for in the metagenome and metatranscriptome (Raymond-Bouchard *et al.*, 2018) (**Table S1**). This aimed to identify potential mechanisms used by the High Arctic *Nostoc* mat community and its members to survive in

extreme Arctic conditions and identify which of these genes were expressed. We observed both the presence and expression of osmotic stress genes in the AHI *Nostoc* mat community and its cyanobacterial MAGs (**Figure 3.2**). This is a common mechanism for cold tolerance, as salt acts as a freezing point depressant (Jungblut & Vincent, 2017). We also observed mild salt tolerance of some of our non-axenic cultures (**Figure 3.3**), which are likely expressing some of the osmotic stress genes seen in the AHI *Nostoc* mat community, however, due to their low abundance in the community, we were unable to obtain high or medium quality bins for these organisms. Genomic and transcriptomic analyses of the non-axenic cultures from the AHI *Nostoc* mat could be used to identify the mechanisms of their cold and salt tolerance. To gain more insights into the cold adaptation mechanisms in photoautotrophic mat members, three medium-quality Cyanobacteriota MAGs were further analyzed. The MAGs, as well as the metagenome, possessed and expressed multiple cold adaptation genes, which aligns with the broader understanding that Arctic microorganisms need to utilize multiple strategies for cold tolerance as the environment is associated with other stressors such as high salinity, low water availability, and freeze-thaw cycles (Lionard *et al.*, 2012, Christmas *et al.*, 2016, Jungblut & Vincent, 2017, Goordial, 2021).

Future work could include replicating the methods of Raymond-Bouchard *et al.* (2018), using our Arctic *Nostoc* mat metagenome and a temperate *Nostoc* mat metagenome. This would allow us to validate the methods, in addition to potentially finding novel cold-adaptation genes. In addition, Raymond-Bouchard *et al.* (2018) evaluated changes in amino acid compositions in cold-adapted organisms; however, this was not considered in this work and would provide additional insights into the mechanisms of cold-adaptation in the High Arctic *Nostoc* mat community.

4.3 Carbon fixation and methane cycling in a High Arctic *Nostoc* mat community

4.3.1 Carbon fixation in a High Arctic *Nostoc* mat community

A summary of the AHI *Nostoc* mat metagenome's carbon fixation and methane cycling can be seen in **Figure 3.9**. The AHI *Nostoc* mat metagenome had all of the tested marker genes for carbon fixation, of which the marker gene for photosynthesis-associated carbon fixation, was also expressed in the metatranscriptome (**Figure 3.4**). In the AHI Vampirovibrionales MAG, there were no marker genes for carbon fixation, which was unsurprising as members of the order are known as non-photosynthetic melanocytes, that instead rely on predation for nutrition (Soo *et al.*, 2015). The AHI *Nostoc* sp. WHI MAG was likely photosynthetically active, which was corroborated by the metatranscriptome taxonomic classification (**Figure 3.2**). However, the marker gene for photosynthesis-associated carbon fixation (*rbcL*) was absent, making it unclear if the organism could fix carbon following electron excitation. To determine if this was an effect of MAG incompleteness, the *rbcL* genes and transcripts would need to be taxonomically classified using NCBI BLAST or another classification tool. Finally, the photosynthetic electron transport chain was incomplete in the AHI *Stenomitos* sp. MAG suggesting that the MAG was not photosynthetically active.

CO₂ flux was obtained to determine if *in situ* activity reflected the carbon fixation activity in the metatranscriptome. There was no statistically significant difference in CO₂ flux between soils with *Nostoc* mats compared to those without (**Figure 3.5**). These soils and the associated *Nostoc* mats acted as a CO₂ source at the time of measurement (**Figure 3.4**), which is common for soils in this area (Altshuler *et al.*, 2019). While heterotrophic metabolisms were not searched for in the metagenome or metatranscriptome, sites containing *Nostoc* mats were expected to have a lower CO₂ flux than sites without. This result may have occurred as the *Nostoc* mats were only

hydrated for three days before measurements were taken, and they may not have resumed photosynthesis yet (Qiu & Gao, 2002, Novis *et al.*, 2007), or may require more intensive *in situ* field samples as the current study was limited to 3 sampling sites.

While ‘omics and *in situ* flux data provide some insight into the community activity, they are only representative of the time that the sampling occurred, which in this case was in the summer when the *Nostoc* mats are most active. To learn more about the low-temperature limits of photosynthesis, the chlorophyll fluorescence of the five non-axenic cultures grown from the MARS *Nostoc* mat, along with a mixed culture was measured at cold and sub-zero temperatures. Half of the cultures showed increasing photosynthetic activity with increasing temperature, which has been previously demonstrated (Lennihan *et al.*, 1994, Novis *et al.*, 2007). Interestingly, MNM2 showed a weak increase in photosynthetic activity with decreasing temperature (**Figure 3.7**). This combined with its ability to grow at -5°C makes MNM2 an excellent candidate for future studies on psychrophilic photoautotrophs. MNM2, MNM3 and the mixed *Nostoc* mat culture showed photosynthetic activity at -10°C (**Figure 3.7**), which expands upon previous evidence that the low-temperature limit of photosynthesis was -5°C (Becker, 1982). This data demonstrates the importance of considering cold-temperature photosynthetic activity rates when modelling photoautotrophic activity in the Arctic.

To gain better insights into true *in situ* carbon fixation, a long-term mesocosm could be set up over the AHI *Nostoc* mats, with an autosampler to obtain CO_2 flux over a year. This would increase our understanding of how CO_2 flux changes in the polar winter and during the spring and fall when temperatures are lower, but photosynthetic and heterotrophic activity has not ceased. A better representation of the spatial dynamics of the *Nostoc* mat community could be determined using a NanoSIMS approach, by feeding a microcosm containing a portion of the

mat $^{13}\text{CO}_2$ and using fluorescent *in situ* hybridization probes for cyanobacteria and general bacteria to determine both if cyanobacteria are fixing carbon and if the heterotrophic members of the community are consuming the product of the cyanobacterial photosynthesis (Li *et al.*, 2023).

4.3.2 Methane cycling in a High Arctic *Nostoc* mat

To consider the AHI *Nostoc* mat's role in methane cycling, the metagenome and its cyanobacterial MAGs were evaluated for marker genes for methanotrophy (*mmoX*) and methanogenesis (*mcrA*). Only the marker gene for methanotrophy was present in the metagenome, while it was absent from the MAGs and metatranscriptome and no marker genes for methanogenesis were detected (**Figure 3.4**). The CH_4 flux of the *Nostoc* mats was obtained to see if the methane cycling transcriptional activity would match *in situ* activity. Soils both with and without *Nostoc* mats were acting as a methane sink at the time of measurement, which has been demonstrated for soils in this area (Altshuler *et al.*, 2022), but the sink decreased in the presence of the *Nostoc* mats (**Figure 3.5**). This suggests that the decrease in methane sink was caused by either an increase in methanogenesis or a decrease in methanotrophy. This could be caused by the rehydration of the mats, as wetter conditions tend to favour methanogenesis, while dryer conditions favour methanotrophy (Liu *et al.*, 2024). Additionally, some cyanobacteria are capable of methanogenesis (Bižić *et al.*, 2020), but this was not indicated by the metagenome, which lacked the methyl coenzyme M reductase (*mcrA*) gene for (**Figure 3.4**). Since none of the tested methane cycling marker genes, *mmoX* and *mcrA* were detected in the metatranscriptome of the AHI *Nostoc* mat (**Figure 3.4**), drawing a conclusion regarding which processes were occurring is not possible. Additionally, the gas flux measurements and the sampling for meta-omic sequencing were done in different years under different environmental conditions, with the 2023 *Nostoc* mats for 'omics were hydrated and in transient pools of water, while the 2024

Nostoc mats for gas flux analyses were dehydrated and the transient pools were dried up, making them difficult to compare directly. A mesocosm approach, as was discussed with respect to CO₂ flux would also be valuable to determine how *in situ* CH₄ flux changes over the course of a year. This would take into consideration both the wet seasons, when the snow is melting, and the dry seasons when water is either frozen or dried up.

4.4 Nitrogen fixation and cycling in a High Arctic *Nostoc* mat community

Marker genes for nitrogen fixation, nitrification, denitrification, and assimilatory and dissimilatory nitrate reduction were selected to evaluate nitrogen cycling in the AHI *Nostoc* mat metagenome. All of the tested nitrogen cycling genes were present in the AHI metagenome, but only nitrogen fixation and assimilatory and dissimilatory nitrate reduction were expressed (**Figure 3.4**). The only MAG that had any of the tested nitrogen cycling genes was the AHI *Nostoc* MAG with the marker gene for nitrogen fixation (*nifH*) which was also responsible for 98% of the total *nifH* transcripts from the metatranscriptome. This suggests that *Nostoc* was fixing nitrogen, and very little of the resulting ammonia was being converted into nitrite or nitrate. Additionally, nitrate reduction transcripts suggested that nitrate was being converted back into ammonia within the community. This was further evidenced by the transient pond water physiochemical measurements, in which the pond containing *Nostoc* had 51% more ammonia but only 12% more nitrate than the adjacent control pond without visible *Nostoc* mats (**Table 3.1**).

Nitrogen fixation rates of the *Nostoc* mat community at cold and sub-zero temperatures were also measured. Due to resource limitations, this was only conducted on a mixed culture from the *Nostoc* mat. Unfortunately, high amounts of ethylene were produced in the control samples at 15 and 5°C, which resulted in negative biological acetylene reduction values

throughout the experiment (**Figure 3.8**). All of the measurements at or below 0°C showed no ethylene production (**Figure 3.8**). This experiment was conducted in carbon- and nitrogen-free media and with nitrogen-free air, which may have caused the photobleaching of cells seen early in the experiment (**Figure S5**), which in turn would cease energy production via photosynthesis (Hsieh *et al.*, 2014). Since nitrogen fixation is an energetically expensive process, it would not occur if insufficient fixed carbon was available in the cells (Esteves-Ferreira *et al.*, 2017). While there was an increase in acetylene production overtime at 15 and 5°C, it was not possible to determine acetylene reduction rates or determine the lower temperature limits for nitrogen fixation in the AHI High Arctic *Nostoc* mat due to a combination of non-biological ethylene production and photobleaching of the *Nostoc* mat culture.

Additional *in situ* acetylene reduction assays could be done on High Arctic *Nostoc* mats, using long-term incubations and auto-sampling, similar to Davey & Marchant (1983). This would allow for a more representative quantification of Arctic nitrogen fixation, allowing for natural nutrient acquisition and a more robust temperature range.

Chapter 5. Final Conclusions and Summary

High Arctic *Nostoc* mats both encode and express the cold tolerance genes required to withstand cold environments in addition to marker genes for carbon and nitrogen fixation. Culture-based analyses identified multiple photoautotrophic mat members that maintained chlorophyll fluorescence, and thus presumed photosynthetic activity, even at sub-zero temperatures. One of these cultures, *Aphanizomenon* sp. NIES81 (MNM2), was also capable of growth at sub-zero temperatures, making it a good candidate for future studies of cold-adapted cyanobacteria. These results demonstrate that High Arctic cyanobacteria are active, and some can grow at sub-zero temperatures.

This activity demonstrates the importance of incorporating cold-adapted photoautotrophic activity into biogeochemical models, especially as the Arctic continues to warm. These communities can comprise a significant portion of terrestrial microbial biomass in rapidly warming polar regions. Arctic biogeochemical models should both consider the spatial distinction between soils and cyanobacterial mats, as they can vary in methane flux. Additionally, there should be greater consideration of cold and sub-zero temperature activity in biogeochemical modelling of Arctic environments, as cyanobacteria, alongside heterotrophic microorganisms, can remain metabolically active below 0°C. This is especially important as the Arctic warms as greater amounts of time will be spent in these sub-zero ranges in which cyanobacteria are photosynthetically active. Further work is therefore needed to expand both *in situ* and culture-based knowledge to determine the role of *Nostoc* mats in High Arctic biogeochemical cycles, including explicit quantitation of their carbon and nitrogen fixation rates at low and sub-zero temperatures so that these communities can be better considered in biogeochemical models.

References

- Altshuler I, Raymond-Bouchard I, Magnuson E, Tremblay J, Greer CW & Whyte LG (2022) Unique high Arctic methane metabolizing community revealed through in situ $^{13}\text{CH}_4$ -DNA-SIP enrichment in concert with genome binning. *Scientific Reports* **12**: 1160.
- Altshuler I, Hamel J, Turney S, Magnuson E, Lévesque R, Greer CW & Whyte LG (2019) Species interactions and distinct microbial communities in high Arctic permafrost affected cryosols are associated with the CH_4 and CO_2 gas fluxes. *Environmental Microbiology* **21**: 3711-3727.
- Arndt KA, Oechel WC, Goodrich JP, Bailey BA, Kalhori A, Hashemi J, Sweeney C & Zona D (2019) Sensitivity of Methane Emissions to Later Soil Freezing in Arctic Tundra Ecosystems. *Journal of Geophysical Research: Biogeosciences* **124**: 2595-2609.
- Becker E (1982) Physiological Studies on Antarctic *Prasiola crispa* and *Nostoc commune* at Low Temperatures. *Polar Biology* **1**: 99-104.
- Bernhard A (2010) The Nitrogen Cycle: Processes, Players, and Human Impact. *Nature Education Knowledge* **3**: 25.
- Bižić M, Klintzsch T, Ionescu D, Hindiyeh MY, Günthel M, Muro-Pastor AM, Eckert W, Urich T, Keppler F & Grossart HP (2020) Aquatic and terrestrial cyanobacteria produce methane. *Science Advances* **6**: eaax5343.
- Bruhwyler L, Parmentier FW, Crill P, Leonard M & Palmer PI (2021) The Arctic Carbon Cycle and Its Response to Changing Climate. *Current Climate Change Reports* **7**: 14-34.
- Capone DG (1993) Determination of Nitrogenase activity in Aquatic Samples Using the Acetylene Reduction Procedure. *Handbook of Methods in Aquatic Microbial Ecology*, (Kemp PF, Sherr BF, Sherr EB & Cole JJ, eds.), p. 621-631. Lewis Publishers, Boca Raton, Fla.
- Chen M-Y, Teng W-K, Zhao L, Han B-P, Song L-R & Shu W-S (2022) Phylogenomics Uncovers Evolutionary Trajectory of Nitrogen Fixation in Cyanobacteria. *Molecular Biology and Evolution* **39**: msac171.
- Christmas NAM, Anesio AM & Sánchez-Baracaldo P (2018) The future of genomics in polar and alpine cyanobacteria. *FEMS Microbiol Ecol* **94**: 10.
- Christmas NAM, Barker G, Anesio AM & Sánchez-Baracaldo P (2016) Genomic mechanisms for cold tolerance and production of exopolysaccharides in the Arctic cyanobacterium *Phormidesmis priestleyi* BC1401. *BMC Genomics* **17**: 14.

Cornet L, Bertrand AR, Hanikenne M, Javaux EJ, Wilmotte A & Baurain D (2018) Metagenomic assembly of new (sub)polar Cyanobacteria and their associated microbiome from non-axenic cultures. *Microbial Genomics* **4**.

Davey A (1983) Effects of abiotic factors on nitrogen fixation by blue-green algae in Antarctica. *Polar Biology* **2**: 95-100.

Davey A & Marchant HJ (1983) Seasonal Variation in Nitrogen Fixation by Nostoc Commune Vaucher at the Vestfold Hills, Antarctica. *Phycologia* **22**: 377-385.

David KA, Apte SK, Banerji A & Thomas J (1980) Acetylene reduction assay for nitrogenase activity: gas chromatographic determination of ethylene per sample in less than one minute. *Appl Environ Microbiol* **39**: 1078-1080.

Davies-Barnard T & Friedlingstein P (2020) The Global Distribution of Biological Nitrogen Fixation in Terrestrial Natural Ecosystems. *Global Biogeochemical Cycles* **34**: e2019GB006387.

Esteves-Ferreira AA, Cavalcanti JHF, Gomes Marçal Vieira Vaz M, Alvarenga LV, Nunes-Nesi A & Araújo WL (2017) Cyanobacterial nitrogenases: phylogenetic diversity, regulation and functional predictions. *Genet Mol Biol* **40**: 261-275.

Evans PN, Boyd JA, Leu AO, Woodcroft BJ, Parks DH, Hugenholtz P & Tyson GW (2019) An evolving view of methane metabolism in the Archaea. *Nature Reviews Microbiology* **17**: 219-232.

Falkowski P, Scholes RJ, Boyle E, *et al.* (2000) The global carbon cycle: a test of our knowledge of earth as a system. *Science* **290**: 291-296.

Fleming ED & Castenholz RW (2008) Effects of nitrogen source on the synthesis of the UV-screening compound, scytonemin, in the cyanobacterium *Nostoc punctiforme* PCC 73102. *FEMS Microbiol Ecol* **63**: 301-308.

Fleming ED & Prufert-Bebout L (2010) Characterization of cyanobacterial communities from high-elevation lakes in the Bolivian Andes. *J Geophys Res-Biogeosci* **115**: 11.

Goordial J (2021) Cryomicrobial Ecology: Still Much To Learn about Life Left Out in the Cold. *mSystems* **6**: e0085221.

Goordial J, Lamarche-Gagnon G, Lay C-Y & Whyte L (2013) Left Out in the Cold: Life in Cryoenvironments. *Polyextremophiles: Life Under Multiple Forms of Stress*, (Seckbach J, Oren A & Stan-Lotter H, eds.), p. 335-363. Springer Netherlands, Dordrecht.

Goordial J, Davila A, Greer CW, Cannam R, DiRuggiero J, McKay CP & Whyte LG (2017) Comparative activity and functional ecology of permafrost soils and lithic niches in a hyper-arid polar desert. *Environ Microbiol* **19**: 443-458.

Goordial J, Raymond-Bouchard I, Zolotarov Y, *et al.* (2016) Cold adaptive traits revealed by comparative genomic analysis of the eurypsychrophile *Rhodococcus* sp. JG3 isolated from high elevation McMurdo Dry Valley permafrost, Antarctica. *FEMS Microbiol Ecol* **92**.

Grim SL, Voorhies AA, Biddanda BA, Jain S, Nold SC, Green R & Dick GJ (2021) Omics-Inferred Partitioning and Expression of Diverse Biogeochemical Functions in a Low-O₂ Cyanobacterial Mat Community. *Msystems* **6**: 16.

Hagopian JC, Reis M, Kitajima JP, Bhattacharya D & de Oliveira MC (2004) Comparative analysis of the complete plastid genome sequence of the red alga *Gracilaria tenuistipitata* var. liui provides insights into the evolution of rhodoplasts and their relationship to other plastids. *J Mol Evol* **59**: 464-477.

Holm-Hansen O (1963) Viability of blue-green algae after freezing. *Physiologia Plantarum* **16**: 530-540.

Holmberg SM & Jørgensen NOG (2023) Insights into abundance, adaptation and activity of prokaryotes in arctic and Antarctic environments. *Polar Biology* **46**: 381-396.

Hsieh P, Pedersen JZ & Bruno L (2014) Photoinhibition of cyanobacteria and its application in cultural heritage conservation. *Photochem Photobiol* **90**: 533-543.

Huo D, Li H, Cai F, Guo X, Qiao Z, Wang W, Yu G & Li R (2021) Genome Evolution of Filamentous Cyanobacterium *Nostoc* Species: From Facultative Symbiosis to Free Living. *Microorganisms* **9**.

Jungblut AD & Vincent WF (2017) Cyanobacteria in Polar and Alpine Ecosystems. *Psychrophiles: From Biodiversity to Biotechnology*, (Margesin R, ed.) p.^pp. 181-206. Springer International Publishing, Cham.

Jungblut AD, Raymond F, Dion MB, *et al.* (2021) Genomic diversity and CRISPR-Cas systems in the cyanobacterium *Nostoc* in the High Arctic. *Environ Microbiol* **23**: 2955-2968.

Kohler TJ, Singley JG, Wlostowski AN & McKnight DM (2023) Nitrogen fixation facilitates stream microbial mat biomass across the McMurdo Dry Valleys, Antarctica. *Biogeochemistry* **166**: 247-268.

Kvídlerová J (2018) Internal structure and photosynthetic performance of *Nostoc* sp. colonies in the high Arctic. *Acta Soc Bot Pol* **87**: 12.

Lee JZ, Everroad RC, Karaoz U, Detweiler AM, Pett-Ridge J, Weber PK, Prufert-Bebout L & Bebout BM (2018) Metagenomics reveals niche partitioning within the phototrophic zone of a microbial mat. *Plos One* **13**: 19.

Lemaux PG & Grossman AR (1985) Major light-harvesting polypeptides encoded in polycistronic transcripts in a eukaryotic alga. *EMBO J* **4**: 1911-1919.

Lennihan R, Chapin DM & Dickson LG (1994) Nitrogen fixation and photosynthesis in high arctic forms of *Nostoc commune* *Canadian Journal of Botany* **72**: 940-945.

Li Q, Chang J, Li L, Lin X & Li Y (2023) Research progress of nano-scale secondary ion mass spectrometry (NanoSIMS) in soil science: Evolution, applications, and challenges. *Science of The Total Environment* **905**: 167257.

Li Z, Tong D, Nie X, Xiao H, Jiao P, Jiang J, Li Q & Liao W (2021) New insight into soil carbon fixation rate: The intensive co-occurrence network of autotrophic bacteria increases the carbon fixation rate in depositional sites. *Agriculture, Ecosystems & Environment* **320**: 107579.

Lim PP, Pearce DA, Convey P, Lee LS, Chan KG & Tan GYA (2020) Effects of freeze-thaw cycles on High Arctic soil bacterial communities. *Polar Science* **23**: 100487.

Lionard M, Péquin B, Lovejoy C & Vincent WF (2012) Benthic cyanobacterial mats in the high Arctic: multi-layer structure and fluorescence responses to osmotic stress. *Front Microbiol* **3**: 10.

Liu Y, Zhang W, Danielsen BK, Elberling B, Hansen BU & Westergaard-Nielsen A (2024) Snow redistribution decreases winter soil carbon loss in the Arctic dry heath tundra. *Agricultural and Forest Meteorology* **356**: 110158.

Luttge U, Budel B, Ball E, Strube F & Weber P (1995) Photosynthesis of terrestrial cyanobacteria under light and desiccation stress as expressed by chlorophyll fluorescence and gas-exchange. *J Exp Bot* **46**: 309-319.

Martineau C, Whyte Lyle G & Greer Charles W (2010) Stable Isotope Probing Analysis of the Diversity and Activity of Methanotrophic Bacteria in Soils from the Canadian High Arctic. *Applied and Environmental Microbiology* **76**: 5773-5784.

Monchamp M-E, Spaak P & Pomati F (2019) Long Term Diversity and Distribution of Non-photosynthetic Cyanobacteria in Peri-Alpine Lakes. *Front Microbiol* **9**.

Moon T, Ahlstrom A, Goelzer H, Lipscomb W & Nowicki S (2018) Rising Oceans Guaranteed: Arctic Land Ice Loss and Sea Level Rise. *Curr Clim Change Rep* **4**: 211-222.

Morgan-Kiss RM, Priscu JC, Pocock T, Gudynaite-Savitch L & Huner NP (2006) Adaptation and acclimation of photosynthetic microorganisms to permanently cold environments. *Microbiol Mol Biol Rev* **70**: 222-252.

Mulkidjanian AY, Koonin EV, Makarova KS, *et al.* (2006) The cyanobacterial genome core and the origin of photosynthesis. *Proc Natl Acad Sci U S A* **103**: 13126-13131.

Mykytczuk NCS, Foote SJ, Omelon CR, Southam G, Greer CW & Whyte LG (2013) Bacterial growth at -15°C ; molecular insights from the permafrost bacterium *Planococcus halocryophilus* Or1. *The ISME Journal* **7**: 1211-1226.

Nakazawa T (2020) Current understanding of the global cycling of carbon dioxide, methane, and nitrous oxide. *Proc Jpn Acad Ser B Phys Biol Sci* **96**: 394-419.

Nash MV, Anesio AM, Barker G, Tranter M, Varliero G, Eloie-Fadrosch EA, Nielsen T, Turpin-Jelfs T, Benning LG & Sanchez-Baracaldo P (2018) Metagenomic insights into diazotrophic communities across Arctic glacier forefields. *FEMS Microbiol Ecol* **94**.

Nikrad MP, Kerkhof LJ & Haggblom MM (2016) The subzero microbiome: microbial activity in frozen and thawing soils. *FEMS Microbiol Ecol* **92**: fiw081.

Novis PM, Whitehead D, Gregorich EG, Hunt JE, Sparrow AD, Hopkins DW, Elberling B & Greenfield LG (2007) Annual carbon fixation in terrestrial populations of *Nostoc commune* (Cyanobacteria) from an Antarctic dry valley is driven by temperature regime. *Glob Change Biol* **13**: 1224-1237.

Overland J, Dunlea E, Box JE, Corell R, Forsius M, Kattsov V, Skovgård Olsen M, Pawlak J, Reiersen L & Wang M (2019) The urgency of Arctic change. *Polar Science* **21**: 6-13.

Pereira SB, Mota R, Vieira CP, Vieira J & Tamagnini P (2015) Phylum-wide analysis of genes/proteins related to the last steps of assembly and export of extracellular polymeric substances (EPS) in cyanobacteria. *Sci Rep* **5**: 14835.

Pessi IS, Pushkareva E, Lara Y, Borderie F, Wilmotte A & Elster J (2019) Marked Succession of Cyanobacterial Communities Following Glacier Retreat in the High Arctic. *Microb Ecol* **77**: 136-147.

Price PB (2007) Microbial life in glacial ice and implications for a cold origin of life. *FEMS Microbiol Ecol* **59**: 217-231.

Qiu BS & Gao KS (2002) Daily production and photosynthetic characteristics of *Nostoc flagelliforme* grown under ambient and elevated CO_2 conditions. *J Appl Phycol* **14**: 77-83.

Raymond-Bouchard I, Goordial J, Zolotarov Y, Ronholm J, Stromvik M, Bakermans C & Whyte LG (2018) Conserved genomic and amino acid traits of cold adaptation in subzero-growing Arctic permafrost bacteria. *FEMS Microbiol Ecol* **94**.

Raymond JA, Janech MG & Mangiagalli M (2021) Ice-binding proteins associated with an Antarctic cyanobacterium, *Nostoc* sp. HG1. *Applied and Environmental Microbiology* **87**.

Reichle DE (2020) Chapter 10-The global carbon cycle and the biosphere. *The Global Carbon Cycle and Climate Change: Scaling Ecological Energetics from Organism to the Biosphere*, p.^pp. 183-208. Elsevier.

Reith M & Douglas S (1990) Localization of beta-phycoerythrin to the thylakoid lumen of *Cryptomonas phi* does not involve a signal peptide. *Plant Mol Biol* **15**: 585-592.

Reynaud PA (1984) Influence of PH on Nitrogen Fixation of Cyanobacteria from Acid Paddy Fields. *Advances in Nitrogen Fixation Research: Proceedings of the 5th International Symposium on Nitrogen Fixation, Noordwijkerhout, The Netherlands, August 28 – September 3, 1983*, (Veeger C & Newton WE, eds.), p.^pp. 356-356. Springer Netherlands, Dordrecht.

Rozwalak P, Podkowa P, Buda J, *et al.* (2022) Cryoconite - From minerals and organic matter to bioengineered sediments on glacier's surfaces. *Science of The Total Environment* **807**.

Sakamoto T & Murata N (2002) Regulation of the desaturation of fatty acids and its role in tolerance to cold and salt stress. *Current Opinion in Microbiology* **5**: 206-210.

Shen L, Zhang S & Chen G (2021) Regulated strategies of cold-adapted microorganisms in response to cold: a review. *Environ Sci Pollut Res Int* **28**: 68006-68024.

Shevela D, Pishchalnikov R, Eichacker LA & Govindjee (2013) Oxygenic photosynthesis in cyanobacteria. *Stress Biology of Cyanobacteria: Molecular Mechanisms to Cellular Response*, (Srivastava AK, Rai AN & Neilan BA, eds.), p.^pp. 3-40. CRC Press.

Singleton CM, McCalley CK, Woodcroft BJ, *et al.* (2018) Methanotrophy across a natural permafrost thaw environment. *The ISME Journal* **12**: 2544-2558.

Sohm JA, Niederberger TD, Parker AE, Tirindelli J, Gunderson T, Cary SC, Capone DG & Carpenter EJ (2020) Microbial Mats of the McMurdo Dry Valleys, Antarctica: Oases of Biological Activity in a Very Cold Desert. *Front Microbiol* **11**: 537960.

Soo RM, Woodcroft BJ, Parks DH, Tyson GW & Hugenholtz P (2015) Back from the dead; the curious tale of the predatory cyanobacterium *Vampirovibrio chlorellavorus*. *PeerJ* **3**: e968.

Sparacino-Watkins C, Stolz JF & Basu P (2014) Nitrate and periplasmic nitrate reductases. *Chem Soc Rev* **43**: 676-706.

Stewart WD, Fitzgerald GP & Burris RH (1967) In situ studies on N₂ fixation using the acetylene reduction technique. *Proc Natl Acad Sci U S A* **58**: 2071-2078.

Stirbet A, Lazár D, Papageorgiou GC & Govindjee (2019) Chlorophyll a Fluorescence in Cyanobacteria: Relation to Photosynthesis. *Cyanobacteria: From Basic Science to Applications*, (Mishra AK, Tiwari DN & Rai AN, eds.), p.^pp. 79-130. Academic Press.

Trotsenko YA & Khmelenina VN (2005) Aerobic methanotrophic bacteria of cold ecosystems. *FEMS Microbiol Ecol* **53**: 15-26.

United States Environmental Protection Agency (2024) Global Methane Initiative: Importance of Methane. Vol. 2024 p.^pp.

Varin T, Lovejoy C, Jungblut AD, Vincent WF & Corbeil J (2012) Metagenomic Analysis of Stress Genes in Microbial Mat Communities from Antarctica and the High Arctic. *Applied and Environmental Microbiology* **78**: 549-559.

Vincent WF (2002) Cyanobacterial Dominance in the Polar Regions. *The Ecology of Cyanobacteria: Their Diversity in Time and Space*, (Whitton BA & Potts M, eds.), p.^pp. 321-340. Kluwer Academic Publishers.

Vincent WF (2007) Cold Tolerance in Cyanobacteria and Life in the Cryosphere. *Algae and Cyanobacteria in Extreme Environments*, Vol. 11 (Seckbach J, ed.) p.^pp. 287-301. Springer, Dordrecht.

Voigt C, Virkkala A-M, Hould Gosselin G, *et al.* (2023) Arctic soil methane sink increases with drier conditions and higher ecosystem respiration. *Nature Climate Change* **13**: 1095-1104.

Yu H, Jia S & Dai Y (2009) Growth characteristics of the cyanobacterium *Nostoc flagelliforme* in photoautotrophic, mixotrophic and heterotrophic cultivation. *J Appl Phycol* **21**: 127-133.

Zhu X-G, Long SP & Ort DR (2008) What is the maximum efficiency with which photosynthesis can convert solar energy into biomass? *Current Opinion in Biotechnology* **19**: 153-159.

Zielke M, Solheim B, Spjelkavik S & Olsen RA (2005) Nitrogen Fixation in the High Arctic: Role of Vegetation and Environmental Conditions. *Arctic, Antarctic, and Alpine Research* **37**: 372-387.

Ziolkowski LA, Mykytczuk NCS, Omelon CR, Johnson H, Whyte LG & Slater GF (2013) Arctic gypsum endoliths: a biogeochemical characterization of a viable and active microbial community. *Biogeosciences* **10**: 7661-7675.

Appendix 1. Supplementary Materials for Chapter 3

A.1 Targeted genes for metagenomic and metatranscriptomic analysis of a High Arctic

Nostoc mat community

Table S1. List of cold tolerance genes adapted from Raymond-Bouchard *et al.* (2018; Table 3)

Gene description	ID
Cold shock, stress and HSP proteins	
CspA; Cold shock protein, CspA family	KO:K03704, COG1278
UspA; Universal stress protein, UspA family	KO:K06149, COG0589
HSP10, GroES; Co-chaperonin GroES (HSP10)	KO:K04078, COG0234
HSP60, GroEL; Chaperonin GroEL (HSP60 family)	KO:K04077, COG0459
HSP70, DnaK; Molecular chaperone DnaK (HSP70)	KO:K04043, COG0443
HSP20, IbpA; Molecular chaperone IbpA, HSP20 family	KO:K04080, COG0071
HSP90; Molecular chaperone, HSP90 family	KO:K04079, COG0326
GrpE; Molecular chaperone GrpE (heat shock protein)	KO:K03687, COG0576
Ribosomal 50S subunit-recycling heat shock protein	KO:K04762, COG1188
DNA replication and repair	
DNA gyrase/topoisomerase I, subunits A&B	KO:K02469, KO:K02470, COG0187, COG0188
RecR; Recombinational DNA repair protein RecR	KO:K06187, COG0353
RecA; RecA-superfamily ATPase, KaiC/GvpD/RAD55 family	COG0467
RecA/RadA; RecA/RadA recombinase	COG0468
RecN; DNA repair ATPase RecN	KO:K03631, COG0497
RecQ; Superfamily II DNA helicase RecQ	KO:K03654, COG0514
Rad3; Rad3-related DNA helicase	KO:K03722, COG1199
Membrane and peptidoglycan alteration	
3-oxoacyl-(acyl-carrier-protein) synthase	KO:K09458, COG0304
3-oxoacyl-[acyl-carrier-protein] synthase III (KASIII)	KO:K00648, COG0332
3-oxoacyl-[acyl-carrier-protein] reductase	KO:K00059, EC:1.1.1.100
Glycosyltransferase involved in cell wall biosynthesis	COG0438, COG0463
3-hydroxyacyl-CoA dehydrogenase	KO:K00074, COG1250
Fatty-acid desaturase	COG1398, COG3239
D-alanyl-D-alanine carboxypeptidase	KO:K01286, COG1686, COG2027
Carotenoid biosynthesis	
Phytoene dehydrogenase-related protein	KO:K09845, COG1233
Phytoene/squalene synthetase	COG1562
crtB; Beta Carotene synthesis, 15-cis-phytoene synthase [EC:2.5.1.32]	KO:K02291

Polysaccharide capsule	
Capsular polysaccharide biosyn. protein EpsC	KO:K19421, COG1086
Capsule polysaccharide export protein	KO:K10107, COG3524
Capsular polysaccharide biosynthesis protein	KO:K19420, COG3944, COG4421
Exopolysaccharide biosynthesis protein	KO:K01125, COG4632
Exopolymeric Substance Export protein (Wza)	KO:K01991, COG1596
Osmotic stress	
ABC proline/glycine betaine transport, ATPase component	KO:K05847, KO:K02000, COG1125, COG4175
ABC proline/glycine betaine transport, permease	KO:K05846, KO:K02001, COG1174, COG4176
Choline-glycine betaine transporter	KO:K02168, COG1292
Osmoprotectant binding protein	KO:K05845, COG1732
Choline dehydrogenase or related flavoprotein	KO:K00108, COG2303
Trehalose-6-phosphate synthase	KO:K00697, COG0380
Trehalose-6-phosphatase	KO:K01087, COG1877
Maltooligosyltrehalose synthase	KO:K06044, COG3280
Na ⁺ /proline symporter	KO:K11928, COG0591
Na ⁺ /H ⁺ antiporters	KO:K03313, KO:K05571, KO:K00341, KO:K12137, KO:K24163, KO:K03893, COG3004, COG1055, COG0025, COG0651, COG1009, COG1320
Oxidative stress	
Catalase	KO:K03781, COG0753
Peroxiredoxin	KO:K14171, KO:K03564, COG0678, COG1225
Glutathione peroxidase	KO:K00432, COG0386
Spermidine synthase	KO:K00797, COG0421
Thioredoxin reductase	KO:K00384, COG0492
Glyoxylase or related hydrolase, β -lactamase superfam II	KO:K01069, COG0491
Toxin/Antitoxin modules	
Ser/Thr kinase RdoA, MazF antagonist	COG2334
Antitoxin component of MazEF	KO:K07172, COG2336
mRNA-interferase, toxin component of MazEF	KO:K07171, COG2337
mRNA interferase YafQ, toxin component of YafQ-DinJ	KO:K19157, COG3041
Antitoxin component of RelBE or YafQ-DinJ	KO:K18918, COG3077
Translation and transcription factors	
tRNA-dihydrouridine synthase	KO:K05539, COG0042
tRNA A37 threonylcarbamoyladenosine dehydratase	COG1179
Translation elongation factor EF-Tu, GTPase	KO:K02358, COG0050
Translation elongation factor EF-G, GTPase	KO:K02355, COG0480

Translation initiation factor IF-2, GTPase	KO:K02519, COG0532
Translation initiation factor IF-3	KO:K02520, COG0290
Transcription antitermination factor NusA	KO:K02600, COG0195
Transcription termination factor NusB	KO:K03625, COG0781
Superfamily II DNA and RNA helicase	KO:K05590, COG1061, KO:K10843, COG0513
Superfamily II DNA or RNA helicase, SNF2	KO:K03580, COG0553
Superfamily II RNA helicase	KO:K03727, COG4581

Table S2. Selected genes to evaluate carbon fixation, methane cycling and nitrogen cycling

Gene description	ID
Carbon Fixation and Methane Cycling	
psbA; photosystem II P680 reaction center D1 protein [EC:1.10.3.9]	KO:K02703, COG5716, TIGR01151
psaA; photosystem I P700 chlorophyll a apoprotein A1 [EC:1.97.1.12]	KO:K02689, COG5701
petB; cytochrome b6	KO:K02635
apcA; allophycocyanin alpha subunit	KO:K02092, COG5684
cpcA; phycocyanin alpha chain	KO:K02284, COG5687
cpeA, mpeA; phycoerythrin alpha chain	KO:K05376
LHCA1; light-harvesting complex I chlorophyll a/b binding protein 1	KO:K08907
rbcl, cbbL; ribulose-bisphosphate carboxylase large chain [EC:4.1.1.39]	KO:K01601, COG1850
mmoX; methane monooxygenase component A alpha chain for methanotrophy [EC:1.14.13.25]	KO:K16157
mcrA; methyl-coenzyme M reductase alpha subunit for methanogenesis [EC:2.8.4.1]	KO:K00399
Nitrogen Cycling	
nasC, nasA, assimilatory nitrate reductase catalytic subunit [EC:1.7.99.-]	KO:K00372
nirK, nitrite reductase (NO-forming) [EC:1.7.2.1]	KO:K00368, TIGR02376
nrFA, nitrite reductase (cytochrome c-552) [EC:1.7.2.2]	KO:K03385, COG3303
nifH; nitrogenase iron protein NifH	KO:K02588, COG1348
pmoA-amOA; methane/ammonia monooxygenase subunit A [EC:1.14.18.3 1.14.99.39]	KO:K10944

A.2 High Arctic Nostoc mat metagenome assembly statistics

Table S3. Metagenome assembly statistics

contigs	total bp	min bp	max bp	average bp	N50
8,315,956	4,996,314,154	200	319,232	600	633

A.3 In situ gas flux analyses of High Arctic Nostoc mats

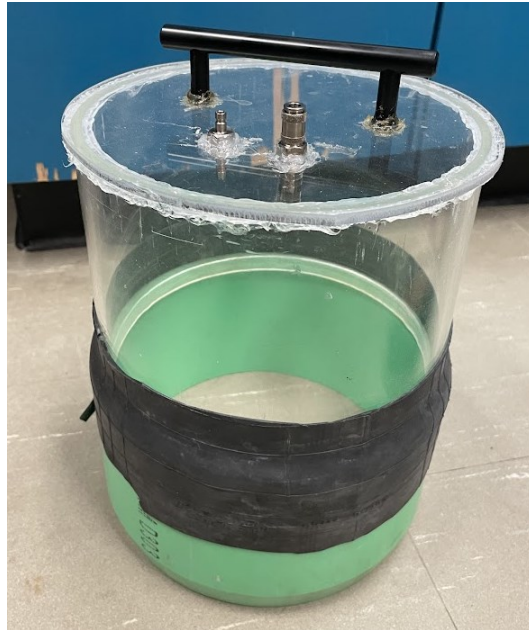


Figure S1. Clear gas flux chamber sealed with a soil collar.

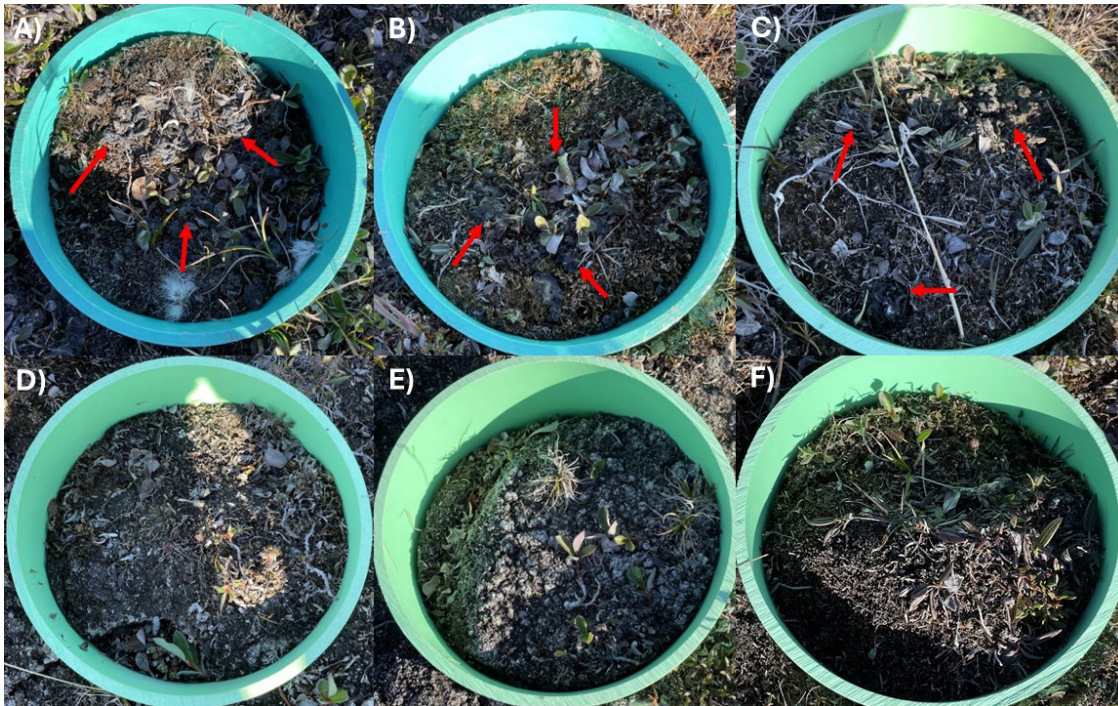


Figure S2. Gas flux sites A) N1, B) N2, C) N3, D) C1, E) C2, and F) C3. N sites contain portions of Nostoc mats (indicated by red arrows), while C sites were nearby soil sites with no mats.

A.4 Isolation and characterization of photoautotrophs from High Arctic environments

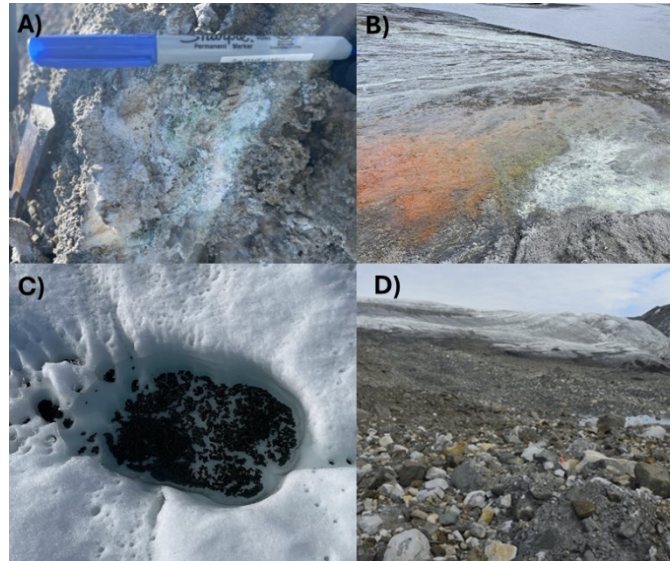


Figure S3. Photoautotroph culture sampling sites. A) Gypsum Hill endolith (GHE) containing green striations. B) Gypsum Hill Springs microbial mats. Samples were derived from the white mat on the left (GHSWM), and the green portion in the center (GHSGM). C) White Glacier Cryoconite material (WGCM). D) White Glacier Forefield (WGF) soils that were deglaciated approx. 50 years ago.

Table S4. Identification and characterization of photoautotrophic cultures from high Arctic environments.

ID	Kingdom	Identity	Growth temperature (°C)	NaCl tolerance (%)	Growth on BG11 _o
Gypsum Hill Endolith (GHE)					
GHE1	Eukarya	<i>Stichococcus</i> sp.	0-15	0-5	Yes
GHE2	Eukarya	<i>Stichococcus</i> sp.	5-15	0-2.5	Yes
GHE3	Bacteria	<i>Scytonema</i> sp. UTEX_2349	15-25	0	Yes
Gypsum Hill Springs Microbial Mats (GHSM)					
GHSWM1	Eukarya	<i>Chlamydomonas</i> sp.	5-15	0-2.5	No
GHSGMA1	Eukarya	<i>Chlamydomonas</i> sp.	5-15	0-2.5	No
GHSGMB1	Eukarya	<i>Chlamydomonas</i> sp.	5-25	0-2.5	No
GHSGMB2	Bacteria	<i>Nitzschia</i> sp.	0-25	0	No
White Glacier Cryoconite Material (WGCM)					
WGCM1	Eukarya	Unknown Chlorophyceae	0-25	0	Yes
WGCM2	Eukarya	Unknown Chlorophyceae	0-15	0	Yes
WGCM3	Eukarya	<i>Chloromonas</i> sp.	5-15	0	Yes
White Glacier Forefield (WGF)					
WGF1	Eukarya	Unknown Chlorophyceae	5-15	0	Yes
WGF2	Eukarya	<i>Stichococcus</i> sp.	0-15	0-2.5	Yes
WGF3	Eukarya	<i>Stichococcus</i> sp.	0-25	0-5	Yes
WGF4	Eukarya	Unknown Trebouxiophyceae	5-15	0	Yes

A.5 Acetylene reduction assay supplemental figures

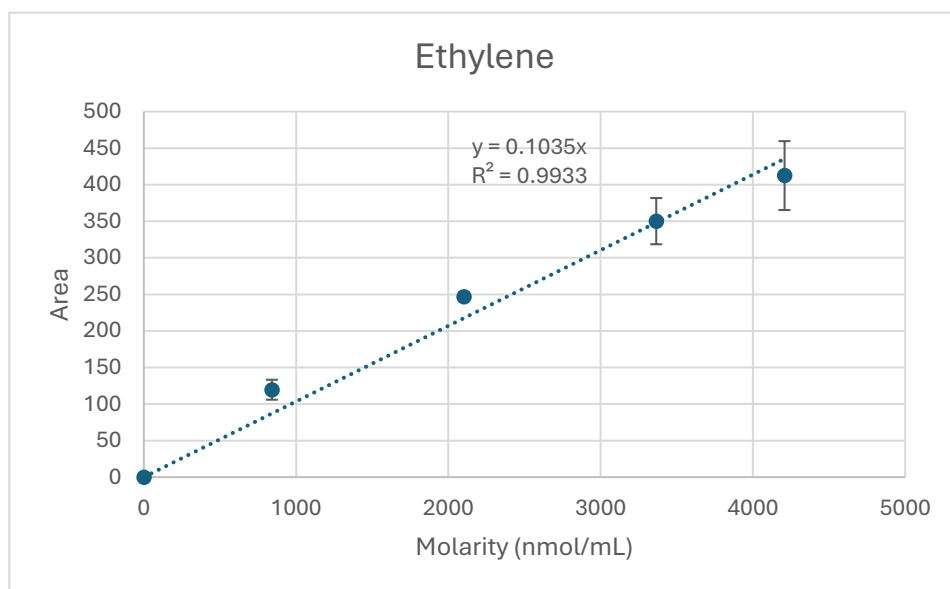


Figure S4. Example ethylene standard curve generated by running standards with known ethylene concentrations through the gas chromatograph, with three technical replicates. Equation was adjusted for a set y intercept of 0.



Figure S5. Tube containing photobleached cell content following 30-day incubation under nitrogen free conditions. Arrow indicates the cell pellet.